Investigation of Superconductors Thermal Stability Using Different Macroscopic Heat Conduction Models

By
Mohammed Q. Odat

Supervisor
Professor Mohammed Hamdan

Co-Supervisor
Dr. Moh'd Al-Nimr

Submitted in the Partial Fulfillment of the Requirements for the Degree of Doctor of Philosophy in Mechanical Engineering

Faculty of Graduate studies
University of Jordan

January 2001

This thesis was successfully defend and approved on: Jan. 11, 2001

Examination Committee	*Signature*
Prof. Mohammed Hamadan, Supervisor and Chairman, Prof. Of Mechanical Engineering, University of Jordan	
Dr. Moh'd Al-Nimr , Co-supervisor, Associate Prof. of Mechanical Engineering, Jordan University of Science and Technology	Moh'd Al-Nimr 1/14/2001
Prof. Mohammed Al-Saad, Member Prof. of Mechanical Engineering, University of Jordan	
Dr. Mohammoud Abu-Zied, Member Associate Prof. of Mechanical Engineering, Mu'ta University	1/14/2001
Dr. Ali Badran, Member Associate Prof. of Mechanical Engineering, University of Jordan	A. Badran 1/17/2001

Dedication

This thesis is dedicated to my mother, wife, sons, daughter, brothers, and sisters, for their love and support throughout my live.

Acknowledgements

I would like to express my sincerest gratitude to my thesis advisors Prof. Mohammed Hamdan and Dr. Moh'd Al-Nimr, for suggesting to me the superconductivity stability area and for their invaluable guidance, insistent encouragement, and support. They have been a source of profound inspiration, and working with them has it self been a rewarding experience. Also I would like to thank my committee members Prof. Mohammed Al-Saad, Dr. Mahmoud Abu-Zied, and Dr. Ali Badran for their valuable comments.

Also, I would like to thank Amman College for Engineering Technology– Al-Balqa Applied University for their support throughout my study.

I would like to express my gratitude to everyone who taught me.

Finally and not final I would like to thank my mother, my wife, my sisters and my brothers- for their deep love and continuous encouragement.

Table of contents

List of Tables

List of Figures

List of Appendices

Nomenclature

A	Cross sectional area of conductor	(m^2)
A_m	Matrix cross sectional area	(m^2)
B	Disturbance Intensity	(---)
C	Volumetric heat capacity	($Jm^{-3}K^{-1}$)
dis(x,t)	Heat disturbance	(Wm^{-3})
Ds	Dimensionless disturbance function	(---)
Ds	Dimensionless heat disturbance	(---)
E	Electric field	($V\ m^{-1}$)
E	Energy of heat disturbance	(J)
f	Volume fraction of stabilizer in conductor	(----)
g(T)	Temperature dependence Joule heating	(Wm^{-3})
G_C	Maximum Joule heating for non-composite superconductor	(Wm^{-2})
g_{max}	The maximum Joule heating with the whole current in the stabilizer	(Wm^{-3})
h	Convective heat transfer coefficient	($Wm^{-2}K^{-1}$)
H	Lateral cooling factor	(---)
H_B	Magnetic field	(T)
H_{Bc}	Critical magnetic field	(T)
H_{Bcl}	Lower critical magnetic field	(T)
H_c	Critical lateral cooling factor (---)	
I_c	Critical current	(Am)
I_m	Matrix current	(Am)
I_o	The current at T_o	(Am)
I_{sc}	Superconductor current	(Am)
I_t	Total current	(Am)

J	Current density	(Am/m^2)
J_c	Critical current density	(Am/m^2)
k	Thermal conductivity of conductor	$(Wm^{-1}K^{-1})$
2l	Length of conductor subjected ro heat disturbances	(m)
P	Perimeter of conductor	(m)
Q	Dimensionless capacity of Joule heating source	(---)
q	heat flux vector	(Wm^{-2})
Q_c	Dimensionless critical Joule heating	(----)
r	material position vector	(m)
R	Relaxation times ratio (τ_T/τ_q) dimensionless	(---)
t	Time	(s)
T	Temperature	(K)
T_c	Critical temperature	(K)
T_{cl}	Current sharing temperature	(K)
t_i	Duration of heat disturbance	(s)
T_i	Initial temperature	(K)
$\dot{T}_i$	Initial time-rate of temperature	(K/sec)
T_o	Temperature far from normal region (ambient temperature)	(K)
T_t	Transition temperature	(K)
V	Voltage	(volt)
x	Co-ordinate along conductor	(m)

Greek letters

β	Dimensionless time	(---)
ε	Dimensionless heat disturbance energy	(---)
φ	Dimensionless lateral cooling factor	(---)

θ	Dimensionless temperature	(---)
$\theta 1$	Dimensionless maximum temperature	(---)
θ_{cl}	Dimensionless current sharing temperature	(---)
ρ	Conductor electrical resistivity	(Ω m)
ρ_o	Stabilizer electrical resistivity	(Ω m)
ξ	Dimensionless co-ordinate along conductor	(---)
τ_I	Dimensionless duration time of heat disturbance	(---)
τ_q	Phase lag of heat flux	(s)
τ_T	Phase lag of temperature gradient.	(s)
α	Thermal diffusivity	($m^2 s^{-1}$)
ω	Speed of heat propagation	(ms^{-1})

Subscripts

c_l	Current sharing
.m	Metal matrix
max	maximum
o	Operating
sc	Superconductor

Abstract

Investigation of Superconductors Thermal Stability Using Different Macroscopic Heat Conduction Models

By
Mohammed Q. Odat

Supervisor
Professor Mohammed Hamdan

Co-Supervisor
Dr. Moh'd Al-Nimr

Superconducting magnets are subjected to a thermal instability, leading to the loss of superconductivity, known as "quench," in which the critical values of field, temperature, and current density are exceeded and fail to recover. This phenomenon generally begins by external localized disturbances, which create a normal (resistive) zone. The normal zone may grow or collapse depending on the balance between the resulting Joule heating in the wire and the heat losses from the wire. If the heat is not conducted away from the normal zone faster than it is generated, the normal zone will grow and the temperature will increase and the superconductor is said to be unstable. Thermal stability, i.e., the possibility of self-recovery of a superconductor after a quench, is one of the most important issues of superconductor devices design. The thermal stability of a superconductor is determined quantitatively by some limiting parameters, called stability indicators or parameters, which delimit the stable operation region of the superconductor. The parameters of stability are used in the design and operation of superconducting devices.

This thesis presents a numerical investigation for calculating the stability parameters; which include the superconductor maximum temperature and the critical energy. The calculation of these parameters is conducted based on different macroscopic heat conduction models, which are the classical diffusion model, the wave

model, and the dual-lag-phase model. The essential part of this work is the usage of the wave and dual phase lag models, which can be used for the description of fast-changing or high heating rate heat processes in the superconductors. These models take into account the finite speed of heat flux propagation and the precedence of temperature gradient-heat flux.

Thermal stability is simulated by a numerical code using finite-difference method for the diffusion model, and FlexPDE finite-element code for the wave and dual-phase-lag models. The numerical methods for calculation the stability parameters of the uncooled and cooled superconductor takes into account transient heat transfer in the conductor and coolant, and the finite duration and finite length of heat disturbances.

The present study indicates that the use of the wave and dual phase-lag-model have a dominant effect on the prediction of superconductor thermal stability. Also, the simulation demonstrates that there is a critical Joule heating for each disturbance intensity, and the stability region estimated based on dual-phase-lag model seems to be overestimated. For small values of disturbances the wave model predicts a narrower thermal stability region compared to the stability region obtained using the diffusion model, and the situation is reversed at disturbance of higher intensity.

Also, the results of this investigation indicate that lateral cooling has a significant influence on the improvement of superconductor thermal stability, and the disturbance length and duration time have a negative effect on the thermal stability, which are physically justified.

Using the elaborated numerical methods, the basic variables characterizing the superconductor stability parameters have been carried out. On the basis of this investigation, a number of general conclusions are drawn. The comparison of the calculated values of the stability parameters with calculated ones taken from the literature is made as well. The comparison shows a reasonable agreement.

1-Introduction

This chapter provides an introduction to the thermal stability of superconducting wires, the concept of superconductivity, superconductor types, and superconductor current and future applications. Superconducting materials can carry current without electrical resistivity, when they are cooled below a critical temperature. Application in power engineering became much more feasible when materials with relatively high critical temperature of 90-120 K were discovered.

1.1 Superconductivity

Superconductivity is the name given to the phenomenon observed when an electric current passes through a material cooled to a temperature below its "critical temperature (T_c)". This observation is that the material conducts electricity without any 'resistance' that is, it conducts without losing any of its electric energy. When electricity flows through a normal wire, it loses a lot of its energy, usually in the form of heat. How much energy is lost depends on the 'resistance' of the circuit. The more the resistance, the more heat is lost.

Toaster ovens, for example, are specifically designed to have a high resistance. In the case of the toaster, however, resistance is the desired effect: if there was no resistance in a toaster, your bread would never become toasted. The energy from the electricity is converted into heat by passing through a section of wires that have a lot of resistance. However, toasters are an exception. Most of the time, one needs to save energy, rather than converting it to heat. This is accomplished by using a superconducting wire. Superconducting wires are those that do not loose any energy to

heat. In other words, they have zero resistance. The problem with superconductors is that they need to be cooled to extremely low temperatures before they will have zero resistance.

1.1.1 Discovery of Superconductivity

The electrical resistivity of some materials becomes zero at low temperatures, defining a state known as superconductivity. In 1911, a Dutch physicist, Karmerlingh Onnes, discovered this condition when he cooled mercury to 4.2 K (the boiling point of liquid helium at atmospheric pressure) and detected no measurable resistance. He later discovered that several other metals, such as lead and tin, also exhibite the same change of state. He designed an experiment to show that energy was not lost when flowing as electricity through a superconductor. He took a ring of wire and placed it in a bath of liquid helium. Next, he started a flow of electricity through the wire, then removed the source of the electricity. Normally, the wire would have almost immediately lost the electric current, but over a year later, still in the bath of liquid helium, he found that the wire still had a current flowing in it that was the same strength as when he first started the current flowing. However, the early superconductors did not promise any practical advantage because they could not carry significant current densities while maintaining their superconducting state. Superconducting material with critical current densities high enough to permit design improvement over the use of normal conductive metals, such as copper, were not discovered for several decades.

The electrical resistivity of all metals and alloys decreases when they are cooled. To understand why this occurs, we must consider what causes a conductor to have a resistance. The current in a conductor is carried by conduction electrons, which are free to move through materials. Electrons have; of course, a wave-like nature, and an

electron travelling through a metal can be represented by a plane wave moving in the same direction. A metal has a crystalline structure with the atoms lying on a regular repetitive lattice, and it is a property of a plane wave that it can pass through a perfectly periodic structure without being scattered into other directions. Hence an electron is able to pass through a perfect crystal without any loss of momentum in its original direction. In other words, if in a perfect crystal we start a current flowing (which is equivalent to giving the conduction electrons a net momentum in the direction of the current) the current will experience no resistance. However, any fault in the periodicity of the crystal will scatter the electron wave and introduce some resistance. There are two effects, which can spoil the perfect periodicity of a crystal lattice and so introduce resistance. At temperature above absolute zero the atoms are vibrating and will be displaced by various amounts from their equilibrium positions; furthermore, foreign atoms or other defects randomly distributed can interrupt the prefect periodicity. Both the thermal vibration and any impurities or imperfections scatter the moving conduction electrons and give rise to electrical resistance.

One can now see why the electrical resistivity decreases when a metal or alloy is cooled. When the temperature is lowered, the thermal vibrations of atom decreases and the conduction electrons are less frequently scattered.

Certain materials, however, show a very remarkable behavior. When they are cooled their electrical resistance decreases in the usual way, but upon reaching a temperature a few degrees above absolute zero they suddenly loose all trace of electrical resistance (Fig. 1.1). They are then said to have passed into the superconducting state. The transformation to the superconducting state may occur even if the metal is so impure that it would otherwise have had a large residual resistivity. The temperature at

which a superconductor looses resistance is called its superconducting transition or critical; this temperature, written T_c, is different for each material.

1.1.2 Type I- Superconductors

The Type I category of superconductors is comprised mainly of pure metals that normally show some conductivity at room temperature. They require incredible cooling to slow down molecular vibrations sufficiently to facilitate unimpeded electron flow in accordance with what is known as BCS theory. BCS theory suggests that electrons team up in "Cooper pairs" in order to help each other overcome molecular obstacles much like race cars on a track drafting each other in order to go faster. Type I superconductors - also known as the "soft" superconductors were discovered first and require the coldest temperatures to become superconductive. They are characterized by a very sharp transition to a superconducting state (see Fig. (1.1)). In normal conducting materials such as copper, the electrical resistance depends linearly on the temperature, (see dash line in Fig. (1.1)). Table (1.1) shows a list of known as Type I superconductors along with the critical (transition) temperature, below which each superconductor will be shifted to the normal state. Copper, silver and gold, are three of the best metallic conductors that do not rank among the superconductive elements. Table (2.2) shows the normal resistivity of various materials.

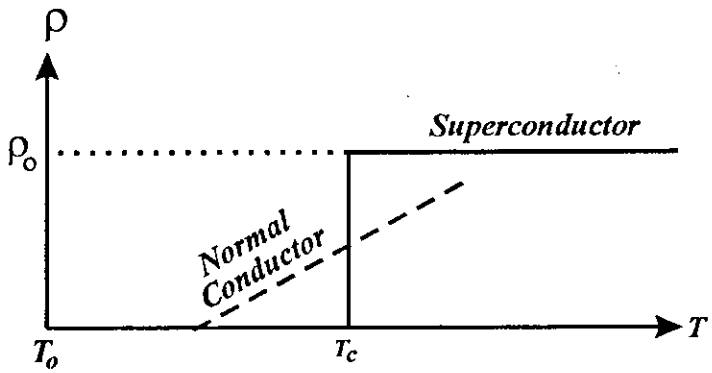

Fig (1.1): Dependence of Electrical resistivity on temperature for type I-superconductor

Table (1.1): Critical temperatures of some type I- superconductors.

Material	**Critical temperature (K)**	**Material**	**Critical temperature (K)**
Aluminum	1.175	Hafnium	0.128
Beryllium	0.026	Tungsten	0.0154
Indium	3.40	Americium	0.6
Lanthanum	4.9	Molybdenum	0.915
Lead	7.2	Gallium	1.10
Mercury *	4.15	Osmium	0.66
Platinum	0.0019	Rhodium	0.000325
Protactinium	1.4	Titanium	0.40
Tantalum	4.47	Zinc	0.85
Thorium	1.38	Uranium	0.20
Tin	3.72	Zirconium	0.61

*First superconductor discovered (1911)

1.1.3 Type II -High Temperature Superconductors (HTS)

In the early 1960s, Nb3Sn and NbTi were found to exhibit superior current-carrying performance even at high magnetic fields. Their critical current densities are greater than those of copper conductor in well-designed water-cooled copper magnets. These superconductors are classified, as type II. Type I and type II superconductors differ in their response to external magnetic fields. Below a critical field, H_{Bc1}, a body of either type will completely exclude the field from its interior while it is superconducting. This behavior is known as the Meissner effect. This effect was discovered in 1933. When a magnetic field surrounds a superconductor it cannot penetrate it, unless the field is strong enough to remove it from its superconductive state. The magnitude of H_{Bc1} varies with material and temperature. Above H_{Bc1} type I superconductors becomes non-superconducting; Type II materials allow field penetration throughout the body while reaming superconducting until the field reaches H_{Bc2}, which is several orders of magnitude greater than H_{Bc1}. Type II superconductors are chatercterised by two critical fields. Magnetic fields weaker than the lower critical field H_{Bc1} are completely excluded from the bulk of the material by superconducting screening currents flowing in a very thin layer at the surface. Magnetic fields between H_{Bc1} and H_{Bc2} penetrate the material in the form of 'flux lines', each carrying the flux quantum of 2×10^{-15} Weber. Both fields depend on temperature and they are zero at the critical temperature. Also,. The transient thermal behavior of high-T_c materials differs from that of low- T_c superconductors. Type I and type II will be completely superconducting at operating temperature below a critical temperature T_{c1} (which is called current sharing temperature in the case of type II and critical or transition temperature in the case of type I). Above T_{c1} type I superconductor becomes non-

superconducting while, type II remains superconducting until the temperature reaches T_c, which is considerably greater than T_{c1}.

High temperature superconducting (HTS) materials are ceramic and therefore brittle in nature. The production of long lengths of wires or tapes suitable for winding magnets has limited the application of high-temperature superconductors. The solutions used in manufacturing high performance superconductors (such as Nb3Sn) are being pursued in the fabrication of HTS wires. Using this approach, filamentary wires (of BSSCO materials) and thin tapes (of YBCO compounds) have been manufactured with properties that approach ideal limit (highly textured or nearly single crystal). BSCCO-2212 shows good inter-grain current transfer even though the inter- grain current density is substantially smaller than that for the YBCO compound and for BSCCO 2223. Although the properties of BSSCO (2212 and 2223 compounds) are exceptional when compared to low temperature superconductors, the properties of YBCO are even better. Indeed, if the magnetic field direction is nearly parallel to the YBCO then the current density of YBCO at high fields (> 10T) and at 77 K approaches that of Nb3Sn at 4 K and 0 T. BSSCO wires also require a large silver fraction, increasing the cost of the wires and decreasing the emerging current density.

The critical current density of type II superconductors varies with temperature and magnetic field. There is a maximum temperature, T_c, as there is a maximum field H_{c2} and with these limits, the materials are in superconducting state. Figure (1.3) shows three-dimensional plots defining the critical surfaces for NbTi and BSCCO-2223 (High temperature superconductors compound of bismuth (Bi). lead (Pb), strontium (Sr), calcium (Ca), copper (Cu) and oxygen (O). –BiPbSrCaCuO- often known by BSCCO-2223, (Mukai H. *et al.*, 1993).

Except for the elements Vanadium, Technetium and Niobium, the type II category of superconductors is comprised of metallic compounds and alloys. The recently discovered superconducting "Perovskites" (metal-oxide ceramics that normally have a ratio of 2 metal atoms to every 3 oxygen atoms) belong to this type II group. They achieve higher T_c's than type I superconductors by a mechanism that is still not completely understood. Conventional wisdom holds that it relates to the planar layering within the crystalline structure. Although, other recent research suggests the holes of hypocharged oxygen in the charge reservoirs are responsible. (Holes are positively charged vacancies within the lattice.) The superconducting cuprates (Copper-Oxides) have achieved astonishingly high T_c's when you consider that by 1985 known Tc's had only reached 23 K. To date, the highest T_c attained at ambient pressure has been 138 K. One theory (Kresin, *et al*, 1998) predicts an upper limit of about 200 K for the layered cuprates. Others assert there is no limit. Either way, it is almost certain that other, more synergistic compounds still wait discovery

. Type II superconductors - also known as the "hard" superconductors differ from Type I in that their transition from a normal to a superconducting state is gradual across a region of "mixed state" behavior called the current sharing region. A type II will also allow some penetration by an external magnetic field into its surface, and type I will not. While there are far too many to list in totality, some of the more interesting Type II superconductors are listed below by similarity and with descending T_c's. Table (1.2) shows the resistivity coefficient of some high temperature superconductor.

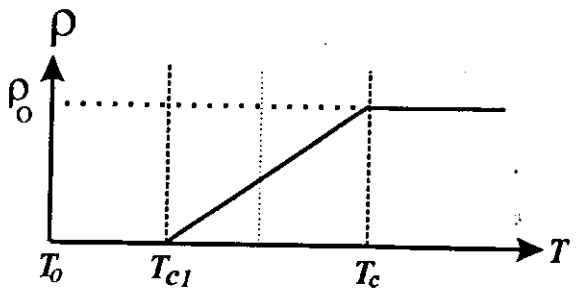

Fig (1.2): Dependence of Electrical resistivity on temperature for type II-superconductor

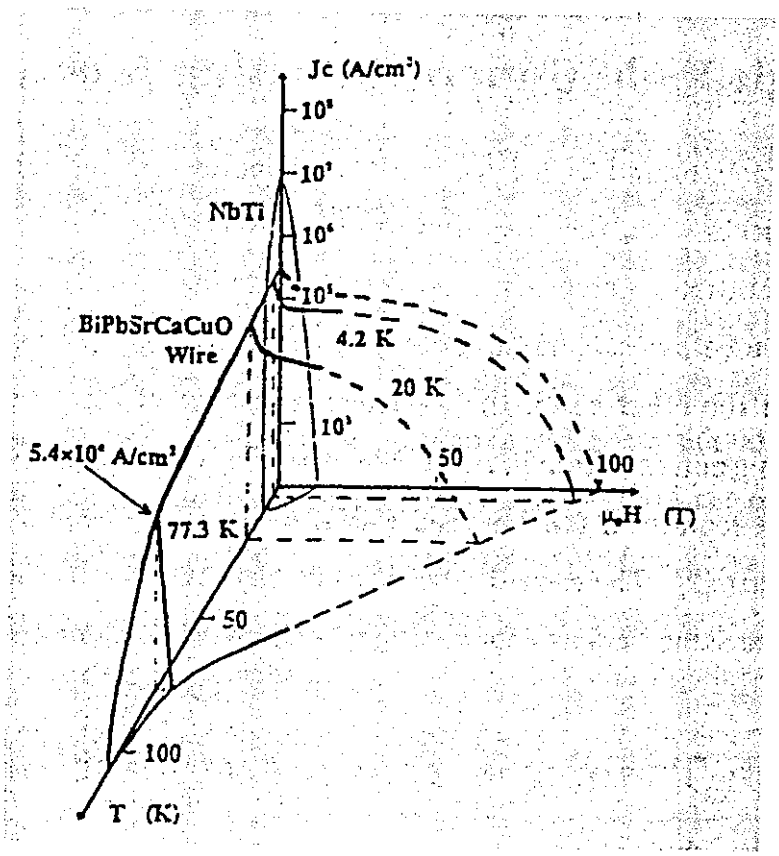

Fig (1.3): Critical surfaces for NbTi and BSCCO-2223 (Mukai et al. 1993)

Table (1.3): Critical temperatures for various high temperature superconductors

Material	Critical Temperature (K)	Critical current A/cm^2
$HgBa_2Ca_2Cu_3O_8$	133-135	272.27
$Tl_2Ba_2Ca_3Cu_4O_{12}$	99	271.96
$Bi_2Sr_2CaCu_2O_9$	110	269.43
$Bi_2Sr_2CaCu_2O_8$	80	269.00
$Ca_{1-x}Sr_xCuO_2$	110	265.97
Nb_Ti	9.8	500000
Nb_3Sn	18.05	255.10
Nb_3Ge	23.2	200000
$YBa_2Cu_3O_7$	90	183.15
Bi-Sr-Ca-Cu-O	105	168.15
Tl-Ba-Ca-Cu-O	125	148.15

The occurrence of superconductivity in high-T_c materials is not yet fully understood. It is not completely explained by the BCS theory, which satisfactorily describes the low-temperature superconductors. Nevertheless the high-T_c materials are known to be type-II superconductors. A magnetic field penetrates a type-II material in

the form of flux lines. Transport current causes a Lorentz force that tends to move the flux lines through the material in a direction perpendicular to the current. This motion is called flux flow and it is a dissipative process. The motion of flux lines corresponds to a change of the internal magnetic field, which causes an electric field according to Faraday's law. The electric field (*E*) increases linearly with the transport-current density. The flux-flow resistivity is usually higher than the resistivity of a good normal conductor. Flux flow is therefore undesirable. The flux lines in high-temperature superconductors are pinned at defects in the crystal structure. At high current densities the flux lines are de-pinned and flux flow is observed. The critical-current density is determined by the density of the pinning centers and by the strength of the pinning forces.

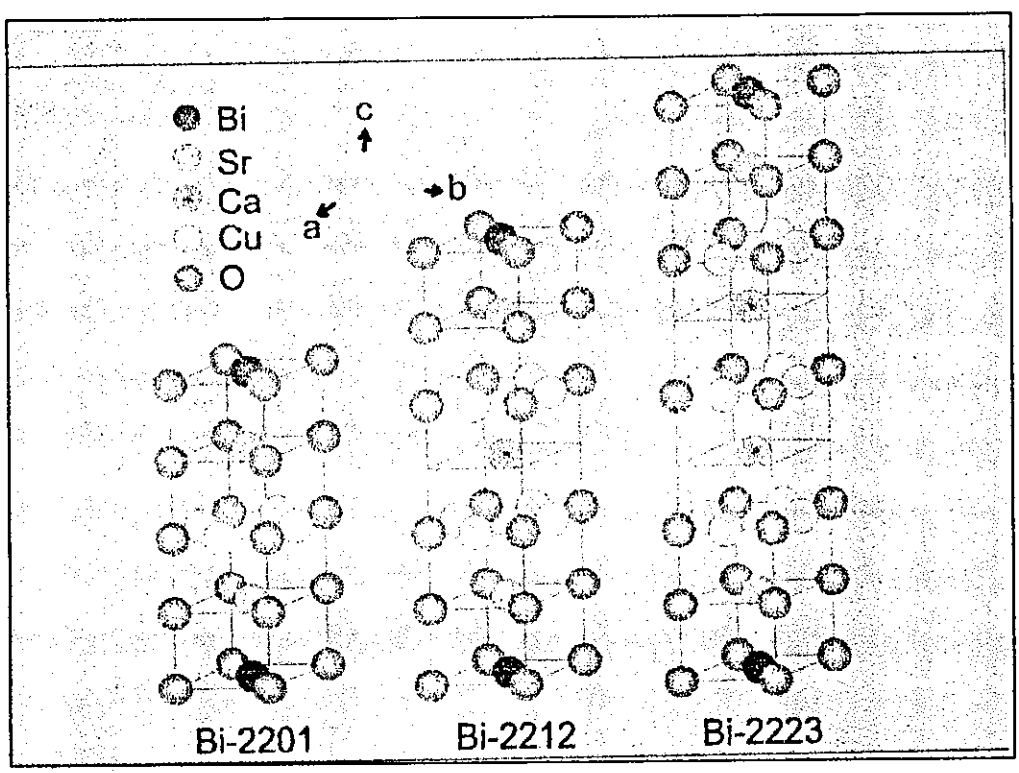

Figure (1.4) Unit cells of three different Bi-compounds.

1.1.4 Applications of Superconductivity

With the discovery of higher temperature superconductors, a wide variety of uses have been devised to use this new technology. Most of this technology is still being worked on, but a few uses are in effect today. The superconductor applications may be classified as current uses and future uses. The *current uses of superconductivity are*:

a) (Magnetic Resonance Imaging) MRI: The MRI is commonly found in hospitals, where it is used to obtain detailed images of the insides of patients. With the advent of superconductors, this can be done without exposing the patient to X-rays or having to inject them with some kind of dye. Because MRIs use low temperature superconductors, this process is very expensive. When higher temperature superconductors take their place in the MRI, this process will become more affordable and may some day do away with X-rays. As of now, the MRI is considered the most successful use of superconductors.

b) Josephson Junctions: This is a device made up of two superconductors with a thin oxide barrier between. This device is extremely sensitive to magnetic fields and may soon be used in a variety of devices.

c) (Superconducting Quantum Interference Device) SQUIDs: This device uses two Josephson Junctions to create a device that is very sensitive in measuring magnetic fields. SQUIDs are used to monitor electromagnetic signals generated by the brain. The U.S Navy uses these SQUIDs to detect submarines and mines in the ocean.

The expected future uses of superconductivity may be summarized as:

a) Computers: The miniaturization and increased speed of computer chips are limited by the generation of heat and the charging time of capacitors due to the resistance of the interconnecting metal films. The use of new superconductive films and Josephson Junctions may result in more densely packed chips, which could transmit information

more rapidly. The Josephson junction is capable of switching 100 times faster than a transistor.

b)Nuclear Fusion: Scientists hope that in the future, powerful superconducting magnets will allow the use of Fusion as a primary power source across the world. Fusion reactions are so violent that as of now, they cannot be contained. Physicists hope that future superconducting magnets will be capable of generating magnetic fields that can contain fusion reactions.

c)Generators: One benefit of superconductors might be in power systems. Generators wound with superconductors rather than conventional copper wire could generate the same amount of electricity with smaller devices and less work.

d) Maglev trains: While these are not in common use today, a major railway system is being built in Japan that will allow the train to hover off of the ground because of superconductors, thus doing away with some of the friction.

e) Transmission Cables: Transmission cables may be created that could carry a current without energy loss. This will increase the capacity of the transmission system, saving money, space, and energy.

f) Superconducting Super Collider: This consisted of an oval ring 52 miles around, precise in all of its dimensions with in a thousandth of an inch. Two beams of protons, guided by magnets would race around the giant ring in opposite directions at very nearly the speed of light, then steered to a head-on collision. This would possibley recreate the state of the universe just after the Big Bang. This plan was interrupted part way through because the U.S. decided to stop funding. Many scientist hope that in the future, the Superconducting Super Collider will be finished.

Of course there are many other ways in which superconductors will be able to benefit society. Once superconductors with higher critical temperature have been found, many of today's ideas will turn into reality.

1.2 Thermal Stability of Superconductors

Thermal stability denotes the case of self-recovery of a superconducting state after a quench. Therefore, superconductors must operate at a low enough temperature so that the critical current (which is also determined by the operating field) is larger than the operating current. Operating under the critical current does not guarantee stable operation in the superconducting state. There are inevitably random points of localized heat dissipation throughout a superconductor when it is carrying current. These may heat small regions into the normal state. Heat dissipated by normal region will spread and drive adjacent conductor to normal state. In essence, the normal region grows. This event is called as normal zone propagation (NZP), or quench propagation. It is the main thermal behavior of superconducting magnets driven normal. We can protect against random disturbances by embedding the superconductor in a conductive metallic matrix, referred to as a stabilizer, this allows the current to flow around a small normal region with only a small increase in voltage. Also, the high thermal conductivity of the metal matrix will conduct heat away from a normal zone and bring it back into superconducting state. However, the stabilizer can not prevent magnets from quenching from all sources of heat dissipation. For example, mechanical disturbances, such as epoxy cracking under changing stress, can cause a large enough thermal power input to propagate a quench in a superconductor with stabilizer. We require a theoretical basis for designing superconducting magnets that will ensure stable operation. Stekly (1968) first proposed the concept of cryostability, where the normal state Joule heating is

balanced by convective cooling by a liquid cryogen, making the normal zone propagation impossible. However, cryostability criterion is the extreme of conservative design. All superconducting magnets may be operated in a stably manner with higher current densities. In this study we will use the history of superconductor maximum temperature as a stability criterion

In this thesis, we study the thermal stability of type I and type II superconducting wires operating dry. Dry operation means there is no cryogen in contact with the conductor and the wire operation is adiabatic. Also, consider the laterally cooled wire is considered. The study will be based on three different macroscopic conduction model, which are: the diffusion model (classical Fourier's law), the wave model and the dual-phase-lag-model. If we were to use cryostability as a stability criterion, the adiabatic superconducting wire will be unstable because the cooling term is zero. In practice, adiabatic superconductors may operate in a sable state even with higher stability compared to cryostable one due to the absence of cooling channels within the wire.

1.2.1 Initiation of Normal Zones

There are many postulates for the mechanism by which a normal zone is created in superconducting wires. Since the superconducting state is defined in terms of the temperature, magnetic field and the current density, a variation that cause any of these parameters to exceed the critical value could cause a normal zone to develop. Another equally important source of disturbances is the Lorentz force (IxH_B) on the conductor which cause brittle fracturing of the epoxy and conductor notion. These disturbances can occur anywhere in the winding or encompass the entire coil. In all cases a disturbance can be thought of as being a sudden release of energy which heats the

conductor. Not all disturbances, though, cause a quench. Critical energy density is required to create a normal zone, which will grow with time. The initiation of the normal zone is, however, of secondary importance to the problem of quench to lead to a quench of the magnet system.

1.3 Goals of This Thesis

The specific goals of this thesis are:

- Investigate the behavior and the thermal stability of a wire type superconductor based on one-dimensional, transient heat diffusion equation (i.e. the parabolic one step model). The transverse heat loss will be taken into account by introducing the convective term in the energy equation, while the temperature will be assumed to be radically lumped. In this thesis we will consider superconductor wire subjected to a centrally located, finite, and linear disturbance heat source. The centrally located heat source is considered because such a heat source results in the largest possible normal zone, as heat needs to diffuse the maximum distance in order to dissipate through convection on the surface.
- The entire work in item one above will be repeated based on the hyperbolic one-step model and its extension dual phase lag model.
- The stability criterion will be derived numerically based on the above analysis. This criterion determines the maximum allowable Joule heating (from which we can calculate the critical current density for a certain superconductor), and the critical disturbance strength that ensure stability. This criterion will be based on the time behavior of the maximum temperature of the superconductor. If the maximum temperature of the superconductor drops below the critical value, then the normal

zone will collapse and the superconductor is stable. Whereas, when the normal zone grows with time, the superconductor will not be stable.

- Investigate the effect of several designs and operating parameters on the superconductor thermal stability. These parameters include the Joule heating, the lateral cooling, the current sharing temperature and the disturbance characteristics such as intensity, length, and duration time.
-

1.4 Organization of Thesis

This thesis covers the theoretical investigation of superconductor thermal stability based on the three different macroscopic heat conduction models. Chapter 1 introduces the principles of superconductivity and the different types of superconductors. Chapter 2 is a literature review, which covers much of the history of superconductor thermal stability research. The conclusions from these literatures are pointed out.

In chapter 3 formulation of the governing equations for the superconductor thermal stability based on the different three models is presented. Also, the superconductor thermal stability criterion is derived based on the time histroy of conductor maximum temperature.

In chapter 4 the investigation results obtained based on the former macroscopic heat conduction models are presented and discussed.

Chapter 5 presents a brief summary on the main conclusion of this thesis and recommendation for further works. Then at the end of the thesis the references and the program listing are presented.

2-Theoretical Background

2.1 Introduction

Thermal stability is one of the major issues in the design of superconducting devices, which may be used in electronic applications and in electric power transmission cables. These devices must be designed in such a way that they are stable against thermal disturbances. Thermal stability denotes a situation where a superconductor can carry the operating current without resistance at all times even if a localized thermal disturbance has been released.

A superconductor is considered stable if it does not quench when it is exposed to a disturbance; i.e. performs an undesirable phase transmission from superconducting to normal conducting state. For example, a tiny conductor motion of only a few micrometers can initiate a quench in high current density magnet. Other examples of disturbances are: absorption of particulate or infrared radiation or short-term failures of cooling. Disturbances immediately transfer into heat pulses that increase the temperature of the superconductor, which in turn reduces its critical current density. As a result, the transport current can become greater than the critical current, locally or over the whole superconductor cross-section, which would send the superconductor into the resistive state. The absence of thermal stability increases the superconductor temperature, and creates a state of Ohmic resistance within the superconductor Quenching may thus cause damage to the superconductor by Joule heating.

The electrical resistivity of a superconductor vanishes below its critical temperature, T_c. At temperature immediately above T_c, the resistivity jumps to a finite level, so the superconductor returns to its normal (i.e. resistive) state. At subcritical temperatures ($T < T_c$) the superconductor can carry very large current without any

resistive heating (Joule heating), while at supercritical temperatures ($T > T_c$), this current causes Joule heating which may damage the superconductivity of the wire.

Unfortunately, the disturbances can locally raise the temperature to supercritical levels ($T > T_c$). This possibility leads to the importance of the superconductor's stability. Superconductor thermal stability implies that the superconductor temperature must drop below its critical temperature if a thermal disturbance of any kind raised its temperature. This can be achieved by cooling the superconductor by axial or transverse conduction through the cold superconducting surrounding material. Other mechanisms of superconductor cooling are to convect heat to the surrounding fluid or to use heat sink within the superconductor domain.

It is an engineering discipline emerging from the need for design of superconducting devices that operate safely under practical conditions. The problem of thermal stability of superconductors has its roots in the monotonic decrease of critical current density with temperature. The theory of thermal stability is concerned with the predictions of consequences of thermal disturbances and their effects on the performance and safety of superconductors.

Using superconductors of very small sizes leads to unique electrical and thermal phenomena. The presence of high electrical fields energizes the electrons and throws them far from equilibrium with lattice. This makes heat generation a non-equilibrium process; this process is treated in the literature using different models. These models will be discussed later. In heavy-duty applications (such as power transmission), the disturbance may lead to a very high heating rate, which indeed increases the significance of the wave behavior of the heat conduction. In this work, the wave behavior model of the heat conduction (i.e. the classical hyperbolic one-step model) and the dual-phase-lag model will be considered to investigate the thermal stability of the

superconductor. All reported similar analysis has been based on the diffusion behavior (Fourier's law) of the heat conduction. Thus, the problem that will be considered in this study is the effect of applying the wave and the dual-phase-lag model to the superconductor thermal stability.

The present analysis considers a bare superconductor wire subjected to a centrally located thermal disturbance of finite width, and a finite duration time as shown in Figs. (3.2) and (3.5).

2.2 Literature Review

This thesis involved theoretical analysis of a superconductor wire thermal stability based on different macroscopic conduction models. Therefore, an extensive review of the literature was performed focusing on many different case studies. The references are organized at the end of this thesis. Following is a summary of some of the more interesting and/or germane results found relative to this investigation.

Low-temperature and high temperature superconducting magnet design is a field that has matured, partially through the process of having some spectacular failures, (Buckel, 1991) and (Wilson, 1983). Although the science of high temperature superconducting (HTSC) coil design is still in its infancy, there have been several attempts to build prototype of HTSC coils to determine how close to design limits these coils may be operated. A literature review was performed prior to the thermal analysis of superconductor wires in order to determine the state-of-the-art, and, more importantly, to gain understanding of some analysis shortage that have been made previously.

The papers reviewed focus on many unique features of HTSC wires as compared to their low temperature superconducting (LTSC) counterparts, are included:

The current state-of-the art for HTSC is a silver-sheathed tape form. Therefore, standard coil winding techniques, which rely on wires of round or square cross section, may not be used. Nb-Ti low temperature superconductor is available in round wire geometry, and standard coil geometry may be used.

While all superconductors' critical current densities (Jc) are degraded by applied magnetic field, HTSC is anisotropic in that regard. The Jc is degraded more by an applied field perpendicular to the wide tape surface than a field parallel to the tape. The degradation may be anisotropic by a factor of 10 to 1 or more. The effect is more pronounced at higher temperature than lower temperature, (Bellis and Iwasa, 1993).

HTSC tape is much less prone to degradation in critical current density Jc due to flux jumping because of the higher heat capacity of the material, (Wipf, 1978)

While low temperature superconducting magnets may be made self-protecting (that is, if the magnet quenches, the normal zone propagates quickly and the magnet energy is dissipated through the whole magnet volume) the slow thermal time constant in HTSC coils precludes self-protection. Therefore, active normal-zone detection and protection is warranted for large coils. Sensing voltage taps may be placed inside the magnet winding to sense normal regions, (Zhao and Iwasa, 1991).

The critical current density J_c is more affected by tensile and compressive strain in HTSC than in LTSC. While Nb-Ti wire may be strained up to 1% with no significant affect on J_c, strains in HTSC must be kept $e < 0.2$-0.4% or so, (Deviatkin, 1997) or significant degradation occurs. Furthermore, HTSC wire may be irreversibly damaged by strains in excess of a few tenths of a percent. This means that practical HTSC coils must be designed with a minimum bend radius of a few centimeters. If higher strains are necessary, the wind-and-react method may be used where the coil is

wound with unreacted superconductor, and heat-treated after winding, (Nakagawa and Umeda, 1996).

The thermal behavior of superconductors is treated in the literature based on diffusion heat conduction model. A summary of these works will be presented below. In the literature, there are basically four models that describe the mechanism of heat conduction in very thin films or during short-pulse laser heating. So far, the only application that involves very fast heating is found in laser heating applications, (Al-Nimr and Arpaci, 1999 &2000). The first model is the parabolic one-step model, which is based on the classical Fourier conduction law. This model assumes that the solid lattice and electron gas are in local thermal equilibrium and that heat flux merges instantaneously when temperature gradient exist. The expression electron gas is a terminology to describe the thermal behavior of the electrons. The second model used is the hyperbolic one-step model, (Al-Huniti and Al-Nimr, 2000), and (Al-Nimr *et al.* 2000) Basically, the hyperbolic one-step heat conduction model consists of two models: the classical hyperbolic heat conduction model and the dual-phase-lag model, (Al-Nimr and Al-Huniti,. 2000). The classical hyperbolic one-step was first postulated for gases by Maxwell in 1867, and developed for electron gas by other workers (Kim *et. al* 1990) and (Chen *et al.* 1994). In this model, it is assumed that both lattice and electron gas in local thermal equilibrium, while the heat flux (the effect), and the temperature gradients (the cause) across a material volume occur at different instant of time. The time delay, between the heat flux and the temperature gradient is the relaxation time (0.1 ~ 1 ps). The dual-phase-lag model was proposed by (Tzou, 1995 a to c). The dual-phase-lag model allows either the temperature gradient (the cause) to precede the heat flux vector (the effect) by time τ_q, or the heat flux vector to precede the temperature gradient by time τ_T, in the transient process. For the case of $\tau_q > \tau_T$, the temperature gradient

established across a material volume is a result of the heat flow, implying that the heat flux vector is the cause and the temperature gradient is the effect. For $\tau_q<\tau_T$, on the other hand, heat flow is induced by the temperature gradient established at an earlier time, implying that the temperature gradient is the cause, while the heat flux is the effect. The third and the fourth models are the parabolic and the hyperbolic two-step models (Al-Nimr. and Arpaci, 1999 & 2000), (Al-Nimr *et al.* 1999), (Qui and Tien, 1992), (Tzuo *et al.* 1994). In these models, it is assumed that solid lattice has different temperature than electron gas and the difference between these two temperatures depends on the coupling factor between both domains. The coupling factor represents a sort of heat transfer coefficient between the electron gas and the solid lattice. However, in the parabolic two-step model, it is assumed that both heat flux and temperature gradients are local in time. This means that heat flux in electron gas merges instantaneously as the temperature gradient in the electron gas exist. While the hyperbolic two-step model, which has been proposed by (Qui and Tien, 1998), assumes that the flux and the temperature gradient are non-local in time, i.e. the heat flux lags the temperature gradient by a thermal relaxation time. Microscopic analysis is carried out when the temperature of the electron gas and the solid lattice are not equal, then two energy equations one for the electron gas and the other for the solid lattice must be derived. While the macroscopic model is adopted, when both electron gas and solid lattice has the same temperature. The microscopic mechanisms of energy deposition become important when the material thickness is very small or the heating process is relatively fast.

Most previous analytical works of superconductors thermal stability considered the one-dimension heat diffusion equation (i.e. the parabolic one-step model) in the longitudinal direction based on the assumption of uniform temperature in the transverse

direction (Bejan and Tien, 1978). Stability concerned with normal zone behavior in transverse direction has seldom been studied. Stekly and Zar, (1965) presented a criterion for cryogenics stability of a one-dimensional composite superconductor. They performed a balance between generation of heat by Joule heating and the heat transfer to the cryogenic coolant. If the latter exceeds the former, the composite superconductor is completely stable. Maddock *et al.* (1969) proposed a criterion that includes the effect of axial conduction and the temperature dependence of cryogenic heat transfer coefficient. Both of these studies considered the long-time behavior of normal zone employing steady state analysis. Bejan and Tien, (1978) removed this constraint and investigate cryogenic stability accounting for small-time transient behavior of the normal zone. All of these three stability criteria assume the existence of a normal zone that produces Joule heating within the composite superconductor. Then they examine the conditions under which this normal zone grows or collapse. The cryogenic stability criteria developed for this case predicts whether this normal zone grows or collapses. In superconducting composite superconductor filament are embedded in a metal matrix of copper or aluminum. When the filaments become normally resistive due to the thermal disturbance, the current is shared the filaments and the matrix, The electrical conductivity of the matrix greatly reduce the Joule heating and have a strong stabilizing effect.

In constract, intrinsic thermal stability refers to a situation where the thermal energy initially deposited diffuse to the boundary of the superconductor without the occurrence of Joule heating at any time (Flik and Tien, 1990). The superconductor is able to carry the operating current without resistance at all times, although its superconducting capacity is reduced due to temperature field developed as a consequence of heat diffusion. There is no negative effect if a composite

superconductor is not intrinsically stable, as long as it is cryogenically stable. On the contrary, if a thin-film pure superconductor is not intrinsically stable, the ensuing Joule heating is likely to destroy the film due to the resulting high temperatures. The comparatively strong Joule heating is due to the high normal-state resistivity of the superconductors, in particular for the ceramic material. They pointed out that the stability criterion should be based on the consideration of intrinsic stability. They considered the criterion of intrinsic stability of a thin-film superconductor subjected to a heat release from a centrally located line heat source. Their analysis was based on the parabolic one-step model, and they did not include the heat transfer in the transverse direction. They presented a numerical analysis for the maximum operating current density that ensures intrinsic stability.

Ünal *et al.* (1993) investigated thermal stability of an infinite length film superconductor by considering the influence of thermal disturbance from centrally located line heat source. They solved the heat diffusion equation, in the axial direction, analytically through separation of variables. They also addressed the issue of recoverability of a quench superconductor, and studied the recovery mechanism based on the instability parameter, cryogenic cooling rate and Joule heating rate. Their analysis was conducted based on one-dimensional heat diffusion equation (i.e. parabolic one-step model).

Soel and Chyu, (1994) investigated the formation of normal cross-section subsequent current sharing with the stabilizer and the possible recovery of superconductivity for a composite superconductor. They studied the stability of the superconductor by considering the transverse normal behavior subjected to an instantaneous thermal disturbance. They developed a stability criterion based on heat

diffusion analysis. They found that quenching is less likely with smaller current density or a thicker stabilizer.

Ito *et al.* (1992) introduced a numerical analysis of the thermal stability of a superconductor cooled by forced-flow helium. Their analytical model was consists of simultaneous two-dimensional coolant flow equations and one-dimensional heat diffusion equation for the superconductor. They found that the stability limit increase with an increase in the Reynolds number and the diameter of the coolant passage, and with a decrease in the helium temperature and transport current.

Ünal and M. -Chyu (1995) investigated the behavior of a wire type superconductor subjected to an instantaneous thermal disturbance, characterized by a linear heat source of finite length. Their analysis was based on the two-dimensional one-step heat conduction model with or without volumetric heating. They presented numerical results for NbTi superconductor, and developed a stability criterion with regard to different modes. They found that the critical current decreases with both the heat source strength and length, and increase with the conductor diameter.

Wetzko *et al.* (1995) presented a full three-dimensional, numerical analysis of transient fields of Bi-2223/Ag high temperature superconductor. Their analysis was based on the one-step heat conduction model, and they considered a single (point-like) or extended thermal disturbance of finite duration. They concluded that the anisotropy of thermal conductivity has an influence on the intrinsic stability. The higher the anisotropy, the lower the critical current density.

Buznikove *et al.* (1995) Studied the quench process in a superconductor carrying a varying transport current. They obtained an analytical results of the quench process. Their analysis was based on the one-step heat conduction model, ignoring the connective heat to the surrounding medium in the transverse direction. They concluded

that when the current is diminishing at very low rate, the normal zone does not appear so the wire remains stable.

Takehiro and hiromi (1996) investigated numerically the thermal stability of pool-cooled superconductor based on the one-step heat conduction model. They considered a disturbance, which take a space-wise and a time-wise rectangular shape. Their main conclusion of their study was the importance of taking into account the space-wise and the time-wise of the disturbance distribution.

Malinowski (1993) presented a numerical analysis of evolution of normal zones in a composite superconductor based on one dimensional heat conduction equation which take into account the finite speed of thermal wave propagation (i.e. the classical hyperbolic one-step model). In this analysis, the transverse conduction and the convection loss to the surrounding were ignored. He concluded that the temperature profiles obtained from parabolic model and relaxation model of the normal zone could differ considerably particularly with a temperature dependent heat source. He did not address the thermal stability issue. His study was concentrate on the difference between the temperature profile obtained based on diffusion and hyperbolic models.

Romanovskii (1998) investigated the thermal stability of superconducting wire for a finite thermal disturbance at various external magnetic field inductions and intrinsic critical temperatures of superconductor. He found that the cooled superconductor can have no region of full stability over the whole magnetic field various (from zero to critical field).

Malinowski (1999) presented an analytical method for calculation of critical energies of uncooled composite conductor, based on the transient diffusion model. In his model, the dependence of ohmic heat generation on temperature as well as the finite duration and the finite length of thermal disturbances are taken into account while the

thermo-physical parameters of the conductor are assumed to constant. Critical energies determined on the basis of analysis of the time-dependent maximum temperature in the normal zone.

Lehtonen *et al.* (1998) studied thermal stability of Bi-2223/Ag multifilamentary composite conductor against transport current ramps. Their model was based on the two-dimensional; magnetic diffusion and the parabolic heat conduction equations. They obtained a numerical solution for the temperature using thePDE2D software, which is a part of FlexPDE software used in this thesis to solve the hyperbolic wave and dual phase-lag equation.

Abeln *et al.* (1991) studied the stability consideration for design of high-temperature superconductors. Their results demonstrate that the calculation of transient temperature history of superconductor after a thermal disturbance as will as knowledge of the magnitude of this disturbance is necessary when designing a conductor for a particular application. Their analysis shows that the application of simple stability criterion is not sufficient for conductor design.

All previous studies of superconductors thermal stability ignored the wave behavior of the heat conduction (i.e. they used the classical hyperbolic one-step model), and they ignored relaxation time between the temperature gradient. Also they considered the one-dimension heat diffusion equation (i.e. the parabolic one-step model) in the longitudinal direction based on the assumption of uniform temperature in the transverse direction. So this work will concentrate on the wave behavior using the classical hyperbolic one-step model, and dual-phase-lag model.

3-Theoretical Analysis and Governing Equations

3.1 Normal Zone Propagation

The design of superconductor wires has undergone a dramatic progress in the last three decades. Since the discovery of high field superconductors, the desire to create magnets, which generate higher and higher fields, has lead to larger stored energies in the systems and increased concern for the protection of the system from catastrophic release of energy. If a coil with a large stored energy suddenly went to normal state, the consequent release of energy could result in the destruction of the coil and its surroundings. Several design steps have been taken to increase the stability of the magnets and also to control the effect of a quench. One of the important steps is the use of a composite conductor consisting of superconductor surrounded by conductive metal matrix (such as copper or silver) (Stekly and Hoag, 1968). The matrix serves multiple purposes: It provides a conductive path when superconductor operating in normal state, helps maintain a uniform temperature across the conductor cross-section, and promotes thermal diffusion along its length. This is because in the normal state, the resistivity of superconductors is about 1000 times higher than the copper. Since 1966, the use of superconducting wires in a copper matrix has become a standard practice. Further refinement in conductor technology has lead to a composite superconductor with hundreds or thousands of fine filaments of superconductor in a copper or copper alloy matrix. Typical cross section of superconducting wire is shown in Fig. (3.1).

When a superconducting magnet operates below its critical temperature, T_c, the transport current flows entirely through the superconducting filaments, creating minimal heat dissipation. However, if an external energy source causes additional heat dissipation in a localized region, the temperature in that region will rise and the critical

current decreases. Given a large enough heat input, the temperature will enter the current sharing region (a region in which the current flows in both of the superconducting material and metal matrix) at T_{cl}, where the operating current is less than the critical current. At this point, the operating current redistributes itself. The current in excess of the critical current flows through the matrix. Virtually all the current shifts from the superconductor into the metal matrix within the normal zone. This limits the Joule heating and thus reduces the temperature rise within the section. Current flow through the matrix causes Joule heating which may continue to increase the temperature, and decrease the critical current if the heat is not conducted away by the matrix fast enough. If the region is recooled, the quench "recovered". If the temperature of the heated region climbs indefinitely, a normal zone propagates into the superconducting zone of the wire. Whether the quench recovers or propagates depends on the size of the heated region, the initial heat input, thermal properties of the conductor and the insulation, and the operating conditions such as transport current, temperature and field. If the normal zone propagates, the conductor temperature can continue to rise unless the current is shut-off. Therefore, we require an accurate model on the normal zone propagation for designing the protection of superconducting systems. Normal zone propagation is a thermal event that may be modeled using the transient heat conduction equations. Thorough works have been performed over the last three decades to model the normal zone propagation in low-T_c superconductors. For these superconductors, the operating temperature T_0, are typically only few Kelvins below the critical temperature, T_c. Since the transition zone between the fully superconducting and fully normal zone is small, the normal zone propagation may be represented by the propagation of a boundary between superconducting and normal zones, as shown in Fig. (3.2).

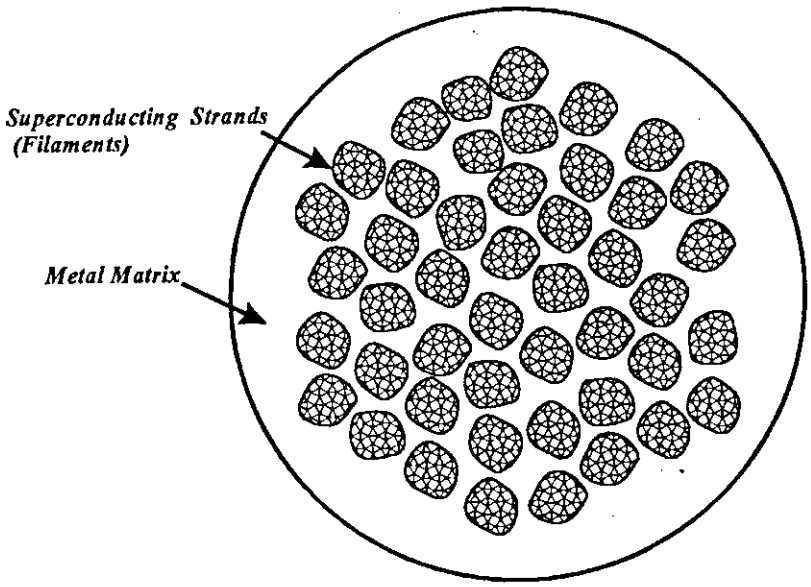

Figure (3.1): Cross section of composite superconductor wire shows filaments of superconductor surrounded by metal matrix.

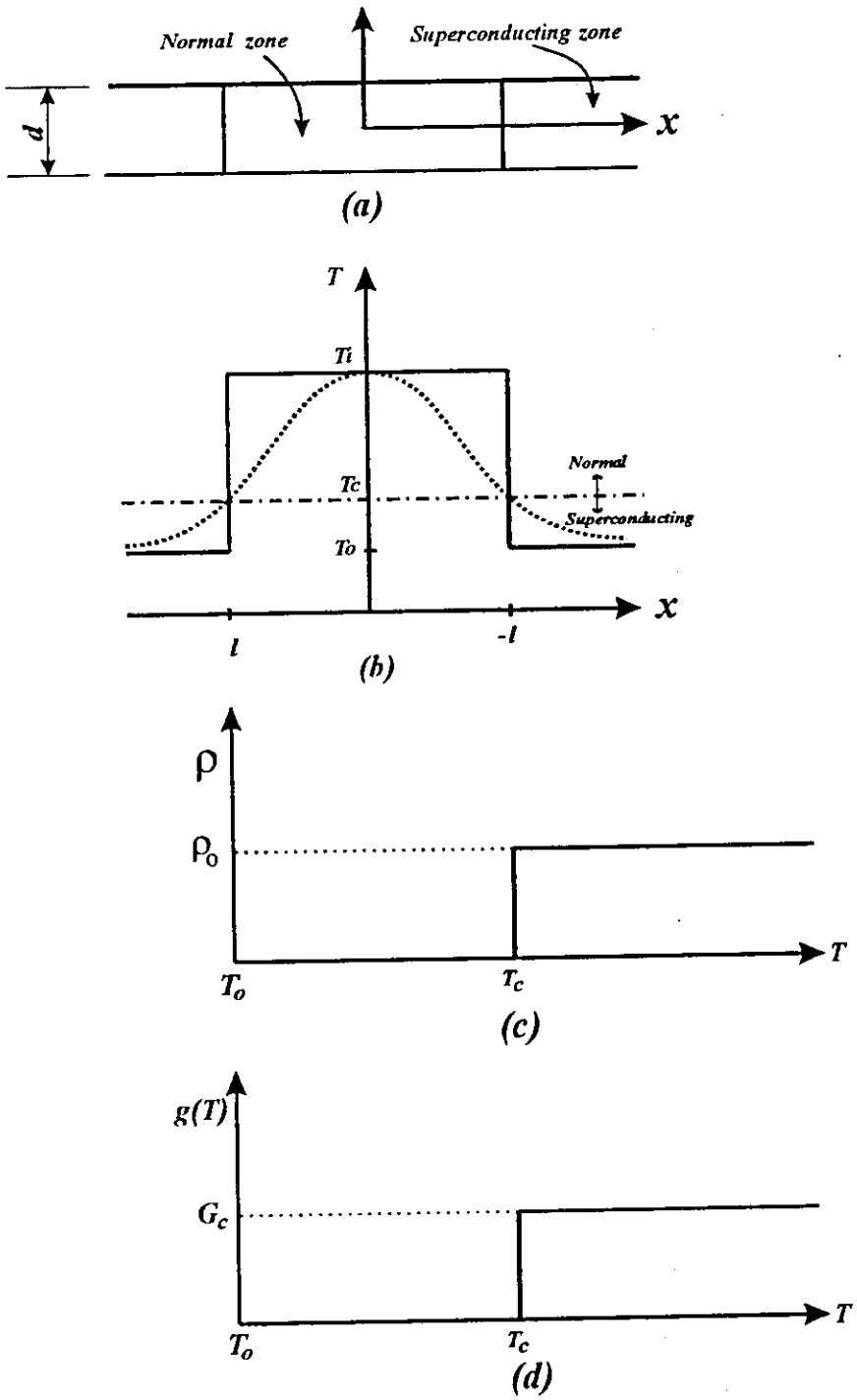

Figure (3.2): Model for type I-superconductor. (a) The different zones of the wire, (b) The initial temperature in the conductor (____) stepwise disturbance and (_ _ .) Gaussian Disturbance (c) The dependence of electrical resistivity on temperature. d) The dependence of Joule heating on temperature.

3.2 Current Sharing and Composite Generation

An important complication introduced into the thermal stability analysis because of the composite nature of magnet conductors is the existence of current sharing between the fully superconducting and fully normal states. Since the conductor transport current cannot shift abruptly from the superconductor to matrix during a quench, there exists a finite length of conductor where current flowing in both regions, as shown in Figs. (3.3), (3.4) and (3.5). This region is referred to as current sharing region. The length of this region is dependent on two factors: 1) the temperature gradient along the conductor, and 2) the absolute temperature range over which current sharing is possible for that particular superconductor. This second factor is in turn dependent on the slope of current versus temperature curve for a given superconductor. It is worth to know that, since the slope of current versus temperature curve is always negative, regardless of particular superconductor, all composite conductor undergoing a quench will experience current sharing over at least a small length of conductor.

It is shown in Fig. (3.3) that as long as the conductor temperature is below T_{cl}, the current sharing temperature, the conductor will be fully superconducting and there will be no heat generation since non-of the transport current is flowing in the matrix. At T_{cl}, is exactly equal to the conductor critical current corresponding to T_{cl}, the current sharing temperature, the conductor will be fully superconducting and there will be no heat generation since non-of the transport current is flowing in the matrix. Above T_{cl}, the superconductor carries $I_c(T)$, which is less than I_t and decreases with temperature. The excess current flows through the matrix I_m. Thus as T is increased above T_{cl}, the superconducting current I_{sc} must decrease and the matrix current, I_m must

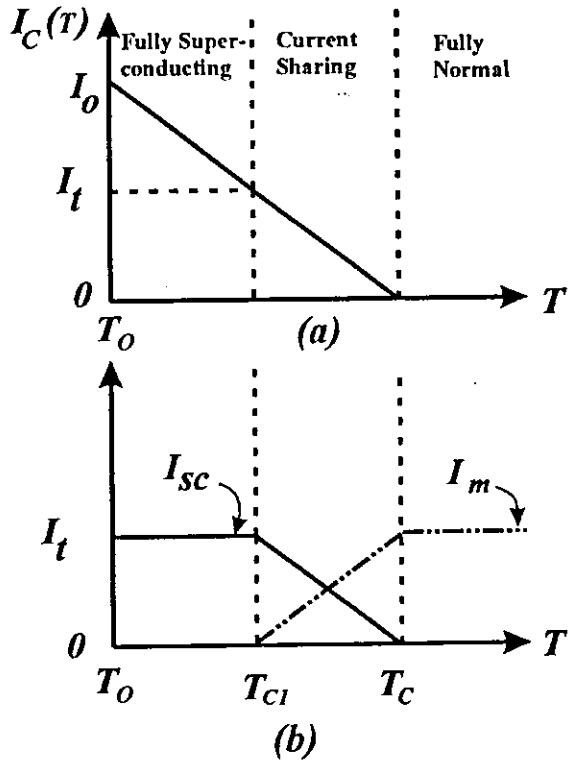

Figure (3.3): a) Upper plot shows a critical current versus temperature curve approximated by a straight line. b) Lower plots show I_{sc} (———) and I_m (— . . —) as conductor temperature increased from T_{c1} to a temperature above T_c.

increase. At the critical temperature and beyond, virtually all the transport current flows in the matrix because the matrix resistivity is much smaller than the superconductor resistivity at normal state. Thus, for temperatures above T_c, $I_m \approx I_t$ and $I_{sc} \approx 0$.

The effect of current sharing is most prominent on the generation term. In non-composite conductors, as soon as the temperature rises past the transition temperature, T_t, the Joule heating will jump to a constant value $G_c=\rho_o J^2$. Where G_c depends only on the transport current, which is assumed to be constant. This is shown in solid line of Fig. (3.4). Note that for the non-composite conductor there is no current sharing temperature and the transition from superconducting to normal zone occurs at T_{ct}.

$$g(T)=\begin{cases}0 & for \quad T<T_{c1}=T_t \\ \dfrac{G_c}{p} & for \quad T\geq T_{c1}=T_t\end{cases} \qquad (3.1)$$

The derivation of equation (3.1) will be presented at the end of this section.

By the phenomenon of current sharing, instead of one critical temperature T_t, there are two critical levels T_{c1}, and T_c, the resistivity increasing linearly from 0 at T_{c1} to ρ_o at T_c. Thus, for composite superconductor the source term varies linearly with temperature, in the current sharing region.

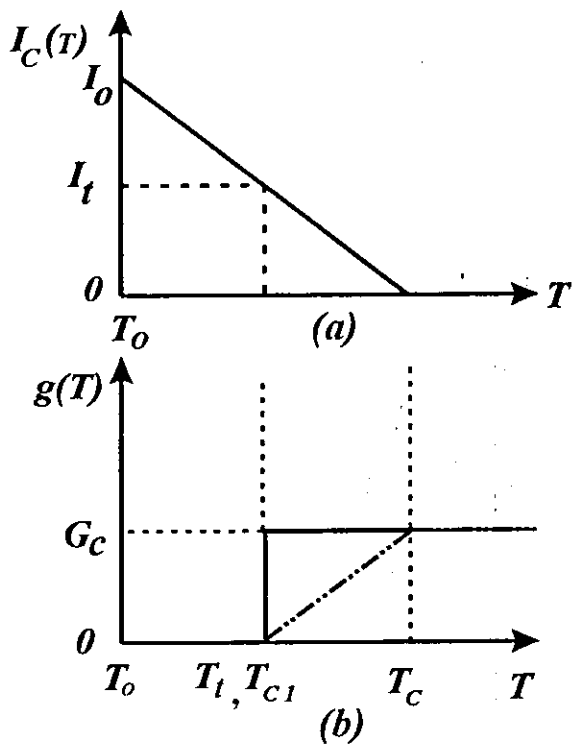

Figure (3.4): For same $I_c(T)$ given in figure (3.3), power generation (Lower plots) for non-composite(———) and composite (— · · —).

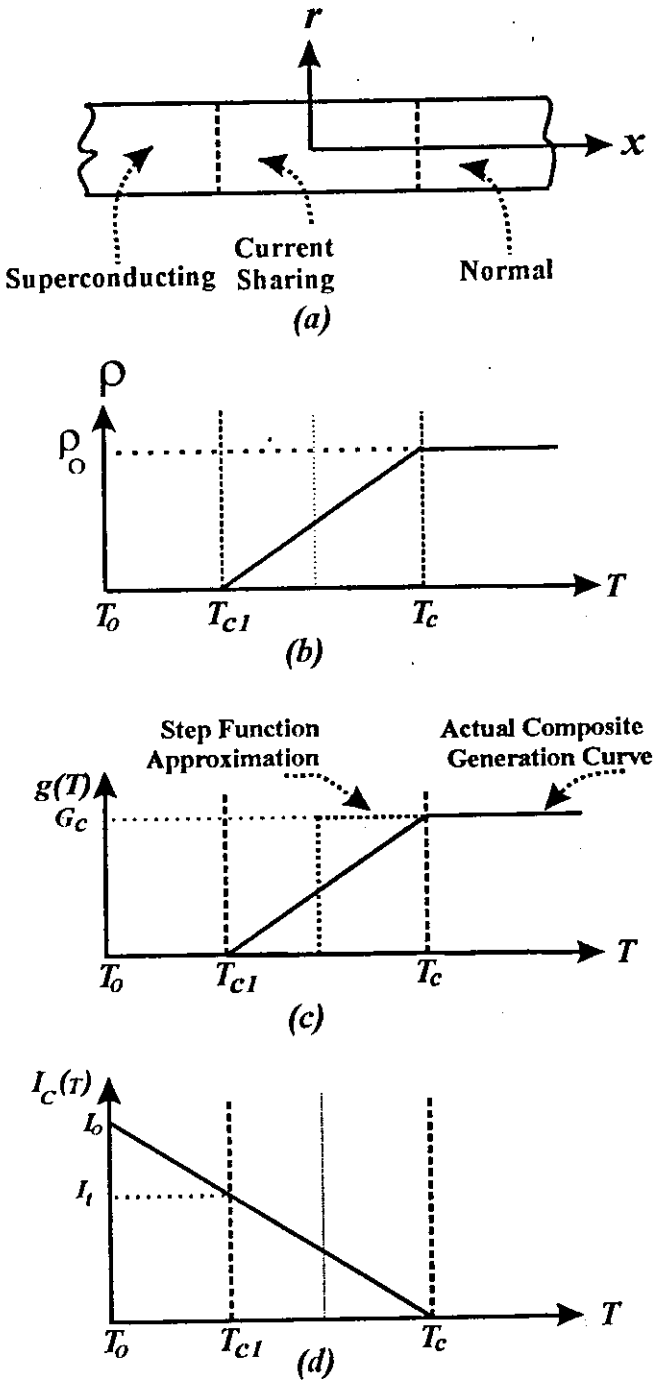

Figure (3.5): a) The different zones of a type II-superconductor wire b) The electrical resistivity c) The volumetric heat generation in the conductor d) The dependence of critical current on temperature

The generation term is not nearly simple in composite case because of current sharing. A better understanding may by obtained by looking at the origin of the generation term Joule heating is the result of transport flowing down a voltage gradient, $\frac{\partial v}{\partial x}$. On the simplest level, the generation power density is simply the transport current density J= I_t/A multiplied by the electrical field E

$$g(T) = J \bullet E = \left(\frac{I_t}{A}\right) \frac{\partial V(T)}{\partial x} \qquad (3.2)$$

Where I_t is the total current, J is the overall current density defined as the transport current divided by the cross-sectional area of the conductor A, and V(T) is the temperature dependent voltage. When the critical current is larger or equal to the operating current, there is theoretically no voltage gradient and g(T) is zero. This corresponds to the case when the operating temperature is less than the transition temperature. During current sharing, the voltage gradient equals to the product of current flowing in the stabilizer matrix and the matrix resistance per length. The voltage V (T) may be computed by multiplying I_m (T) by the matrix resistance:

$$V(T) = I_m(T) \times \frac{\rho_o(T)}{f A} = I_m(T) \times \frac{\rho_o(T)}{A_m} \qquad (3.3)$$

where A is the matrix cross-sectional area of the composite superconductor, f is the volume fraction of the normal metal, A_m, is the cross-section of the metal matrix, ρ_m is the matrix electrical resistivity, and I_m is the current flowing through the metal matrix. Combining equation (3.2) with equation (3.3) gives

$$g(T) = \rho_o(T) \times \left(\frac{I_t}{A}\right)\left(\frac{I_m(T)}{A_m}\right) = \rho_o(T) J J_m(T) \qquad (3.4)$$

Equation (3.4) is the most general form of the generation term for composite conductors. Equation (3.4) may be simplified somewhat by introducing a linear approximation for the I_c versus T curve, as done in Fig. (3.3).

$$I_c(T) = -\frac{I_0}{T_c}T + I_0 \tag{3.5}$$

Where I_0 is the critical current at zero temperature. This approximation may then be used to obtain an expression for the matrix current I_m

$$I_m(T) = \begin{Bmatrix} 0 & for & T \le T_{c1} \\ I_t \times \frac{T - T_c}{T_c - T_{c1}} & for & T_{c1} < T < T_c \\ I_t & for & T \ge T_c \end{Bmatrix} \tag{3.6}$$

The value of T_{c1} is dependent on the transport current I_t. Incorporating this approximation into equation (3.4); the generation term may be expressed as

$$g(T) = \begin{Bmatrix} 0 & for & T \le T_{c1} \\ g_{max} \times \frac{T - T_c}{T_c - T_{c1}} & for & T_{c1} < T < T_c \\ g_{max} & for & T \ge T_c \end{Bmatrix} \tag{3.7}$$

Where, g_{max} is the Joule heating source with the whole current flowing in the stabilizer and g_{max} is given by:

$$g_{max} = \frac{\rho_o J^2}{f P} = \frac{G_c}{f P} \tag{3.8}$$

This linear approximation of g(T) is shown by the dashed line in the lower plot of Fig. (3.4).

To drive equation (3.1), as we know that I_m is the difference between the transport (total) current and the critical current, I_t- I_c. Thus the voltage gradient will be

$$\frac{\partial V}{\partial x} = (I_t - I_c)\frac{\rho_o}{f A} \tag{3.9}$$

Substitute equation (3.9) into equation (3.2), to get:

$$g(T) = I_t (I_t - I_c) \frac{\rho_m}{f A} \qquad (3.10)$$

In normal state, all the current sharing flows through the metal matrix, and since the resistivity of superconducting material resistivity in normal zone is much higher than the resistivity of metal matrix then I_c is much lower than I_m, so in normal state the Joule heating is given by:

$$g(T) = I_t^2 \frac{\rho_o}{f A} = \rho_o \frac{I_t^2}{A_m} \qquad (3.11)$$

In equation (3.11) the current sharing region is neglected which corresponds to low T_c superconductors. In this case the conductor is divided into two distinct regions in x, one superconducting and the other is normal as shown in Fig. (3.2). Introducing the current density J, equation (3.11) may be written as:

$$g(T) = \frac{\rho_o J^2}{P} = \frac{G_c}{P} \qquad (3.12)$$

In superconducting zone g (T) equals zero, so the heat source term in the case on non-composite or type I-superconductor may be written as:

$$g(T) = \begin{cases} 0 & for \quad T < T_{c1} \\ \dfrac{G_c}{P} & for \quad T \geq T_{c1} \end{cases} \qquad (3.13)$$

In summary, because the thermal behavior of superconductors is controlled by the heat generation term, the thermal behaviors of type I and type II are quite different. The generation term for typeI is given by equation (3.1) and for type II by equation (3.7).

3.3 Macroscopic Heat Conduction Models

It is stated in the previous chapter that there are basically three different macroscopic heat conduction models that describe the mechanism of heat conduction process. These models will be used to investigate the thermal stability of superconductors.

The first model is the classical diffusion model which employs Fourier's law of heat conduction. In the classical diffusion model, the heat flux vector q and the temperature gradient across the material volume are assumed to occur at the same instant of time. Thus, the Fourier's law may be written as

$$\mathbf{q}(\mathbf{r},t) = -k\nabla T(\mathbf{r},t) \qquad (3.14)$$

Where r is the position vector of the material volume, t is the physical time, q is the heat flux vector, and k is the thermal conductivity. This model results in an infinite speed of heat propagation, implying that the thermal distribution applied to a certain location in a solid medium can be sensed immediately anywhere in the medium. In other words, a local change in temperature causes an instantaneous response at each point in the medium. Because the heat flux and the temperature gradient are simultaneous, there is no time difference between the cause (temperature gradient) and the effect (heat flow).

The second model is the wave (hyperbolic) model, which assumes the heat flux vector and the temperature gradient to occur at different instants of time. This model results in a finite propagation of the thermal wave. To account for the phenomenon involving the finite propagation velocity of thermal wave, the classical diffusion model should be modified. Cattaneo (1958) and Vernotte (1961) suggested independently a modified model for the heat flux in the form

$$\mathbf{q}(\mathbf{r},t+\tau_q) = -k\nabla T(\mathbf{r},t) \qquad (3.15)$$

Where τ_q is the time delay between the temperature gradient and the heat flux vector, and is usually called relaxation time. The relaxation time, indeed, relates to the thermal wave speed by $\tau_q = \frac{\alpha}{\omega^2}$ where α is the thermal diffusivity and ω the thermal wave speed. Generally, the value of τ_q depends on temperature. As it is evaluated by Vedararz et al. (1994), the value of τ_q is of order of 10^{-11} to 10^{-6} s at cryogenic temperatures and 10^{-14} to 10^{-10}s at room temperature. In the case of ω approaching infinity, the relaxation time decreases to zero, the wave model reduces to the diffusion model.

The constitution law of equation (3.15) assumes that the heat flux vector (the effect) and the temperature gradient (the cause) across a material volume occur at different instants of time, and the time delay between the heat flux and the temperature gradient is the relaxation time τ_q. The first-order Taylor expansion of q in equation (3.15) with respect to t bridges all physical quantities at the same time. This expansion results in

$$\mathbf{q}(\mathbf{r},t) + \tau_q \frac{\partial \mathbf{q}(\mathbf{r},t)}{\partial t} = -k \nabla T(\mathbf{r},t) \qquad (3.16)$$

In equation (3.16) it is assumed that τ_q is small enough so that the first-order Taylor expansion of $q(r,t+\tau_q)$ is an accurate representation for the heat conduction heat flux vector.

The third model is the dual-phase-lag model. The dual-phase-lag-model, states that the heat flux and the temperature gradient occurr at different instants of time during the heat transfer process. If the temperature gradient leads the heat flux in the time history, the temperature gradient is the cause and the heat flux is the effect. Whereas, if the heat flux leads the temperature gradient, the heat flux becomes the cause and the temperature gradient becomes the effect. This concept of dual lagging does not exist

neither in the diffusion model nor in the wave model. The diffusion model assumes that the heat flux and the temperature gradient occur at the same instant of time, and the wave model assumes that the temperature gradient is always the cause for the heat transfer and the heat flux is always the effect.

The dual-phase allows either the temperature gradient (cause) to precede the heat flux (effect) or the heat flux (cause) to precede the temperature gradient (effect) in transient heat conduction processes. This was represented by Tzou (1995 a-c):

$$\mathbf{q}(\mathbf{r},t+\tau_q) = -k\nabla T(\mathbf{r},t+\tau_T) \qquad (3.17)$$

Where τ_T is the phase lag of the temperature gradient and τ_q is the phase lag for the heat flux. For the case of $\tau_T > \tau_q$, The temperature gradient established across a material volume is a result of heat flow, implying that the heat flux is the cause and the temperature gradient is the effect. On the other-hand, for $\tau_T < \tau_q$ heat flow is induced by temperature gradient established at an earlier time, implying that the temperature gradient is the cause and heat flux is the effect. Assuming the time delays τ_T and τ_q are much shorter than the response time in a transient process t, the first-order Taylor series expansion can be applied to equation (3.17), rendering:

$$\mathbf{q}(\mathbf{r},t) + \tau_q \frac{\partial \mathbf{q}(\mathbf{r}.t)}{\partial t} \cong -k\left\{\nabla T(\mathbf{r},t) + \tau_T \frac{\partial}{\partial t}\left[\nabla T(\mathbf{r},t)\right]\right\} \qquad (3.18)$$

3.4 Thermal Stability Governing Equations

3.4.1 Introduction

The theoretical analysis of the superconductor thermal stability will be performed based on the former three macroscopic heat conduction models (the

diffusion, wave, and dual-phase-lag-model). For each model the governing equations with their associated boundary and initial conditions will be derived. Then, these equations will be solved numerically. Different factors will be taken into consideration for each model. These factors include the Joule heating, lateral cooling, current sharing, disturbances length duration time, and nature.

3.4.2 Analysis Based on Diffusion Model

Here, thermal stability of composite superconductor will be studied according to Fourier's heat conduction model, which is a parabolic partial differential equation. Two cases will be considered in this thesis. The first is the laterally cooled superconducting wire and the second is uncooled one. Furthermore, we will consider two cases with respect to the disturbance duration time, one with and the other without disturbance duration time. In this analysis we consider a cylindrical type superconductor wire subjected to heat disturbance which will create a normal zone (Figs 3.2 and 3.3). The temperature field in the normal zone and the quenching process are governed by the transient heat conduction equation. Consider the one-dimensional heat conduction with the assumption of lumped behavior in the transverse radial direction and the constant thermal properties, the transient heat conduction may be written as:

$$C\frac{\partial T}{\partial t} = k\ \frac{\partial^2 T}{\partial x^2} - \frac{hP}{A}(T - T_0) + g(T) \qquad (3.19)$$

Where T is temperature, t is time, x is the spatial coordinate, C is the volumetrically averaged total heat capacity, k is the volumetrically averaged thermal conductivity, h is the heat transfer coefficient, P is the perimeter of the superconductor exposed to coolant, T_0 is the ambient temperature, and g(T) represents the internal Joule heating

density, which depends on operating temperature. When the conductor is superconducting, this term is zero.

The heat capacity and thermal conductivity are volumetrically averaged as follows because of the composite nature of all practical conductors:

$$C = f C_m + (1-f) C_{sc} \tag{3.20}$$

$$k = f k_m + (1-f) k_{sc} \tag{3.21}$$

Where the subscripts m, and sc are for matrix, and superconductor, respectively. f is a void fraction defined as A_m/A, where A_m is the cross section of matrix. Note that f is a volume ratio. In this case, however, it may be written as an area ratio since it is assumed that the matrix-to-superconductor ratio is independent of length. In practical, k may be approximated as $k \approx f\, k_m$, since $k_{sc} << k_m$. For non-composite conductor f=0.0 and $k=k_{sc}$ and $C=C_{sc}$.

Most of previous works on superconductor thermal stability consider an adiabatic superconductor wire, this means that the superconductor is thermally insulated (see for example Malinowski L. (1991) and Jorma et al (1998)) But, this thesis studies the effect of lateral heat on the superconductor thermal stability. In terms of thermal diffusivity, equation (3.19) may be written as:

$$\frac{1}{\alpha}\frac{\partial T}{\partial t} = \frac{\partial^2 T}{\partial x^2} - \frac{hP}{Ak}(T - T_0) + \frac{g(T)}{k} \tag{3.22}$$

where α is the thermal diffusivity. The left hand-side term is the rate of change in thermal energy density. The first term in the right hand side represents the local longitudinal heat conduction density and the second term represents the lateral cooling, and the last term is the Joule heating (internal heat generation).

Disturbances (mechanical or magnetic) represent external heat sources such as conductor motion or epoxy cracking. Disturbances locally raise the temperature above

the critical value. These disturbances may be modeled as an initial condition (T_i) that depends on spatial coordinate of the normal zone. The disturbances are characterized by three parameters, its intensity (value of T_i), length (2l), and duration time (t_i). For, the case of no disturbance duration time, the disturbance may be written as an initial condition only:

$$T(x,0)=\begin{cases} T_i = cons. & for \quad -l \le x \le l \\ T_0 & outside\ this\ region \end{cases} \tag{3.23}$$

Where, T_i is the disturbance intensity.

Referring to Fig. (3.6) and due to the symmetry of the normal zone analysis are limited to the half of the zone (i.e. to the domain x>0 only), in which the problem is stated as follows:

$$\frac{1}{\alpha}\frac{\partial T}{\partial t} = \frac{\partial^2 T}{\partial x^2} - \frac{hP}{Ak}(T-T_0) + \frac{g(T)}{k} \tag{3.24}$$

with the following boundary conditions:

$$\begin{array}{lll} at & x=0, & \dfrac{\partial T}{\partial x}=0 \\ as & x \longrightarrow \infty & T \longrightarrow T_o \end{array} \tag{3.25}$$

and the initial condition at t=0 is:

$$T(x,0)=\begin{cases} T_i & for \quad 0 < x \le l \\ T_o & for \quad x > l \end{cases} \tag{3.26}$$

For more convenience of subsequent analysis, equation (3.24) with its associated boundary and initial condition will be written in dimensionless form by introducing the following dimensionless parameters:

$$\theta = \frac{T-T_o}{T_c-T_o} \quad , \quad \xi = \frac{2x}{d} \quad , \quad \beta = \frac{4\alpha t}{d^2}, \tag{3.27a}$$

$$B = \frac{T_i-T_o}{T_c-T_o} \quad , \quad Q = \frac{d^2 g(T)}{4k(T_c-T_o)} \quad , \quad L = \frac{2l}{d}, \quad H = \frac{hd}{k} \tag{3.27b}$$

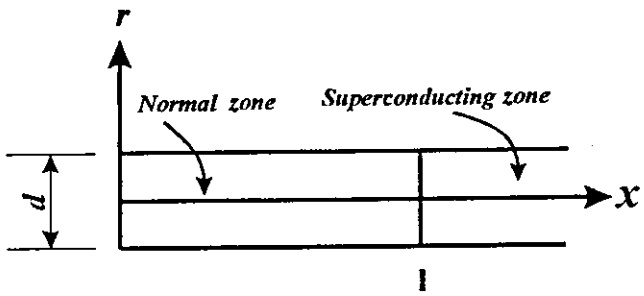

Figure (3.6): The superconductor with the origin in the center of the heat disturbance at x=0

Then problem statement (3.24)-(3.26) becomes:

$$\frac{\partial\theta}{\partial\beta}=\frac{\partial^2\theta}{\partial\xi^2}-H\theta+Q \qquad (3.28)$$

The dimensionless generation term for type I and typeII-superconductor will be given in equation (3.29) and (3.30), respectively.

$$Q=\begin{cases}0 & for \quad \theta<\theta_{c1}\\ \dfrac{d^2Gc}{4Pk(T_c-T_o)} & for \quad \theta\geq\theta_{c1}\end{cases} \qquad (3.29)$$

$$Q=\begin{cases}0 & for \quad \theta\leq\theta_{c1}\\ \dfrac{d^2g_{max}}{4k(Tc-To)}\times\dfrac{\theta-1}{1-\theta_{c1}} & for \quad \theta_{c1}<\theta<1\\ \dfrac{d^2g_{max}}{4k(T_c-T_o)} & for \quad \theta\geq1\end{cases} \qquad (3.30)$$

The boundary conditions will be:

$$\begin{aligned} &at \quad \xi=0, \quad \frac{\partial\theta}{\partial\xi}=0\\ &as \quad \xi\longrightarrow\infty \quad \theta\longrightarrow0\end{aligned} \qquad (3.32)$$

and, the initial conditions are:

$$at \quad \beta=0, \quad \theta=\begin{cases}B & for \quad 0<\xi\leq L\\ 0 & for \quad \xi>L\end{cases} \qquad (3.33a)$$

Equation (3.33) represents a step disturbance. To study the effect of disturbance nature, we will consider the normal (Gaussian) disturbance, which may be written as

$$\theta = \mathbf{B}\exp[-\xi^2 \ln(B)] \qquad (3.33b)$$

The results of superconductor subjected to step and Gaussian initial condition will be compared. Also, note that the term source is present only if the temperature is greater than critical value.

Now, we will study the effect of disturbance duration time, therefore equation (3.19) should be modified by addition of a new term, which represents the disturbance duration

$$C\frac{\partial T}{\partial t} = k\frac{\partial^2 T}{\partial x^2} - \frac{hp}{A}(T - T_o) + g(T) + dis(x,t) \qquad (3.34)$$

where dis(x,t) is the external disturbance which may be a result of conductor motion or epoxy cracking. The disturbance has the form of a rectangular heat pulse

$$dis(x,t) = \begin{cases} \dfrac{E}{2Alt_i} & for \quad -l \le x \le l \ and \ 0 < t < t_i \\ 0 & outside\ this\ region \end{cases} \qquad (3.35)$$

here E represents the energy of heat disturbance.

Introducing the same dimensionless parameters used in equation (3.27) in addition to the following dimensionless parameters

$$\varepsilon = \frac{d^2 E}{8Alk\, t_i(T_c - T_o)}, \qquad \tau_i = \frac{4\alpha t_i}{d^2} \qquad (3.36)$$

where ε is the dimensionless energy of heat disturbance and τ_i is the dimensionless disturbance duration time. Equation (3.34) may be written in dimensionless form as

$$\frac{\partial\theta}{\partial\beta} = \frac{\partial^2\theta}{\partial\xi^2} - H\theta + D_s + Q \qquad (3.37)$$

where Ds is the dimensionless heat disturbance, in the domain $\xi>0$, is given by

$$D_s = \begin{cases} \varepsilon & for \quad 0 \le \xi \le L \; and \; 0 < \tau < \pi \\ 0 & outside \; this \; region \end{cases} \qquad (3.38)$$

The initial and boundary conditions associated with equation (3.37) are the same as equations (3.32) and (3.33).

3.4.3 Investigation of Superconductor Thermal Stability Based on Wave Conduction Model

The classical parabolic heat conduction model breaks down when the time required by the transient process is comparable with the relaxation time. Since, the relaxation time of heat flux increases as the temperature decreases; the wave model is particularly useful for the analysis at very low temperature (cryogenics application). The heat wave propagation speed is usually approximated by the velocity of a free electron gas in the case of metal, and the speed of sound in crystals in the case of non-metals. At room temperature, these speeds are of the order of 9×10^4 ms^{-1} and 5×10^3 ms^{-1}, respectively (Malinowski, 1993).

This section present a numerical analysis of a composite and non-composite superconductor thermal stability with regard to the thermal relaxation processes in the conductor (i.e. based on wave heat conduction equation, which takes into account the finite speed of thermal wave). Here, we will consider a thin, superconductor wire carrying an electrical current. A conductor length of 2l is instantly heated by the heat disturbance source up to temperature T_i, exceeding the critical superconductor temperature at a given current. The heat disturbance will initiate a normal zone that will propagate along the conductor. Because of their low thermal conductivity, the superconducting filaments play almost no role in heat transfer along the conductor. In

flux vector introduces an apparent heat source, $\left(\tau_q/k\right)\left(\partial g/\partial t\right)$, and apparent lateral cooling factor, $\left(\tau_q\varphi/k\right)\left(\partial\varphi/\partial t\right)$, in addition to the real heat source, and the real lateral cooling applied to the conductor.

Our analysis will conducting for the one-dimensional case, with the assumption of constant physical properties As a result, equation (3.42) reduced to:

$$\frac{1}{\omega}\frac{\partial^2 T}{\partial t^2}+\frac{1}{\alpha}\frac{\partial T}{\partial t}=\frac{\partial^2 T}{\partial x^2}-\frac{1}{k}\left(\tau_q\ \frac{\partial\varphi}{\partial t}+\varphi\right)+\frac{1}{k}\left(\tau_q\frac{\partial g}{\partial t}+g\right) \quad (3.43)$$

At the initial time t=0, the temperature field within the conductor is uniform and stationary at a value of T_i. Thus the initial conditions associated with equation (3.43) are:

$$T=\begin{cases} T_i & for \quad 0<x\le l \\ T_o & for \quad x>l \end{cases} \quad (3.44a)$$

and

$$at \ \ t=0, \quad \frac{\partial T}{\partial t}=0 \quad (3.44b)$$

and the boundary conditions are:

$$\begin{aligned} &at && x=0, && \frac{\partial T}{\partial x}=0 \\ &as && x\longrightarrow\infty && T\longrightarrow T_o \end{aligned} \quad (3.45)$$

The steady state capacity of Joule heating for the non-composite superconductor is given by equation (3.1) and for the composite superconductor is given by equation (3.7).

It is more convenient to introduce the following dimensionless parameters:

$$\xi=\frac{x}{2\sqrt{\alpha\tau_q}},\quad \beta=\frac{t}{2\tau_q},\quad \theta=\frac{T-T_o}{T_c-T_o},\quad L=\frac{l}{2\sqrt{\alpha\tau_q}} \qquad (3.46a)$$

$$Q=\frac{4\tau_q\, g(T)}{C(T_c-T_o)}\quad ,\quad H=\frac{4\,\tau_q hP}{C\,A} \qquad (3.46b)$$

Rewrite equation (3.43) and the associated initial and boundary condition in dimensionless form to obtain:

$$\frac{\partial^2\theta}{\partial\beta^2}+\frac{\partial\theta}{\partial\beta}=\nabla^2\theta-H\left(\theta+\frac{1}{2}\frac{\partial\theta}{\partial\beta}\right)+\left(Q+\frac{1}{2}\frac{\partial Q}{\partial\beta}\right) \qquad (3.47)$$

The dimensionless initial conditions associated with equation (3.47) are:

$$at\quad \beta=0,\qquad \theta=\begin{cases} B & for\ 0<\xi\le L \\ 0 & for\quad \xi>L \end{cases} \qquad (3.48a)$$

and

$$at\quad \beta=0,\quad \frac{\partial\theta}{\partial\beta}=0 \qquad (3.48b)$$

and, the dimensionless boundary conditions are:

$$\begin{aligned} &at \qquad \xi=0, \qquad \frac{\partial\theta}{\partial\xi}=0 \\ &as\ \ \xi\longrightarrow\infty \qquad \theta\longrightarrow 0 \end{aligned} \qquad (3.49)$$

The dimensionless generation term for type I and type II superconductor is the same as equation (3.29) and (3.30).

To study the effect of disturbance duration time on superconductor thermal stability based on the wave model, we will use the same corresponding approach used in the case of diffusion model. Equation (3.43) will be modified to be as

$$\frac{1}{\omega}\frac{\partial^2 T}{\partial t^2}+\frac{1}{\alpha}\frac{\partial T}{\partial t}=\frac{\partial^2 T}{\partial x^2}-\frac{1}{k}\left(\tau_q\frac{\partial \varphi}{\partial t}+\varphi\right)+\frac{1}{k}\left(\tau_q\frac{\partial g}{\partial t}+g\right)+\frac{1}{k}\left(\tau_q\frac{\partial dis}{\partial t}+dis\right) \quad (3.50)$$

Also, the delay of heat flux results in an apparent disturbance, $\left(\tau_q dis/k\right)\left(\partial dis/\partial t\right)$, in addition to the real one.

Equation (3.50) may be written in dimensionless form using the dimensionless parameters shown in equation (3.46) and the following dimensionless parameters:

$$\varepsilon=\frac{d^2 E}{8A t_i l k(T_c-T_o)}, \quad \tau_i=\frac{t_i}{2\tau_q} \quad (3.51)$$

The dimensionless form of equation (3.50) is

$$\frac{\partial^2\theta}{\partial\beta^2}+\frac{\partial\theta}{\partial\beta}=\nabla^2\theta-H\left(\theta+\frac{1}{2}\frac{\partial\theta}{\partial\beta}\right)+\left(Q+\frac{1}{2}\frac{\partial Q}{\partial\beta}\right)+\left(Ds+\frac{1}{2}\frac{\partial Ds}{\partial\beta}\right) \quad (3.52)$$

The dimensionless disturbance is given in equation (3.38). The initial and the boundary conditions associated with equation (3.52) are the same as equations (3.48) and (3.49).

3.4.4 Investigation of Superconductor thermal Stability Based on Dual-Phase-Lag Model

This section presents a theoretical investigation of superconductor thermal stability based on the dual-phase-lag model. Applying the dual-phase-lag model to investigate the thermal stability of a superconductor wire will be conducted in this thesis for the first time -up to my knowledge-. As mentioned previously, the dual-phase-lag model allows the temperature gradient to precede the heat flux or the heat flux to precede the temperature gradient, depending on the relative values of time lags (τ_T and τ_q).

To derive the governing equation based on dual-phase-lag model we start from equation (3.18). Assuming constant thermal properties, the divergence of equation (3.18) gives:

$$\nabla.\mathbf{q} + \tau_q \frac{\partial}{\partial t}(\nabla.\mathbf{q}) = -k\nabla^2 T - \tau_T \frac{\partial}{\partial t}(\nabla^2 T) \qquad (3.53)$$

Substituting the expression $\nabla.\mathbf{q}$ from the energy conservation equation (3.40) into equation (3.53) and introducing the thermal diffusivity gives:

$$\frac{1}{\alpha}\frac{\partial T}{\partial t} + \frac{\tau_q}{\alpha}\frac{\partial^2 T}{\partial t^2} = \nabla^2 T + \tau_T \frac{\partial}{\partial t}(\nabla^2 T) + \frac{1}{k}\left[g + \tau_q \frac{\partial g}{\partial t}\right] - \frac{1}{k}\left[\varphi + \tau_q \frac{\partial \varphi}{\partial t}\right] \qquad (3.54)$$

Equation (3.54) describes the temperature response with lagging in the linearized framework accommodating the first order effect of τ_T and τ_q. It captures several representative models in heat transfer as special cases. In the absence of two phase lags, $\tau_T = \tau_q = 0$, equation (3.54) reduces to the diffusion equation employing Fouries's law (equation 3.19). In the absence of phase lag of temperature gradient, $\tau_T = 0$, equation (3.52) reduces to the wave model equation (3.42). Thus, the two popular models used for describing the macroscopic heat conduction are captured in the framework of dual-phase-lag model under special cases. The phase of heat flux vector introduces an apparent heat source, $\left(\tau q/k\right)\left(\partial g/\partial t\right)$, and apparent lateral cooling factor, $\left(\tau \varphi/k\right)\left(\partial \varphi/\partial t\right)$, in addition to the real heat source, and lateral cooling applied to the conductor.

The superconductor wire considered here will be the same as the one previously described. Equation (3.54) will be written for one-dimensional case as

$$\frac{1}{\alpha}\frac{\partial T}{\partial t} + \frac{\tau_q}{\alpha}\frac{\partial^2 T}{\partial t^2} = \frac{\partial^2 T}{\partial x^2} + \tau_T\left(\frac{\partial^3 T}{\partial x^2 \partial t}\right) + \frac{1}{k}\left[g + \tau_q \frac{\partial g}{\partial t}\right] - \frac{1}{k}\left[\varphi + \tau_q \frac{\partial \varphi}{\partial t}\right] \qquad (3.55)$$

The initial and boundary conditions associated with equation (3.55) are the same as equation (3.44) and equation (3. 45).

The lagging response of temperature is characterized by three parameters: the thermal diffusivity, the phase lag of temperature gradient, and the phase lag of the heat flux vector. The dual-phase-lag model introduces a new type of energy equation in conductive heat transfer. As shown in equation (3.55), the mixed-derivative term, containing the first-order derivative with respect to time and the second derivative with respect to apace, appears as the highest order differential in the equation, which will dramatically alter the fundamental characteristics of the solution for temperature. A wave term, the second derivative with respect to time, still exists on the right-hand side of the energy equation, but the mixed-derivative term completely destroys the wave structure.

It is more convenient to write equation (3.55) in dimensionless form by introducing the following dimensionless parameters:

$$\xi = \frac{x}{2\sqrt{\alpha \tau}} \qquad \beta = \frac{t}{2\tau} \qquad \theta = \frac{T - T_o}{T_c - T_o} \tag{3.56a}$$

$$Q = \frac{4\tau_q \, g(T)}{C(T_c - T_o)}, \quad Ds = \frac{4\tau_q \, dis(x,t)}{C(T_c - T_o)}, \quad H = \frac{4\,\tau_q hP}{C\,A}, \quad R = \frac{\tau_T}{2\tau_q} \tag{3.56b}$$

Thus, the dimensionless form of equation (3.55) takes the form:

$$\frac{\partial^2 \theta}{\partial \beta^2} + 2\frac{\partial \theta}{\partial \beta} = \frac{\partial^2 \theta}{\partial \xi^2} + R\frac{\partial^3 \theta}{\partial \xi^2 \partial \beta} + \left(Q + \frac{1}{2}\frac{\partial Q}{\partial \beta} \right) - H\left(\theta + \frac{1}{2}\theta \right) \tag{3.57}$$

The dimensionless initial and boundary conditions associated with equation (3.57), are the same as equation (3.48) and (3.49).

The dimensionless analysis clearly shows that the lagging response is indeed characterized by a single parameter R, the ratio between the phase lags. In the case of $\tau_T = 0$, implying R=0, equation (3.57) reduces to the wave model, and the remaining phase

lag τ_q reduces to the conventional relaxation time. Furthermore, If $\tau_T = \tau_q$, not necessarily equal to zero, and ignoring the generation, and lateral cooling terms, equation (3.55) can be rearranged into the following form:

$$\left(\frac{\partial^2 T}{\partial x^2} - \frac{1}{\alpha}\frac{\partial T}{\partial t}\right) + \tau_q \frac{\partial}{\partial t}\left(\left(\frac{\partial^2 T}{\partial x^2} - \frac{1}{\alpha}\frac{\partial T}{\partial t}\right)\right) = 0 \qquad (3.58)$$

For a homogeneous initial temperature, it has a general solution

$$\frac{\partial^2 T}{\partial x^2} - \frac{1}{\alpha}\frac{\partial T}{\partial t} = 0 \qquad (3.59)$$

Which is the classical diffusion equation. When the two-phase lags are equal, the dual-phase-lag model reduces to the diffusion model employing Fourie's law. This becomes obvious in view of equation (3.18) because equal phase lags imply a trivial shift in time scale, while an instantaneous response between the heat flux vector and the temperature gradient still exists. The dimensionless form of equation (3.56) reduces to:

$$2\frac{\partial \theta}{\partial \beta} = \frac{\partial^2 \theta}{\partial \xi^2} \qquad (3.60)$$

To study the effect of disturbance duration time on superconductor thermal stability based on the dual-phase-lag model, we will use the same corresponding approach used in the case of diffusion and wave model. Equation (3.55) will be modified to be as

$$\frac{1}{\alpha}\frac{\partial T}{\partial t} + \frac{\tau_q}{\alpha}\frac{\partial^2 T}{\partial t^2} = \frac{\partial^2 T}{\partial x^2} + \tau_T\left(\frac{\partial^3 T}{\partial x^2 \partial t}\right) - \frac{1}{k}\left[\varphi + \tau_q \frac{\partial \varphi}{\partial t}\right] + \frac{1}{k}\left[Q + \tau_q \frac{\partial Q}{\partial t}\right] + \frac{1}{k}\left[dis + \tau_q \frac{\partial dis}{\partial t}\right] \qquad (3.61)$$

Also, the lagging between the temperature gradient and the heat flux results in an apparent disturbance, $\left(\tau_q dis/k\right)\left(\partial dis/\partial t\right)$, in addition to the real one.

Equation (3.61) may be written in dimensionless form using the dimensionless parameters shown in equation (3.56) and the dimensionless parameters that described by equation (3.51). The dimensionless form of equation (3.61) is

$$\frac{\partial^2\theta}{\partial\beta^2}+2\frac{\partial\theta}{\partial\beta}=\frac{\partial^2\theta}{\partial\xi^2}+B\frac{\partial^3\theta}{\partial\xi^2\partial\beta}-H\left(\theta+\frac{1}{2}\theta\right)+\left(Q+\frac{1}{2}\frac{\partial Q}{\partial\beta}\right)+\left(Ds+\frac{1}{2}\frac{\partial Ds}{\partial\beta}\right) \quad (3.62)$$

The dimensionless disturbance Ds is given in equation (3.38). The initial and boundary conditions associated with equation (3.62) are the same as those shown in equation (3.47) and (3.48).

3.4.5 Rate Effect

Although the wave structure in the dual-phase-lag model is deserted by the microstructural interaction effect, the presence of the wave term in equation (3.56) or (4.58) allows two initial conditions to specify the lagging response of temperature evolution. One example is the specification of the initial time-rate of change of temperature along with the initial temperature

$$T(x,0)=T_i \quad and \quad \frac{\partial T}{\partial t}(x,0)=\dot{T}_i \ for \ x\in[0,\infty) \quad (3.63)$$

The existence of the initial time-rate of change of temperature corresponds to a non-uniform initial heating. The boundary conditions remain the same as in equation (3.49). The governing equations for the lagging response are given by equation (3.57), but the initial conditions in equation (3.48) are replaced by

$$\theta(\xi,0)=B \ and \ \frac{\partial\theta}{\partial\beta}=\dot{\theta}_i \quad with \quad \dot{\theta}_i=\frac{2\tau_q\dot{T}_i}{T_c-T_o} \quad (3.64)$$

In this section the emphasis, obviously, is placed on the effect of initial temperature rate on the lagging behavior. In the case of a zero rate, the solution of the equation reduced to the same as that of equation (4.57).

3.5 Thermal Stability Criterion

The solution of the transient heat conduction based on the three macroscopic heat conduction models has the general form of

$$\theta=\theta(\xi,\beta,B,Q,H,l,Ds,\varepsilon,\tau) \tag{3.65}$$

Since the problem is symmetric about the ξ =0.0 plane, at all times the maximum conductor temperature (θ1) is at ξ =0.0, (i.e. resides in the original center of the disturbance).

$$\theta 1=\theta(0,\beta,B,Q,H,Ds,l,\tau,\varepsilon) \tag{3.66}$$

On a θ1-β plane, equation (3.66) represents a family of curves, one curve for each combination of Bs, Q, H, B, L, Ds, ε, and τ_i. For example, in the absence of Joule heating, Q tends to zero, most temperature-time curves will eventually drop below the critical level θ_c=1. In other words, for most combination of H, and B the normal zone will collapse and the superconductor is thermally stable. However, as Joule heating increases, one crosses a critical threshold distinguishes between stable and unstable operation. For very large values of Joule heating ,Q tendes to infinity, θ1 will generally rise, always bieng greater than unity, which means that the normal zone will grow and the superconductor is thermally unstable

To check the superconductor thermal stability, the transient behavior of θ1 is plotted for different values of B, H, Q, L, ε, τ_i, and Ds. Two behaviors can be featured out; a) θ1 drops below 1, meaning that the normal zone shrinks to zero, and the superconductor is stable, and b) θ1 does not drop below 1, indicating that the normal zone grows and the superconductor is unstable. For any B, there exists a critical parameter Q_c(B), below which the superconductor is stable.

We are particularly interested in the marginal case, when the conditions

$$\theta 1 = 1 \qquad (3.67)$$

$$\frac{\partial \theta 1}{\partial \beta} = 0 \qquad (3.68)$$

Occur simultaneously. Eliminating β between (3.67) and (3.68) yields a relationship for the critical combination $(Q,H,B)_c$, separating the range of possibilities for collapse (recovery) from separating the range of possibilities causing perpetual normal zone growth. The resulting critical combination can also be expressed as:

$$Q_c = Q_c(H,B) \qquad (3.69)$$

The stability criterion is then

$$\begin{cases} Q < Qc & \textit{for collapse (Stable)} \\ Q > Qc & \textit{for growth (Unstable)} \end{cases} \qquad (3.71)$$

where Q_c is the result of combining conditions (3.67) and (3.68) with the solution for the conductor maximum temperature (3.66). In order to arrive at (3.71) we must first solve the transient heat conduction problem.

3.6 Numerical Model

For low-T_c (type I or non-composite) superconductor analytical methods may be used, but numerical modeling of normal zone propagation shows significant advantages over analytical methods, as demonstrated by Kadambi and Dorri (1986) and Eckart et.al (1981). For the case of high-T_c (typeII or composite) superconductors, the wide temperature span of current sharing makes numerical methods essential. One-dimensional numerical analysis has been performed for high-T_c and low T_c superconductor using finite difference method. Here, we develop a one-dimensional code for the investigation of superconductor thermal stability based on diffusion model. The program listing is presented in the appendix. The numerical solution for the thermal

stability problem based on the wave and dual-phase-lag models have been obtained using the FlexPDE finite element code.

3.6.1 Finite Difference Method

Modeling the spatial variation of an implicit property across an object involves representing the object by a nodal mesh. Each node, corresponding to a small slice of the object, has relevant properties and at least one control variable associated with it. In our study, the control variable is temperature. The simulation proceeds through sufficiently small time steps. For each time step, the value of the control variable at each node is calculated for the next time step based on property and control values of the surrounding nodes. Various finite difference algorithms are available. However, when used properly, each should yield identical results. The algorithms are classified into two categories. The implicit method (backward-difference) uses the control variable values at both the present and next time steps to calculate the value for the next time step. The explicit method (forward-differences) requires only the present property and control values to calculate the value for the next step. The implicit method requires much more computation per iteration, causing it to be time consuming, but it is unconditionally stable. The explicit method requires a special attention to the mesh size and the time step, to maintain numerical stability and prevent faulty results when the mesh size or time steps is too large. Therefore, we will use the implicit method to avoid numerical stability issue. There are many implicit schemes, we will use the most common scheme which known as Crank-Nicolson implicit method.

The basic idea behind the simulation code is to solve a discretized version of equation (3.28) for one-dimensional temperature profiles at discrete instants in dimensionless time. The numerical method is adapted from the methods presented by patanker (1980). To begin, the wire is discretized into approximately 1000 differential

elements dx (slices). Within each element, the temperature assumed to be function of time only. Thus at any given instant of time, the temperature of the element is constant. Hence, equation (3.28) reduces a set of algebraic equations, which may be solved using the tri-diagonal matrix algorithm (Thomas algorithm). By simultaneously solving for temperature of each element, a temperature profile for that given instant of time may be obtained, $\theta(\xi,\beta_i)$.

The basic algorithm is as follows. First, an initial constant temperature profile is assumed. Using this profile, the amount of heat generation is evaluated within each discrete element along the wire. Second, based upon this heat generation, the interconnected discrete equation for each location long the wire are solved simultaneously using the tri-diagonal matrix algorithm (Thomas algorithm), resulting a new temperature profile for the next time step. This new profile is used to update the generation in each element. The loop then repeats itself, marching out the temperature profile in time.

3.7 Method of Solution for the Wave and Dual-Phase Model

The wave model described by equations (4.49) to (4.51) and the dual-phase-lag models described by equations (4.58), (3.50) and (4.51), have been solved numerically by means of FlexPDE program. This section presents a brief explanation about this program.

FlexPDE is a software tool for the solution of systems of partial differential equations. It offers an integrated solution environment, including problem description language, numerical modeling and graphical output of solutions. FlexPDE is developed by the staff that originally developed PDEase2, FlexPDE is a unique, flexible, and powerful general purpose software system for obtaining numerical solutions to the

coupled sets of partial differential equations frequently found in engineering, physics, chemistry, biology, geology, mathematics and other scientific fields.

FlexPDE uses the powerful finite element method to obtain its numerical solutions. FlexPDE does not, however, require its users to have any knowledge of the intricacies of the finite element method or mesh generation. Users who can express their problems as initial value/boundary value problems can use FlexPDE immediately. Problems are posed to FlexPDE by first preparing a simple problem descriptor file using an easy-to-learn natural language originally developed by Nelson and described by Backstrom (1999). While in some ways similar to a computer programming language, the natural language used in FlexPDE descriptor files is not a programming language but rather a natural English-like scripting language and is much simpler to learn. The language of FlexPDE problem descriptors is relational, not procedural. The user describes how the various components of the system relate to one another; he does not describe a sequence of steps to be followed in forming the solution. Based on the relations between problem elements, FlexPDE decides on the sequence of steps needed in finding the solution.

Problem descriptor files may be prepared using either FlexPDE's built-in editor or any other convenient ASCII text editor such as WINDOWS NOTEPAD. Once the problem descriptor file has been prepared, FlexPDE will take over from the user and use its powerful finite element engine to numerically solve the problem. During the process of obtaining the numerical solutions, FlexPDE continuously displays its progress and any intermediate results requested in the descriptor file. While by default all of these "monitors" are displayed on one screen as "thumbnails", any one or more of the thumbnails can be expanded to full screen at any time for detailed viewing and, if

desired, can be sent to the system printer. Upon completion of a problem, FlexPDE displays as many views of the final results as requested in the problem descriptor file.

Equation-Systems

FlexPDE can treat boundary value and eigenvalue problems in one, two, and three space dimensions, as well as initial/boundary value problems in one, two, and three space dimensions plus time. The equations are assumed to be of first or second order in space and first order in time. Equations of higher order must be rewritten as systems of equations of lower order. Equations may be linear or nonlinear, and FlexPDE will automatically apply a solution method, which is appropriate to the system. Only the resources of the computer limit the number of simultaneous equations.

Boundary-Conditions

Boundary conditions may be specified as arbitrary combinations of "value", "natural", "Neumann", "periodic" and "antiperiodic" conditions. "Value" boundary conditions specify the value of a given dependent variable as a function of constants, spatial coordinates, and values or derivatives of dependent variables.

"Natural" boundary conditions depend for their meaning on the way the equations are written, but in the usual case refer to the specification of a boundary flux. Natural boundary conditions are given as functions of constants, spatial coordinates, and values or derivatives of dependent variables. Consider for example the heat equation div(-K*grad(T))=H. Application of the divergence theorem to the left side reduces it to the surface integral of (-K*grad(T)), which is the meaning of the natural boundary condition, ie. the surface flux. "Neumann" boundary conditions specify the outward normal derivative of the variable.

"Periodic" and "antiperiodic" boundary conditions force the values of points on one boundary to replicate or negate values on another boundary, identified by an arbitrary

coordinate transformation expression. Linear extension, azimuthal rotation and other shape periodicities may be specified.

Finite-Element-Model

FlexPDE uses a Galerkinn or Cranck-Nicolson or backward implicit finite element models, with quadratic or cubic basis functions involving nodal values of system variables only. This model assumes that the dependent variables are continuous over the problem domain, but does not require or impose continuity of derivatives of the dependent variables. Second-order terms in the equations will give rise to various forms of flux continuity (through surface integrals generated by integration by parts), and these conditions will be imposed in an integral sense over the cell faces.

Problem-Domains

Problem domains can be arbitrarily complex in one or two space dimensions, but contiguity is assumed. Two-dimensional domains may be made up of an arbitrary number of regions, with differing parameter definitions in all or any region. Three dimensional domains are constructed as layered extrusions of two-dimensional domains, and so are more restricted. Any number of layers may be specified, and material parameters may be different in any layer of any region. Layer interfaces may be non-planar, specified by arbitrary functions of 2D spatial coordinates, but must not intersect.

Adaptive-Meshes

FlexPDE automatically generates an unstructured computational mesh of triangles or tetrahedra, which fill the domain and match region boundaries. The initial mesh is adaptively refined during solution until a user-specified accuracy tolerance is met. In time dependent problems, meshes will be refined where necessary, and un-refined where no longer required, so that mesh density will follow moving fronts.

Problem-Descriptors

FlexPDE uses a sophisticated grammar-based input format, which allows problem descriptions to be written in a compact and readable form, following very closely the mathematical description of the equations and parameters. The problem domain is specified by walking the region boundaries, attaching boundary conditions as appropriate.

Graphical-Output

Graphical output can be requested for any function of independent and dependent variables and constants. Available graphic formats include contour plots, surface plots, elevations (line-outs), vector fields, and displaced meshes. Arbitrary function values, including area and surface integrals, can be reported on any plot, and a summary page can be written with reports of arbitrary function values.

System Requirements

FlexPDE requires the following computer specifications:

Personal computer with a 486 or higher processor (Pentium-class recommended)

Microsoft Windows 95 or Windows NT (version 4.0 or later)

16 Mbytes of memory (32 Mbytes for 3D)

10 Mbytes of free disk space

VGA or higher resolution monitor

Mouse or trackball pointing device.

4-Discussion of Results

4.1 Superconductor Thermal Stability Based on Diffusion Model

The numerical results for superconductor thermal stability based on diffusion heat conduction model are shown in Figs (4.1-4.24).

Figure (4.1) shows the effect of dimensionless Joule heating on type II-superconductor maximum temperature-time history (which is adopted as a criterion for superconductor thermal stability). It is obvious that as the dimensionless Joule heating increases the evolution of temperature with time increases. When the maximum temperature $\theta 1$ collapses below the critical temperature θ_c=1, i.e. for Q<0.29, the superconductor is said to be thermally stable and has the self ability to recover its superconducting state after a quench has been occurred. While, at Q=0.29 the maximum temperature drops to the critical temperature within a certain time τ_c and then it becomes fixed at a value equal to θ_c. This value of dimensionless Joule heating is known as the critical Joule heating, which indeed determines the critical current density for a specific superconducting wire operating at a certain conditions. For a value of dimensionless Joule heating greater than the critical one, the maximum temperature will grow with time, and the superconductor is said to be thermally unstable. In this case the normal zone will propagate until it covers the whole superconductor and eventually the superconductivity will be completely destroyed.

Figures (4.2a, b, and c) illustrate the dependence of temperature profile, θ, (the temperature distribution along the conductor axis) on dimensionless Joule heating at different dimensionless time for type II. By comparing the three curves, it is clear that

when the value of Q is higher than the critical one, the maximum temperature will grow with time, whereas when Q is less than critical value the maximum temperature will collapse. Also, the heat penetration depth, conductor length affected by the disturbance, increases with time. The physical justification of the above behavior is clear.

The effect of dimensionless Joule heating Q on type I-superconductor thermal stability is shown in Fig. (4.3) and (4.4). The behavior here is similar to that of type II, but the value of critical Joule heating is much less. The reason for this behavior is that the transition temperature of type I, θ_{c1}, is lower than the transition (critical) temperature θ_c of type II, thereby increasing the Joule heating dissipation within the type I conductor. So, much more energy is required to raise the temperature of type II superconductors. Thus one can say that type II has a better thermal stability characteristics compared to type I counterparts. Figures (4.4a, b and c) show the temperature disturbution along the axis of type I superconductor wire at different times and for different values of Joule heating. It can be seen that, the higher the Q the higher the maximum temperature, while the thermal penetration depth is independent of Q at the same instance of time. As time elapses the maximum temperature value may increases or decreases depending upon the Joule heating. If The Joule heating is higher than the critical values the maximum temperature increases and vice versa.. Further more, the thermal penetration depth increases steadily with time regardless the Joule heating

The effect of lateral cooling on type II -superconductor thermal stability is shown in Figs. (4.5) and (4.6). It is clear, as shown in Fig. (4.5), that the lateral cooling has a significant effect on superconductor thermal stability. While the superconductor is unstable for $H<0.5$, it will enter the critical stability region at

dimensionless lateral cooling H=0.5, which refereed as critical dimensionless lateral cooling H_c. For H greater than H_c the superconductor transfers to operate in a safe and stable region. The temperature profiles become shallow as H increases (Fig. 4.6).

The effect of lateral cooling on type I-superconductor thermal stability is similar to type I, but the value of H_c is much larger, which means that type I requires more cooling compared to type II counterparts (Fig. (4.7)). Also, this behavior results from the lower transition temperature of type I which indeed required an excessive cooling to maintain the operating temperature below the transition one.

Each value of dimensionless Joule heating Q requires a specified value of dimensionless lateral cooling H to force the superconductor to operate within the thermal stability region. These values are shown in Fig. (4.8) for type II at different values of disturbance intensity. At small values of Q and B, the lateral cooling is of minor importance and therefore the superconductor may be operated adiabatically within the stability region. While, at larger values of Q and B the importance of lateral cooling increases dramatically. Also, it can be seen from Fig. (4.8) that a small increase in Q requires a small increase in H, While a small increase in B requires higher increase in H. Thus, the disturbance intensity plays a major role in superconductor thermal stability.

The required H corresponding to Q at different value of disturbance intensity for type I superconductor is shown in Fig. (4.9). The thermal stability is more sensitive to disturbance intensity compared to Q. The increase of the required H at higher value of disturbance intensity is somewhat sharp, while at low values of Q the increase of the required H is weakly dependent on the disturbance intensity.

The stability curve $Q_c(B)$ separates the field of operating conditions into a region of stable operation, which is of interest to the designer, and a region of

unstable operation conditions, which must be avoided. Figure (4.10) is the relation between the step disturbance intensity B and the critical Joule heating (heat dissipation) at different value of lateral cooling. For H=0.0, Q_c decreases sharply with the increasing disturbance strength B. The stability margin increases dramatically with the cooling magnitude. The maximum rate of increase in the stability margin occurs at the first step of lateral cooling, and then the rate of increase reduces as the lateral cooling increases. Thus the importance of lateral cooling is clarified. For example, at a disturbance intensity of 5, the critical Joule heating will increase by 50% as the amount of lateral heat cooling increases by 100%. Also, it can be seen that the stability region becomes narrower as the disturbance intensity increases, and the rate at which the stability region shrinks is inversely proportional to lateral cooling value. The stability criterion obtained here, from the numerical solution, matches the analytical results obtained by Bejan and Tien (1978) for B>4. Toward small disturbances, B<4, the numerical results of this study lie with 5% under the analytical predictions (see Fig. 4.11). In conclusion, the analytical results verify the results obtained in this work.

Figure (4.12) shows the effect of heat generation on type II superconductor thermal stability subjected to Gaussian disturbance. It can be seen that, the critical heat generation is less than that in the case of step disturbance, which means that step disturbance, has a significant effect on superconductor thermal stability. The effect of disturbance nature on superconductor thermal stability is shown in Figs. (4.13) and (4.14). The stepwise disturbance has a greater influence on superconductor thermal stability compared to the Gaussian counterpart.

Figure (4.15) shows the stability criterion curve (Qc-B) for a superconductor subjected to Gaussian disturbance at different values of lateral cooling. It is clear that

the stability has been improved by increasing the lateral cooling. The increase in stability region becomes greater as the disturbance intensity increases. For example, at B=2 an increase of H from 0 to 1 results in increase in the stability region by a bout 62.5%, while the same increase in H results in about 1022% at B=10. This emphasizes the importance of lateral cooling at larger disturbance intensities.

Figure (4.16) shows the influence disturbance initial length (i.e. the normal zone initial length) on type II superconductor thermal stability. For a point disturbance L=0, the maximum temperature (stability criterion) falls sharply to zero and reaches its steady state value in about 2.5 dimensionless time. So, we can say that a point disturbance will not lead to normal zone propagation. It is clear that as L increases (wider initial normal zone) the temperature evolution increases with time and eventually brings the superconductor to unstable operation.

As the disturbance length increases the type I superconductor thermal stability becomes worse; this is clear from Fig. (4.17).

The maximum temperature evolution with time increases as the duration time increases (Fig. 4.18). At Q=0.25 the type II -superconductor is stable for τ_i less than 0.4, while it shifted to unstable operation at higher dimensionless time (Fig. 4.18a). While for Q=1.0 the type II-superconductor is thermally unstable regardless the duration time (Fig. 4.18b).

The effect of disturbance duration time on type I-superconductor thermal stability is shown in Figs. (4.19) and (4.20). It is obvious that as the duration time decreases the thermal stability will be improved. In this case the superconductor is thermally stable for dimensionless duration time less than 0.35 which less than the corresponding value for type II-superconductor. As the duration time increases the temperature profile becomes sharper, with higher values at the disturbance center.

The type II has better thermal stability characteristics compared to type I counterpart, this result from the two critical temperature for type II, while type I has only one critical temperature (see Figs. 4.21 and 4.22)

Figures (4.23a and b) shows the effect of current sharing temperature on type II -superconductor thermal stability. It can be seen, from Fig. (4.23), the evolution of temperature with time increases as the current sharing temperature decreases, which means that the superconductor thermal stability tends to fail. This behavior can be explained or justified by the fact that the Joule heating increases as the current sharing temperature decreases.

The effect stabilizer to superconductor ratio f on superconductor thermal stability is shown in Fig. (4.24a and b). It is clear that the superconductor thermal stability has been improved as the value f increases. The interoperation of this behavior is that when a normal zone initiates, the current shifts from the superconducting material to the stabilizer (normal metal) material. And, since the resistivity of superconducting material at normal state is much higher than the resistivity of the stabilizer, (1000 times the resistivity of the stabilizer at normal sate). This will lead to a significant decrease in the resulting Joule heating, which mean an improvement in thermal stability.

4.2 Superconductor Thermal Stability Based on Wave Model

The numerical results for superconductor thermal stability based on wave model are shown in Figures (4.25-4.36).

different shapes. In the case of hyperbolic model more energy is concentrated at the edge of the conductor which results in a higher temperature at this region. The higher temperature causes greater growth of heat generation as the capacity of heat sources increases with temperature, and so on.

In the case of a conductor with an internal heat source whose capacity depends on temperature, the differences between temperature profiles obtained from wave and diffusion models do not disappear as the time increases to infinity (Fig. 4.30). Here. For β=15 the temperature profiles obtained from the two models vary a lot (Fig. 4.30c). Long time solutions are shown in Fig. (4.31). It can be seen that the differences between the models increase steadily with time.

As the disturbance length increases the maximum temperature evolution of type II -superconductor increases (Figs. 3.32a and b). Also, It can be noticed that the wave structure decreases as the length increases. In the presence of duration time the wave behavior is more clarified (Fig. 4.32b).

As the disturbance length decreases the type I-superconductor thermal stability improved. Also, it can be seen that the wave structure of the maximum temperature history curve destroyed as the disturbance length increases (Fig. 4.33).

The results in Fig. (4.34) show that the duration time of the disturbance length has a destructive role in thermal stability of type II-superconductor. The superconductor is stable for duration times less than 0.4 and unstable for larger times.

The disturbance duration time has a critical role in superconductor thermal stability, such as the thermal stability is significantly improved as the disturbance duration time decreases. Here, for type I-superconductor the critical duration time equals 0.75 (Fig. 4.35).

The effect of current sharing temperature on type II-superconductor thermal stability is shown in Fig. (4.36). It is clear that the current sharing temperature has a minor effect on thermal stability. Even that the maximum temperature decreases slightly as the current sharing temperature increases.

4.3 Superconductor Thermal Stability Based on Dual-Phase-Lag Model

The numerical results for superconductor thermal stability based on dual-phase-lag model with R=5.0 (i.e. $\tau_T = 2.5\tau_q$), will be shown in Figs. (4.37-4.52).

The results of Fig. (4.37) and Fig. (4.38) show the effect of Joule heating for type II and type I-superconductor respectively. It is clear that the increase in Joule heating forced the superconductor of both types to operate outside the stability region.

The influences of lateral cooling on type II -superconductor and type I-superconductor are shown in Figs. (4.39) and (4.40) respectively. A similar effect has been noticed for both types, with much higher values of H required to stabilize type I-superconductor compared with type II counterparts.

The effect of disturbance length on type II-superconductor and type I-superconductor are shown in Figs. (4.41) and (4.42) respectively. It can be stated that as the disturbance length increases the thermal stability region shrinks.

The effect of disturbance duration time on type II-superconductor and type I-superconductor are shown in Figs. (4.43) and (4.44) respectively. It is clear that as the duration time increases the maximum temperature increasing, eventually the superconductor will shift to operate in unstable region.

Comparison between the stability criterion for type II-superconductor and type I based on the three previous conduction models is shown in Fig. (4.45) and (4.46) for

two values of lateral cooling parameter. For type II-superconductor, at H=0.0, and for low values of B <4, the wave model should be used to determine the thermal stability of type II-superconductor, to ensure a safe and stable operation of the superconducting wires. While, for high values of disturbance intensity B>4 the diffusion model should be used. For, H=1.0, and for very low values of B the wave model should be used, and the diffusion model should be used for the remaining values of B. It seems that the dual-phase-lag model is overestimating the stability region, and thus, it is non-recommended to use in the analysis of superconductor thermal stability. For type I-superconductor (Fig. 4.46) a similar behavior has been seen, with narrower stability region.

Figure (4.47) presents a comparison between maximum temperature history, thermal stability, of type II-superconductor based on three previously mentioned models. The difference between wave and diffusion behaviors is very clear. Also, it can be seen that as R increases the predicted maximum temperature decreases.

A comparison between temperature profiles for type I superconductor with wide disturbance l=1 obtained based on the three macroscopic heat conduction model is shown in Fig. (4.48) at different dimensionless times. At very short time the difference between the profiles is insignificant and the heat penetration in the case of diffusion model is the largest one (Fig. 4.48a). As time passes, the difference between the dual-phase-lag model and diffusion model increases, with increase in the heat penetration distance (Fig. 4.48b and c). At much higher times the shapes of temperature profile obtained based on dual-phase-lag model approach those obtained by the other two models, but the predicted temperature based on dual-phase-lag-model still lower than that predicted by the other two models. Also, the heat penetration distance remains higher. At the same time the thermal penetration depth

into the conductor increases with the ratio R. This is also the effect of microstructural interaction because the ratio R is proportional to temperature gradient lag time.

The effect of current sharing temperature on superconductor thermal stability is illustrated in Fig. (4.49). The minor role played by the current sharing in thermal stability is clarified. The thermal stability improves as the current sharing temperature increases, this refer to the reduction of Joule heating associated the higher values of current sharing temperature.

Based on the wave model, Fig. (4.50) shows the type II-superconductor maximum temperature at various values of initial rates $\theta^{\cdot}$. The curves without a rate effect, rate-0.0, is the similar to that shown in Fig. (4.25). The initial time-rate of change of temperature reflects a uniform heating applied at t=0, resulting in a significant temperature rises throughout the entire body and particularly the center of the disturbance $\theta 1$. when the initial temperature rate increases the maximum value of $\theta 1$ increases and the time at which the maximum occurs is also increases. This is the temperature overshootimg phenomenon that canot be depicted by diffusion model.

Based on dual-phase-lag model with R=5, Fig. (4.51) shows that as the intial temperature rate increases the type II superconductor maximum temperature increases. But, here the nonunifomity in maximum temperature history doesnot vanish. For initial rate less than 1 the superconductor may considered to be stable, since the maximum temperature drops below θ_c.

For type I-superconductor the maximum temperature is somewhat differ from that of type II -superconductor (Fig. 4.52). The difference mainly is in temperature overshooting, for type I the overshooting is reduced this may be due to the gradual increases in the electrical resistivity, compared to abrupt change in resistivity for type

I-superconductor. As in the previous two curves the initial temperature rate plays an important role to the superconductor thermal stability issue.

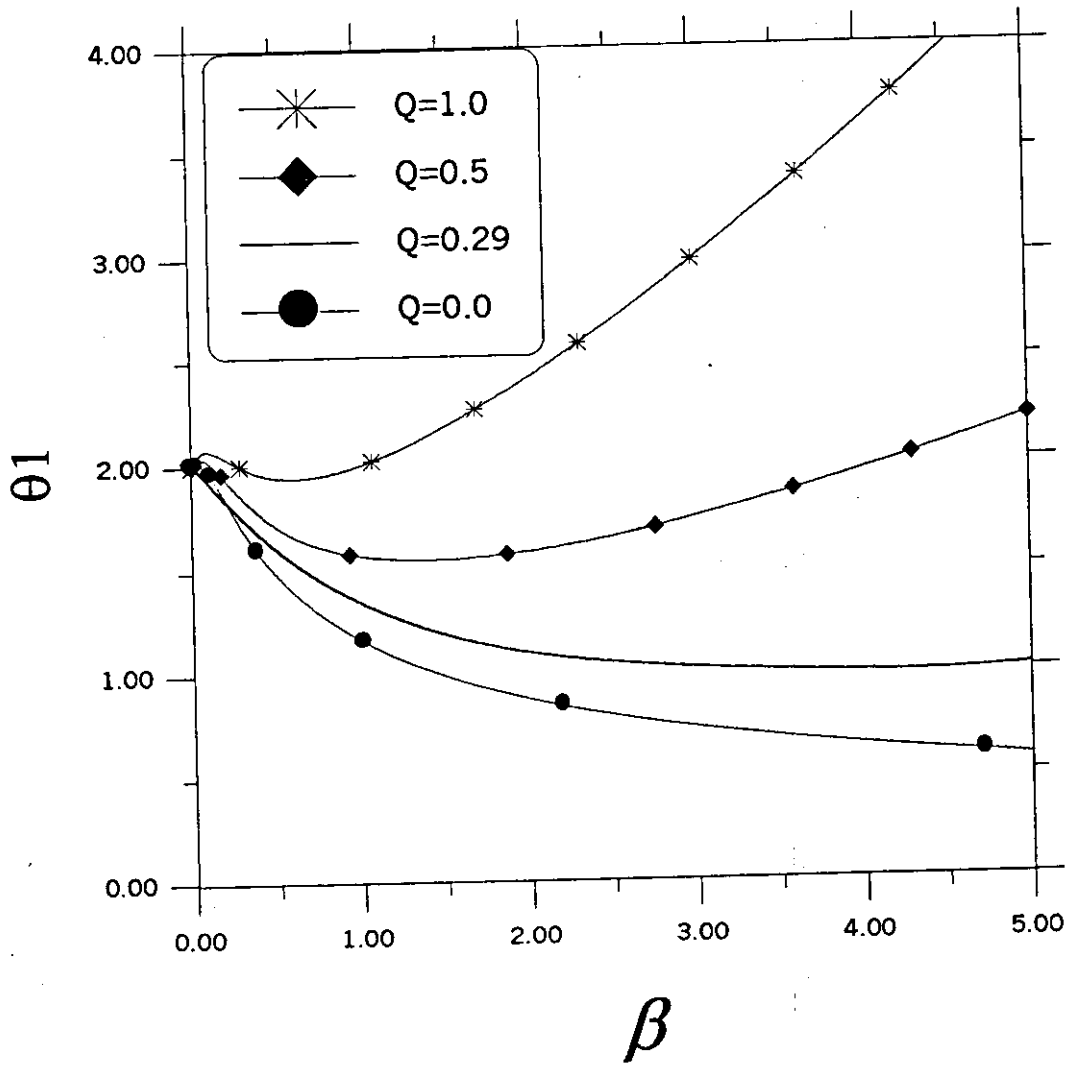

Figure (4.1): Effect of dimensionless Joule heating on typeII-superconductor thermal stability based on diffusion model. (For L=1.0, B=2, H=0.0, ε=0.0, and τ_f=0.0).

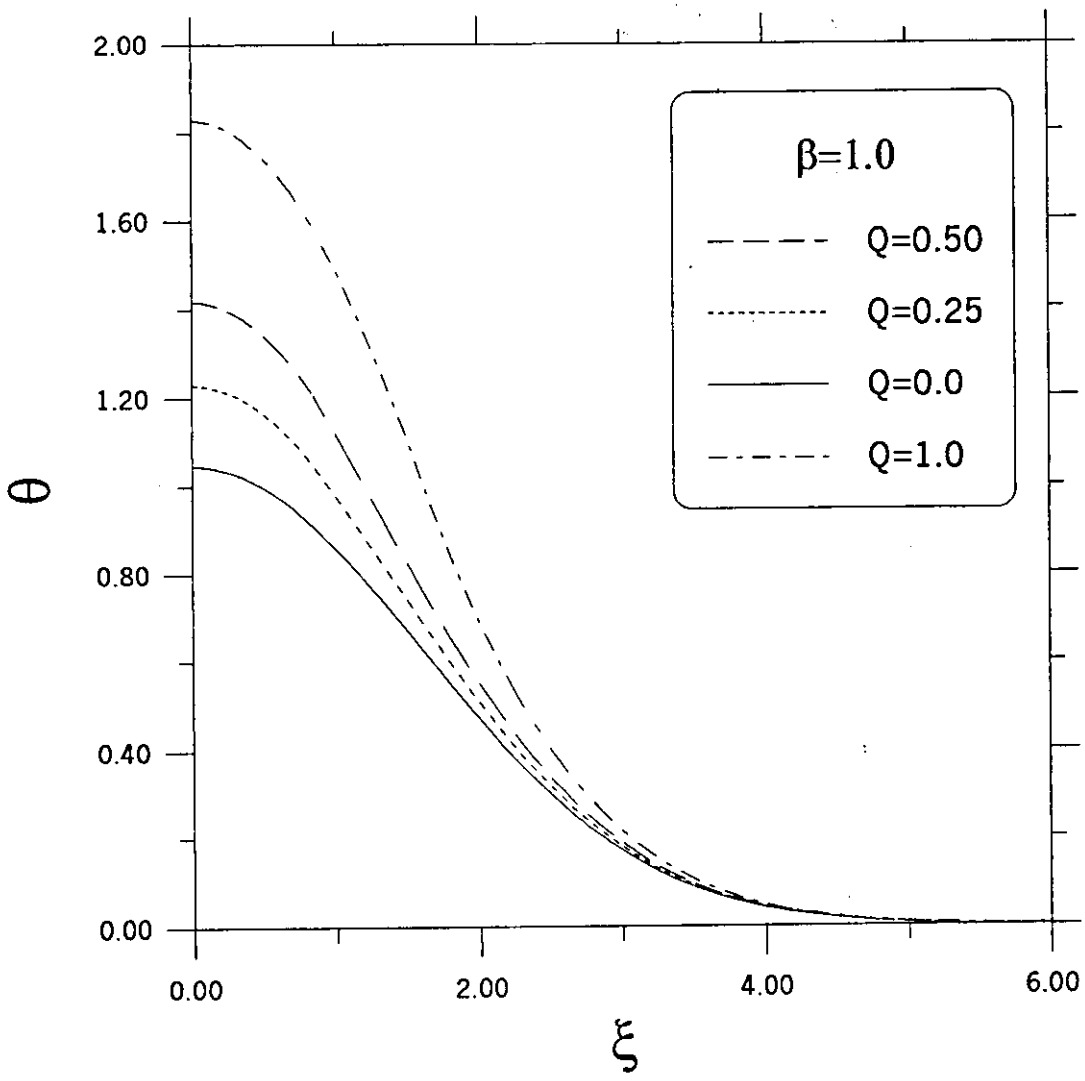

Figure (4.2a): Dependence of temperature profiles on dimensionless Joule heating for typeII-superconductor based on diffusion model. (For L=1.0, B=2.0, ε=0.0, H=0.0, and τ_i=0.0).

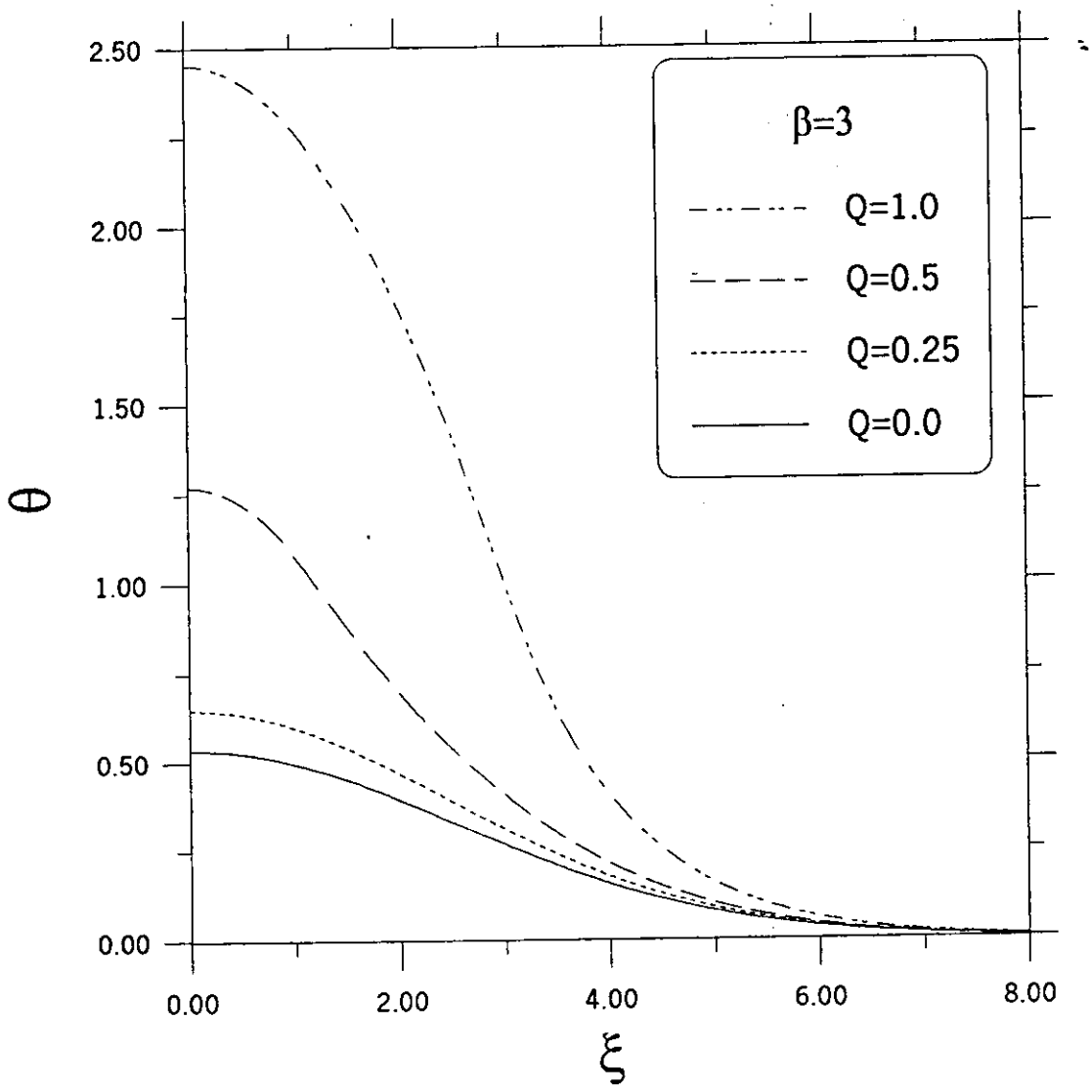

Figure (4.2b): Dependence of temperature profiles on dimensionless Joule heating on typeII-superconductor based on diffusion model. (For L=1.0, H=0.0, B=2.0, ε=0.0, and τ_i=0.0).

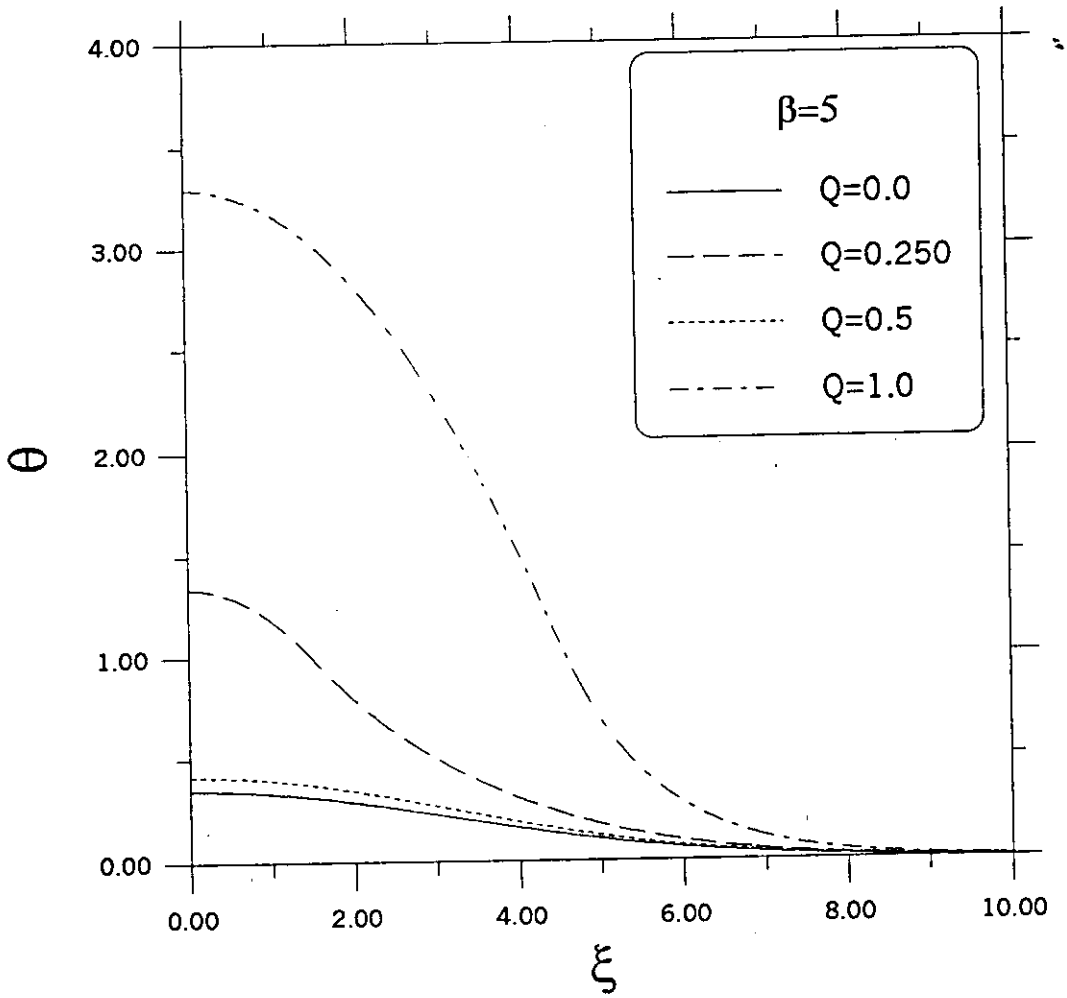

Figure (4.2c): Dependence of temperature profiles on dimensionless Joule heating on typeII-superconductor based on diffusion model. (For L=1.0, H=0.0, B=2.0, ε=0.0, and τ_i=0.0).

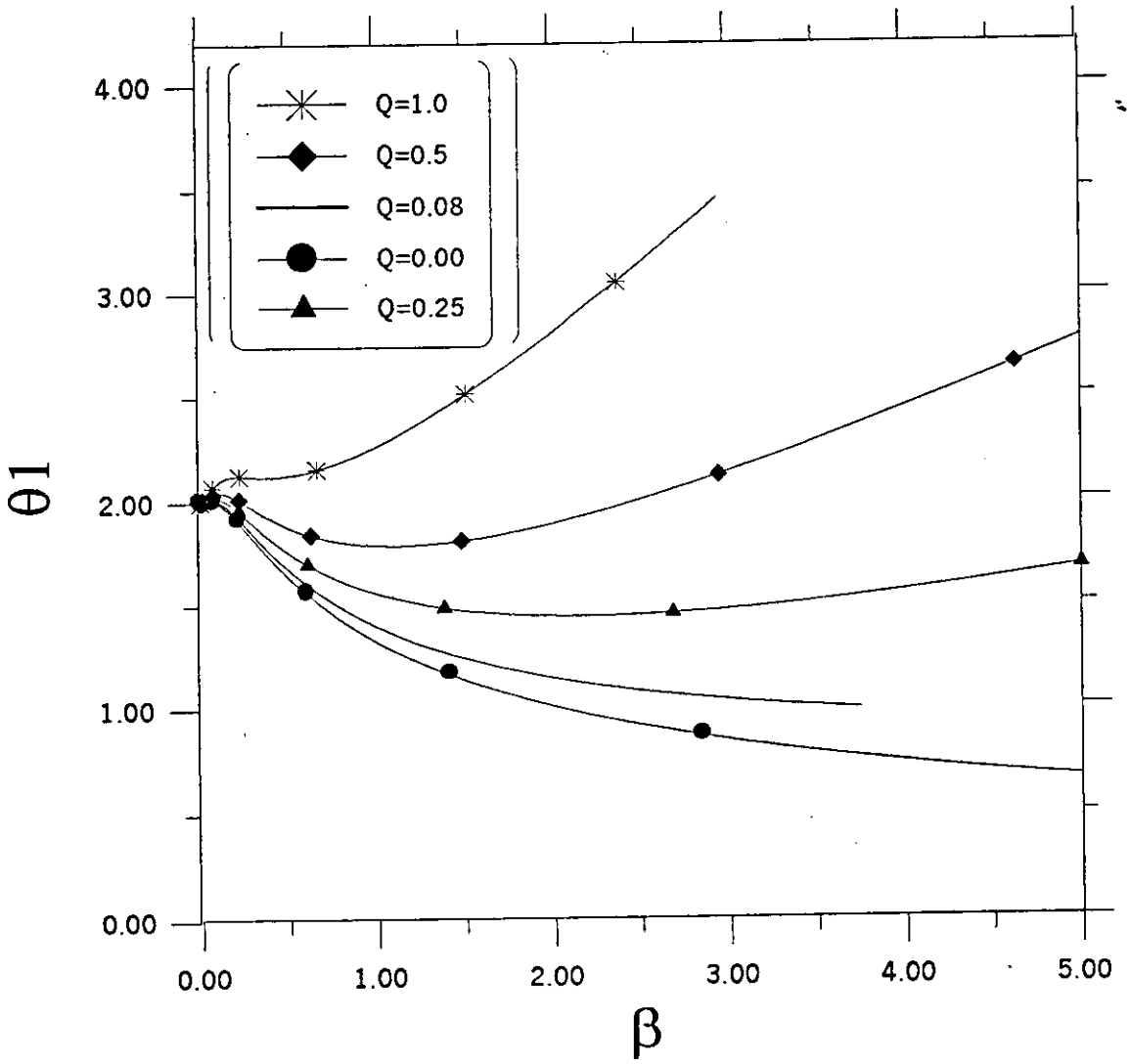

Figure (4.3): Effect of dimensionless Joule heating on typeI-superconductor based on diffusion model. (For L=1.0, ε=0.0, τ_i=0.0, and θ_{c1}=0.1).

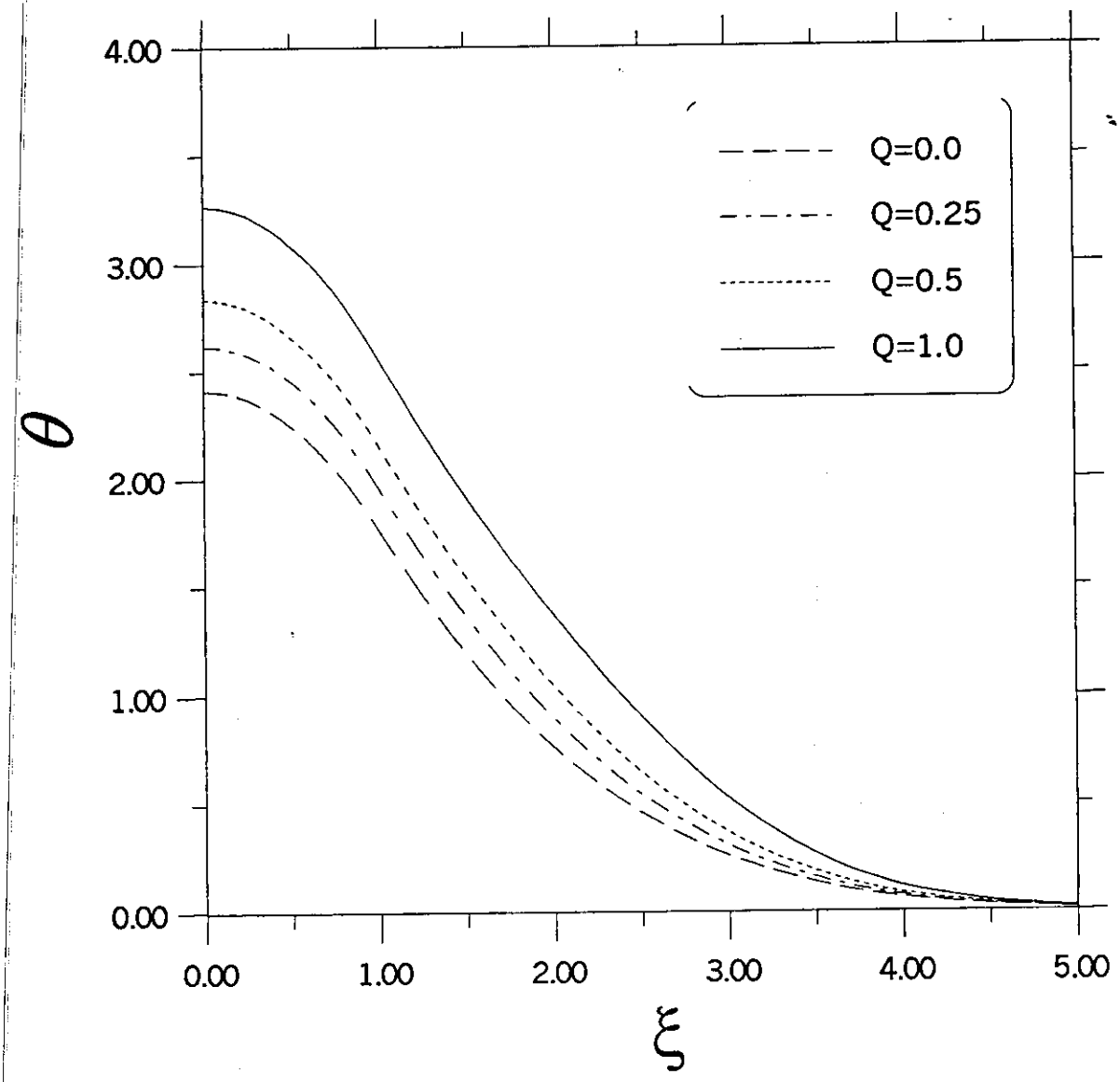

Figure (4.4a): Dependence of temperature profiles on dimensionless Joule heating for type I-superconductor thermal stability based on diffusion model. (For L=1.0, τ_i=0.0, θ_{c1}=0.1, ε=0.0, and H=0.0)

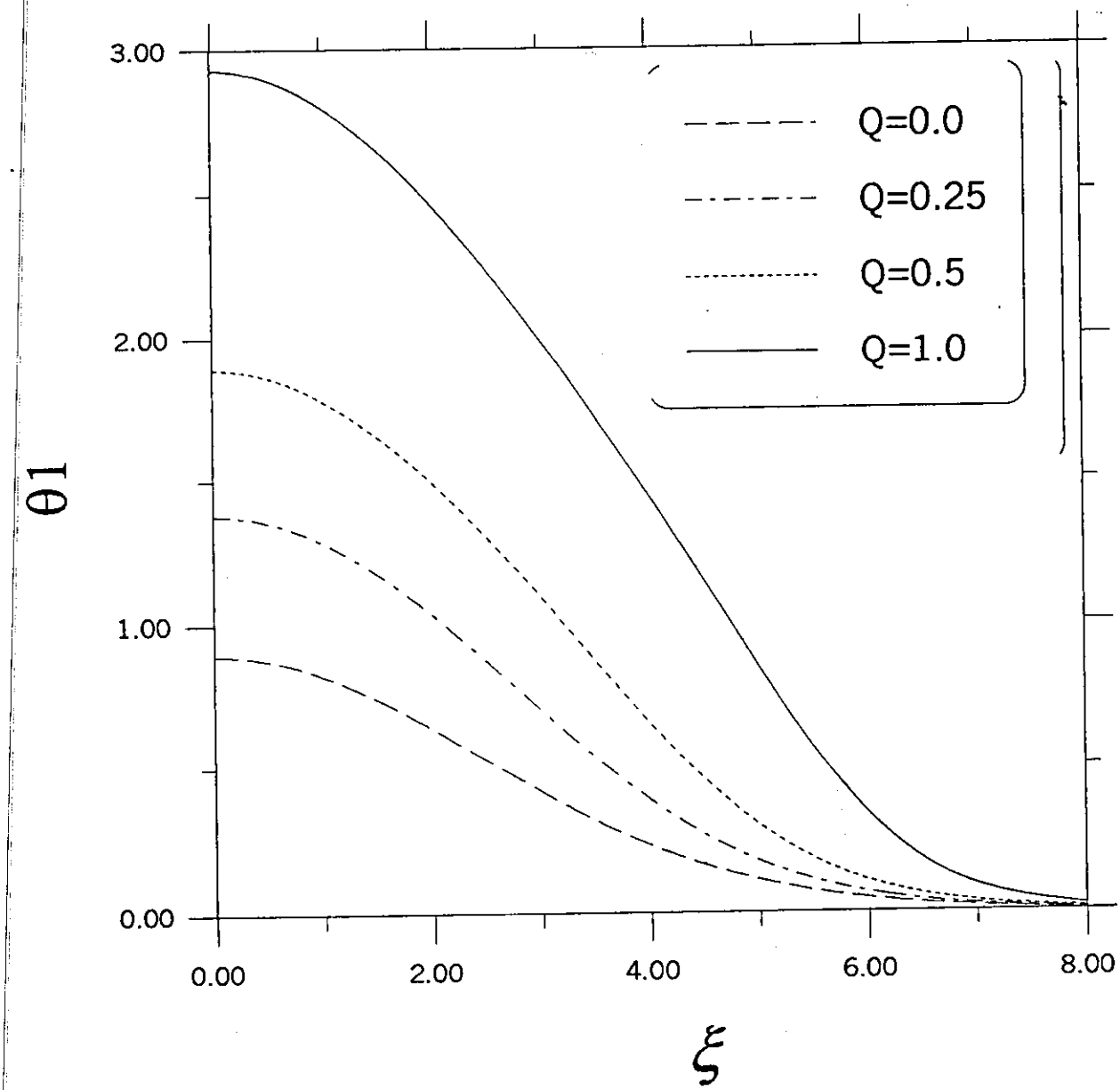

Figure (4.4b): Dependence of temperature profiles on dimensionless Joule heating for typeI-superconductor thermal stability based on diffusion model. (For θ_{cI}=0.1, B=2.0,L=1.0, τ_i=0.0, ε= 0.0,and H=0.0).

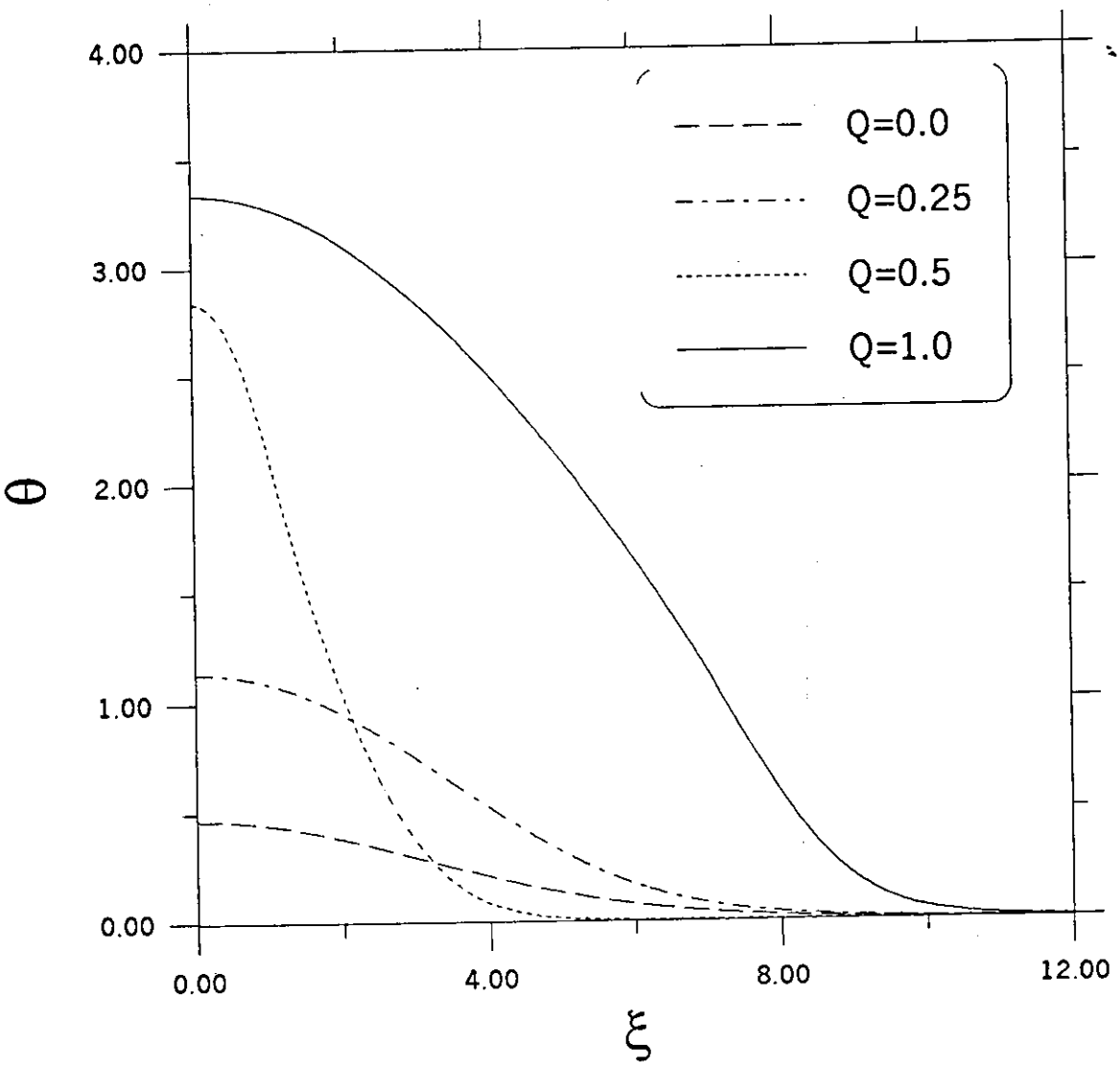

Figure (4.4c): Dependence of temperature profiles on dimensionless Joule heating for typeI-superconductor thermal stability based on diffusion model. (For θ_{c1}=0.1, B=2.0, L=1.0, ε=0.0, τ_i=0.0 and H=0.0)

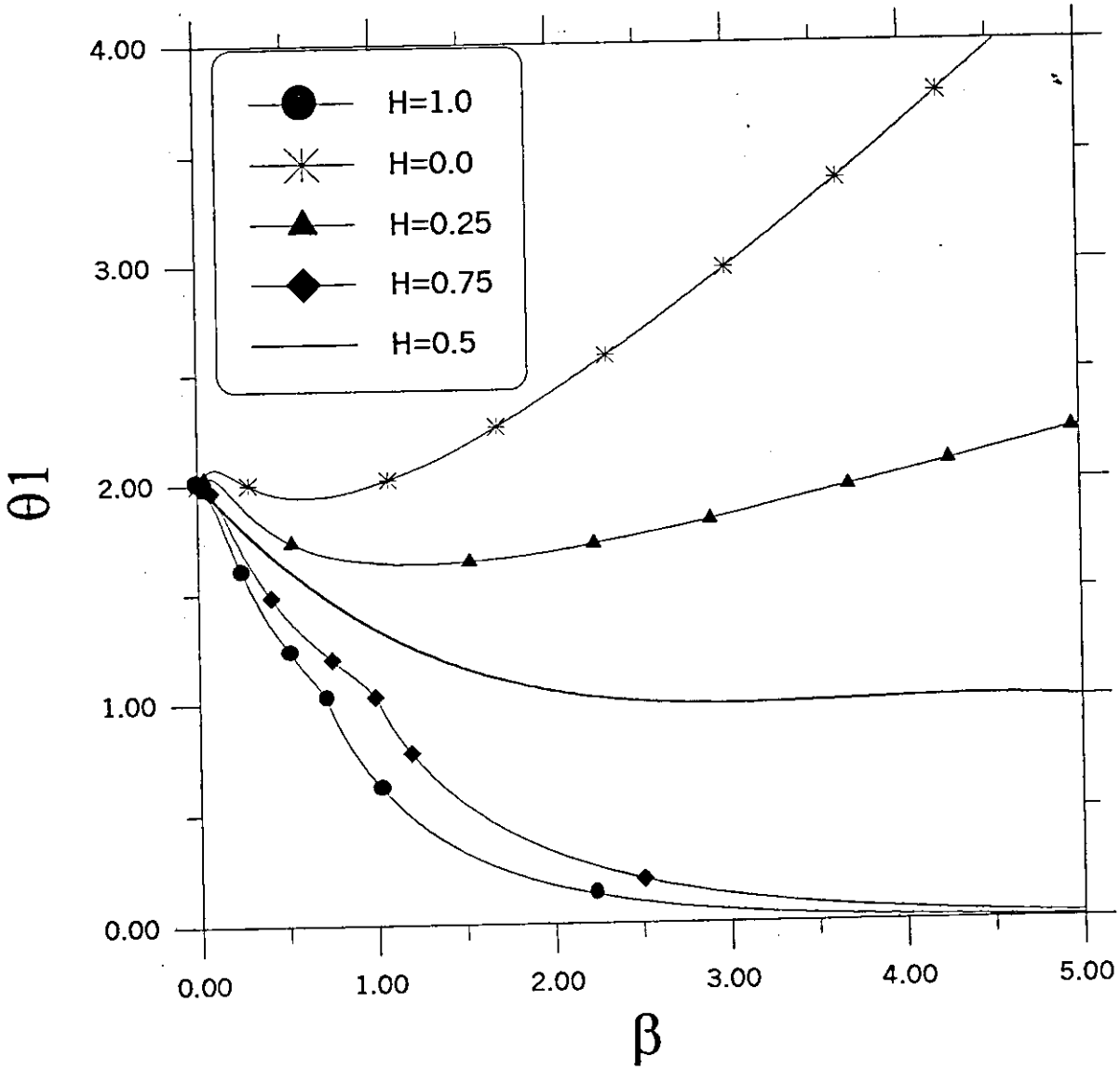

Figure (4.5): Effect of lateral cooling on typeII-superconductor thermal stability based on diffusion model subjected to unit-step disturbance. (For Q=1.0, B=2.0, ε=0.0, L=1, and τ_i=0.0).

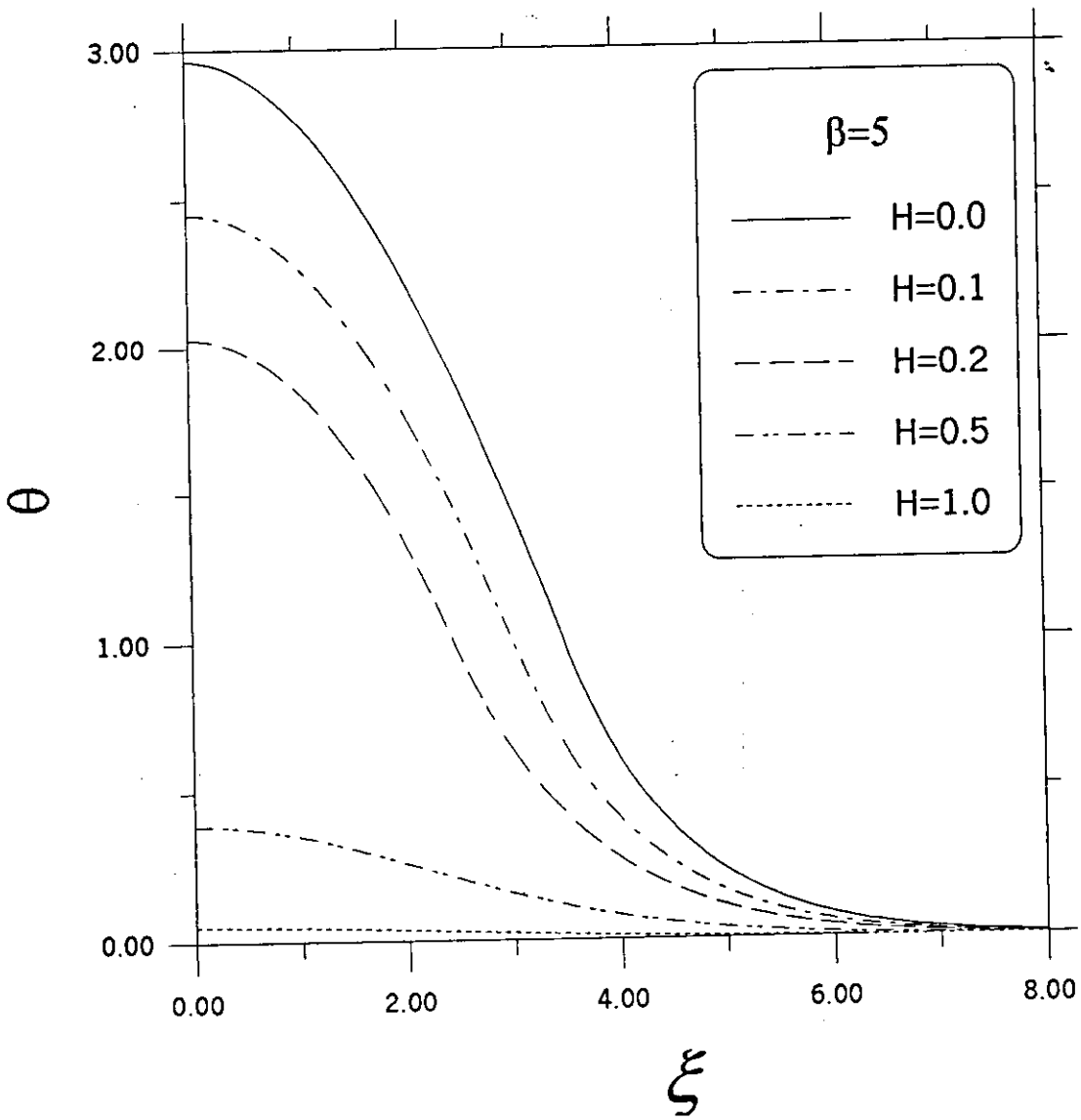

Figure (4.6): *Dependence of temperature profiles on dimensionless lateral cooling for typeII-superconductor based on diffusion model. (For Q=1.0, B=2.0, ε=0.0, L=1.0 and* τ_i*=0.0).*

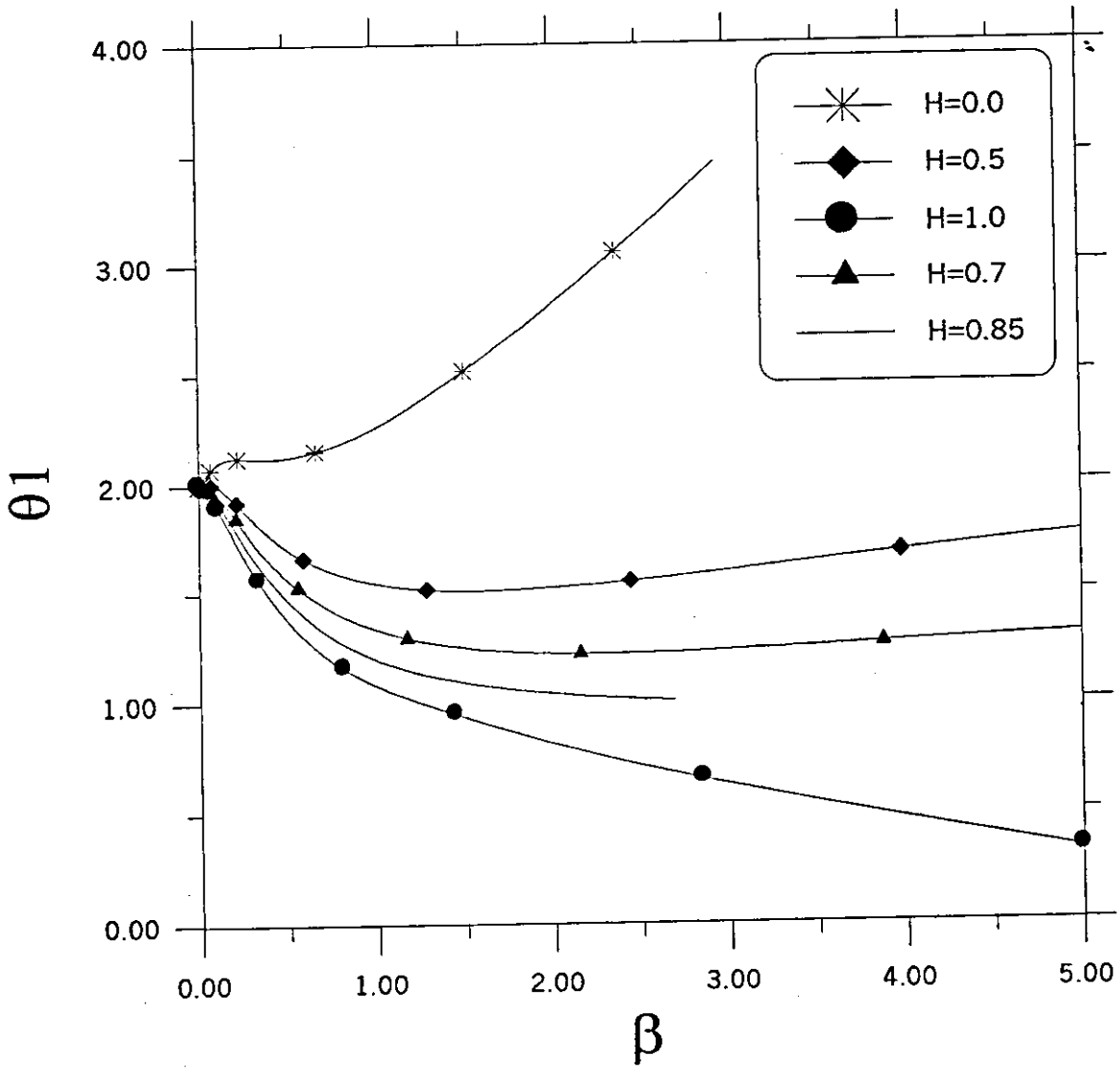

Figure (4.7): Effect of dimensionless lateral cooling on typeI-superconductor based on diffusion model. (For Q=1.0, B=2.0, ε=0.0, θ_{c1}=0.1, τ_i=0.0, and L=1.0).

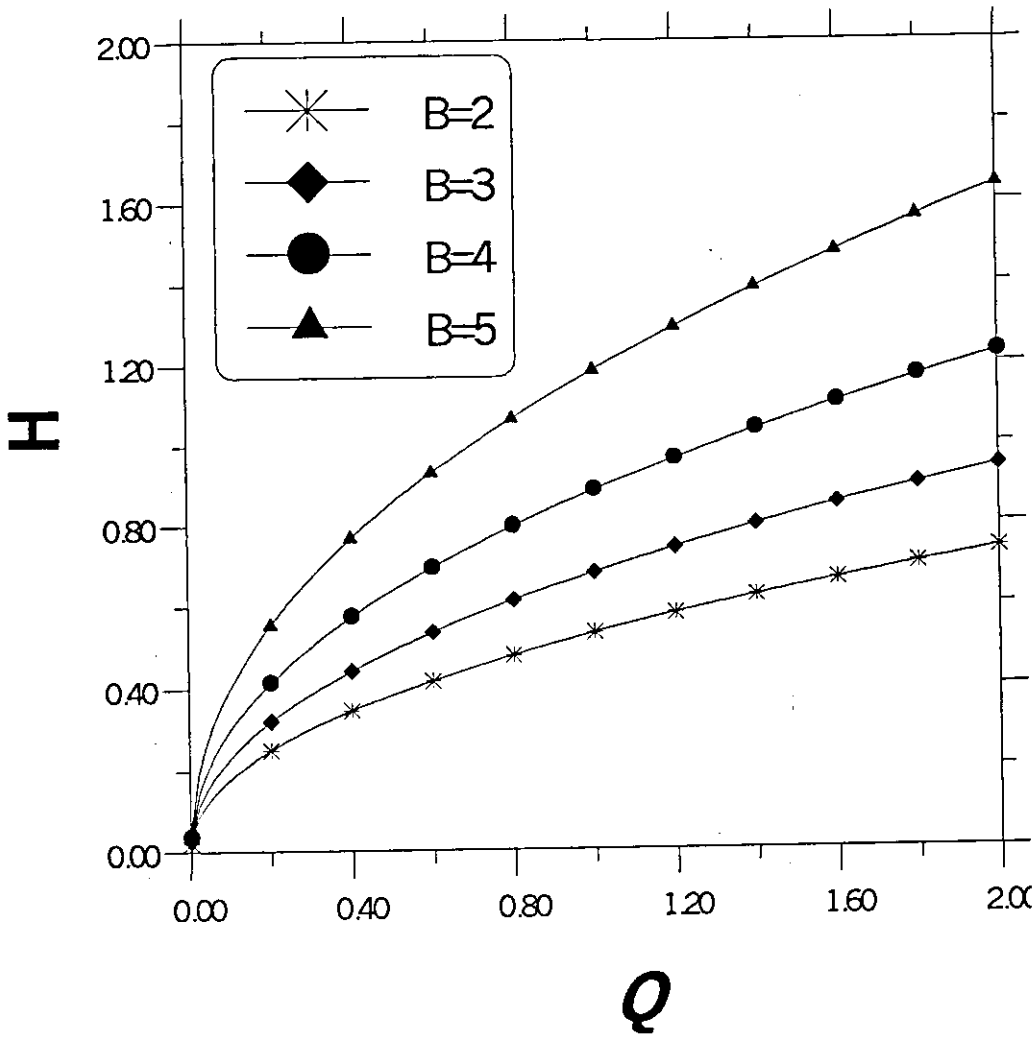

Figure (4.8): Dependence of the required lateral cooling (H) on heat generation (Joule heating) at different values of disturbance intensity for typeII-superconductor based on diffusion model. (For L=1.0, ε=0.0, and τ_i=0.0)

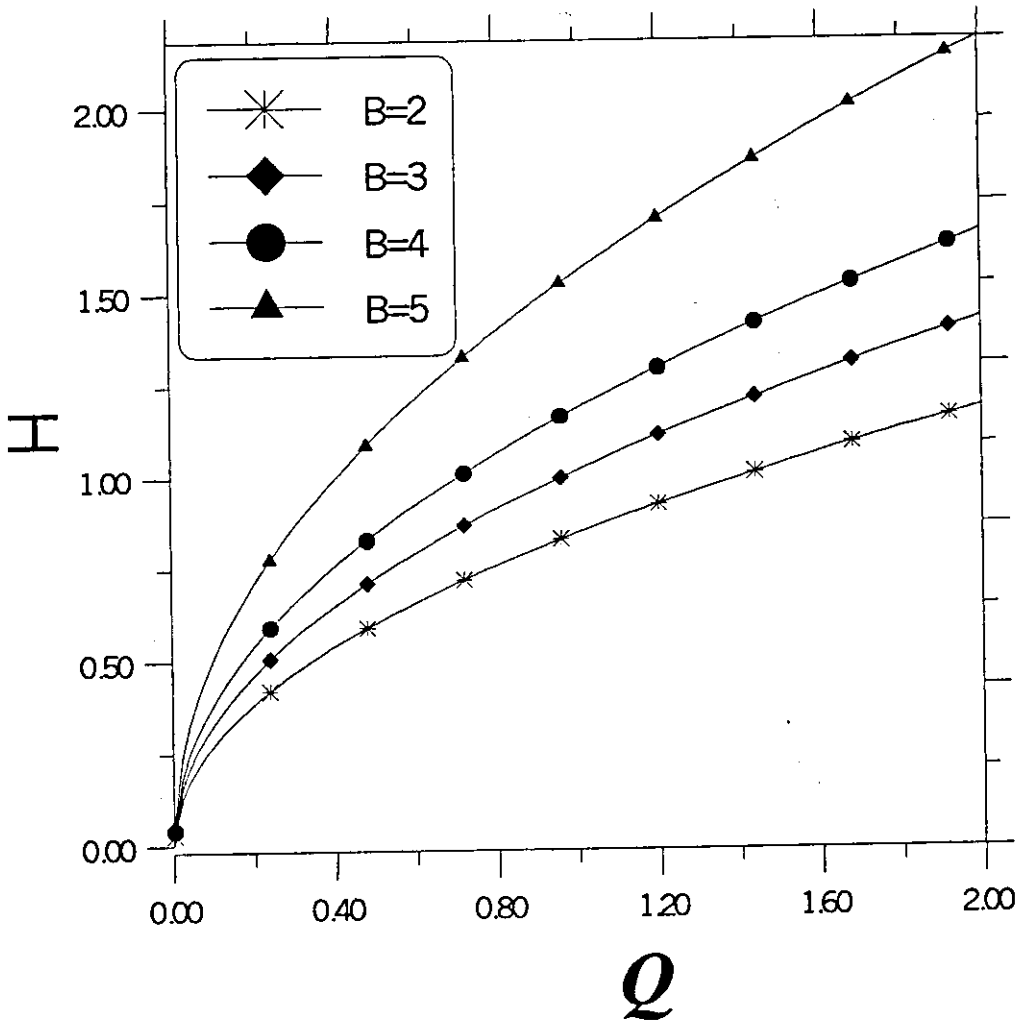

Figure (4.9): Dependence of the required lateral cooling (H) on heat generation (Joule heating) at different values of disturbance intensity for type I-superconductor based on diffusion model. (For L=1, ε=0.0 and, τ_i=0.0)

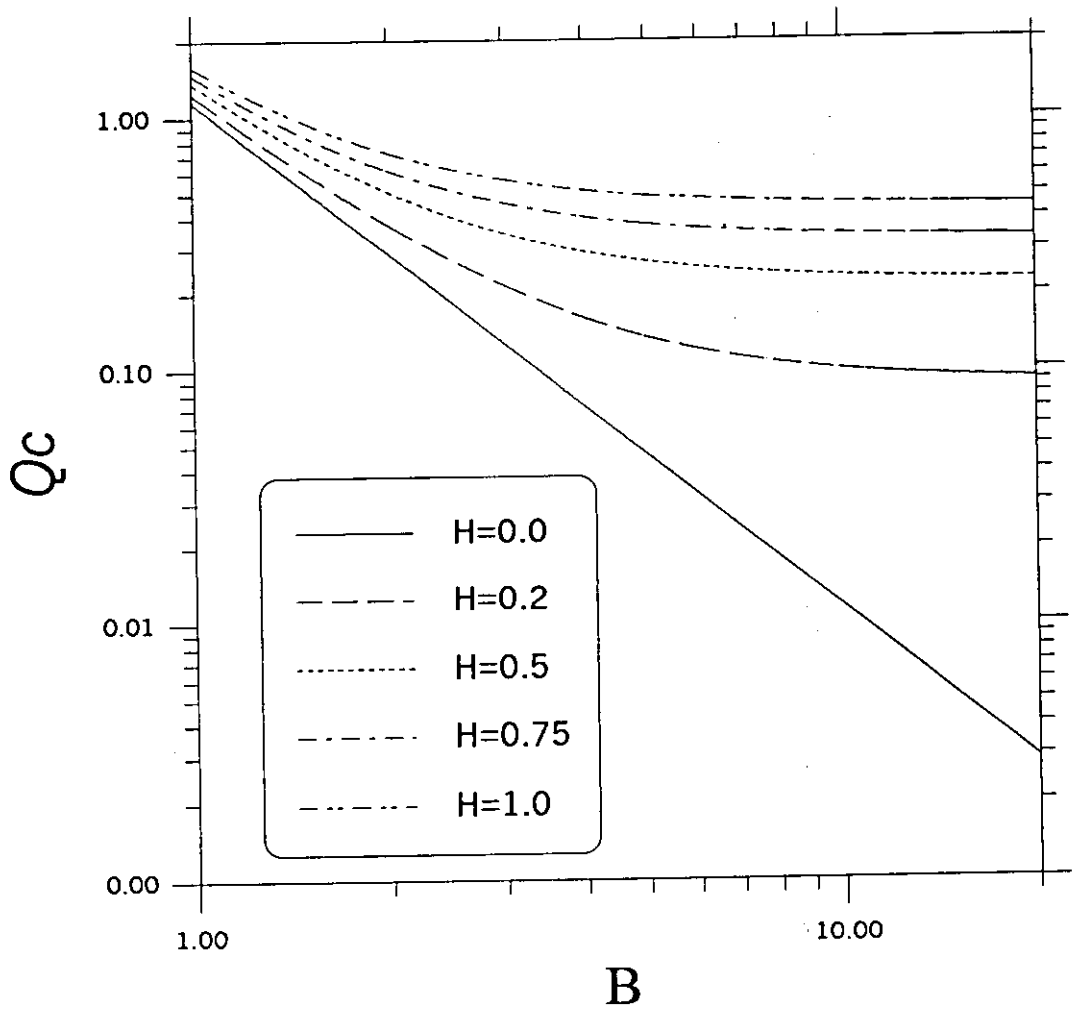

Figure (4.10): The stability criterion for typeII-superconductor subjected to stepwise type disturbance, based on diffusion heat conduction model. (For L=1.0, ε=0.0 and, τ_i=0.0)

(For L=1.0, H=0.0, and τ_i=0.0).

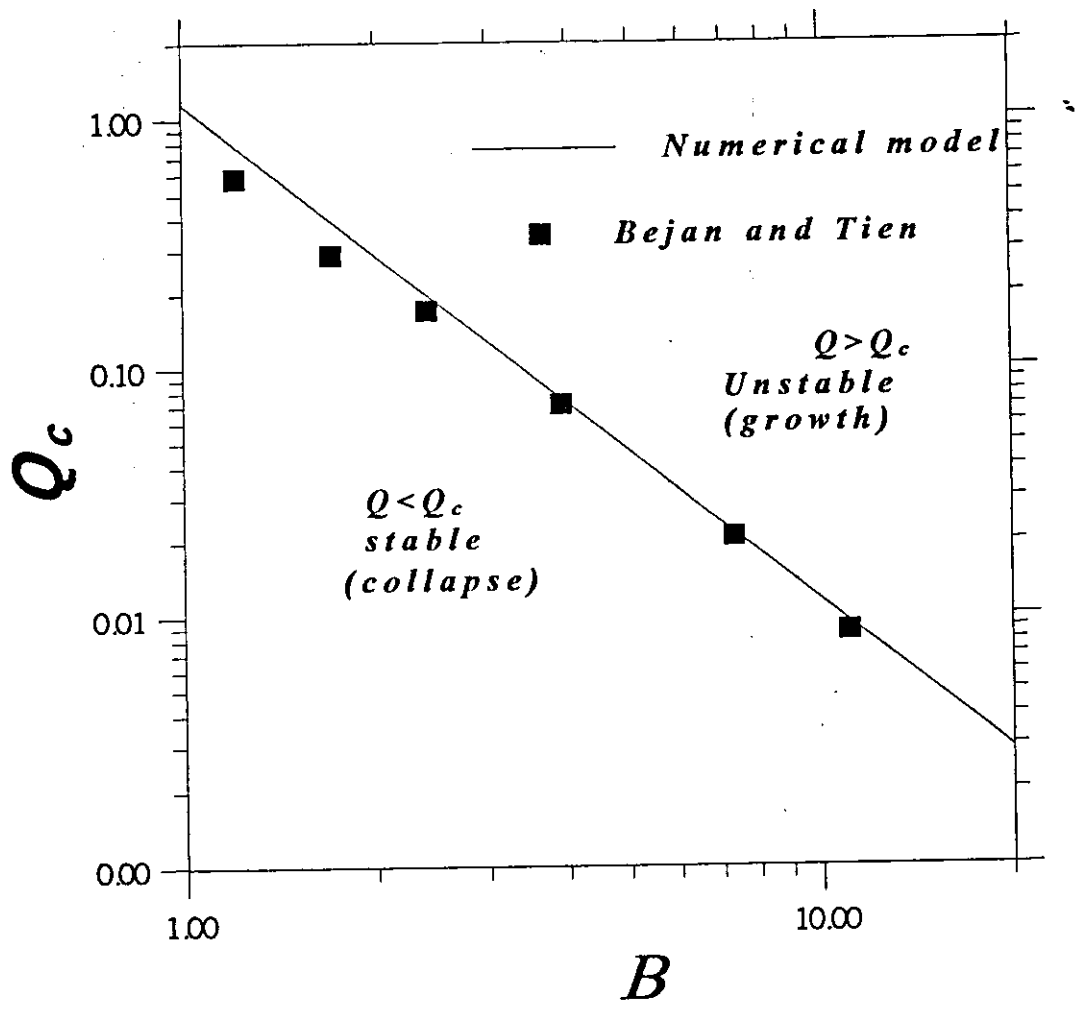

Figure (4.11): Comparison between the results obtained in this study and the results reported by Bejan and Tien (1978). (For L=1.0, ε=0.0, H=0.0 and τ_i=0.0).

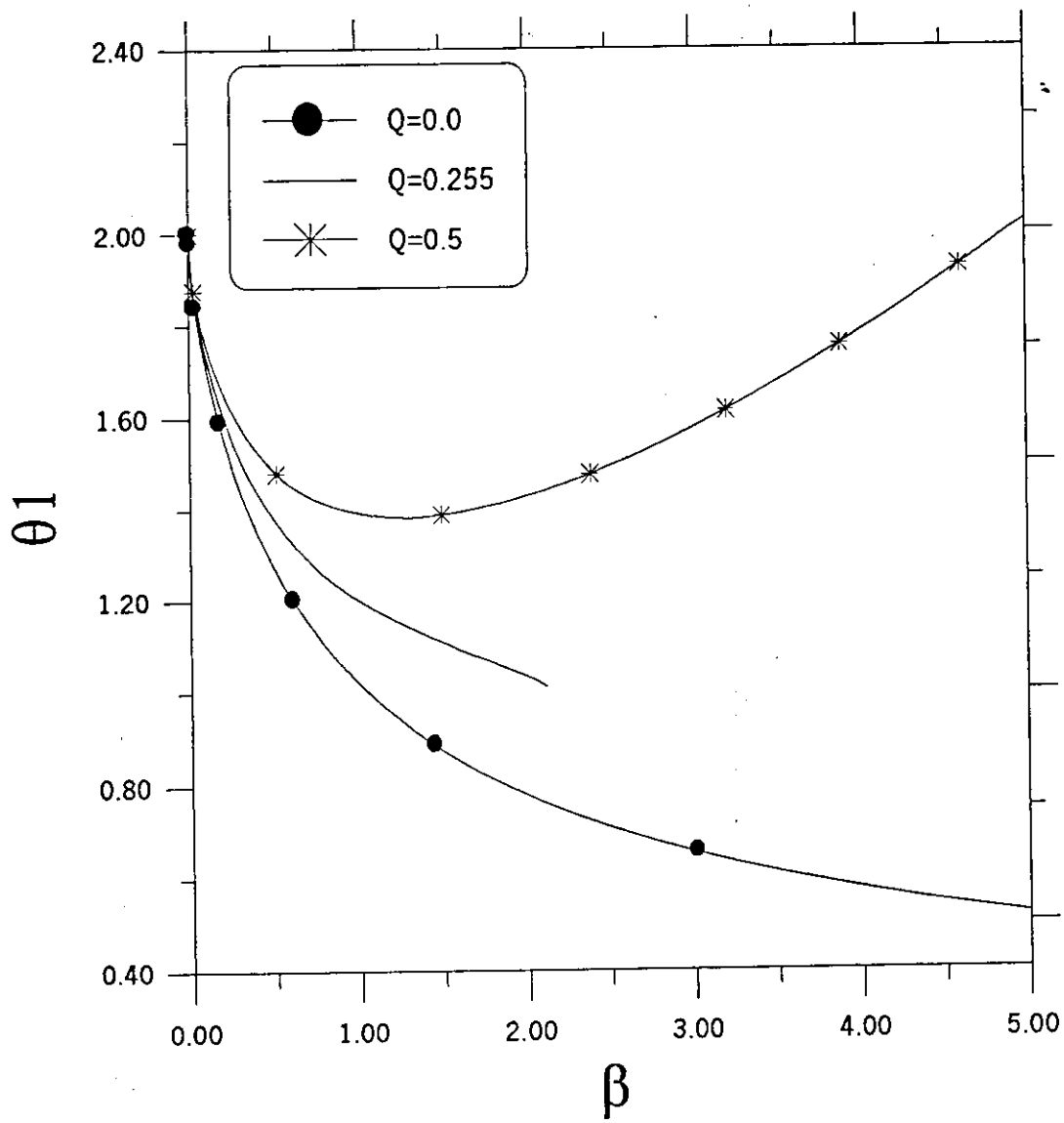

Figure (4.12): Effect of dimensionless Joule heating on typeII-superconductor, subjected to Gaussian heat disturbance, based on diffusion model. (For L=1.0, H=0.0, ε= 0.0, and τ_i=0.0)

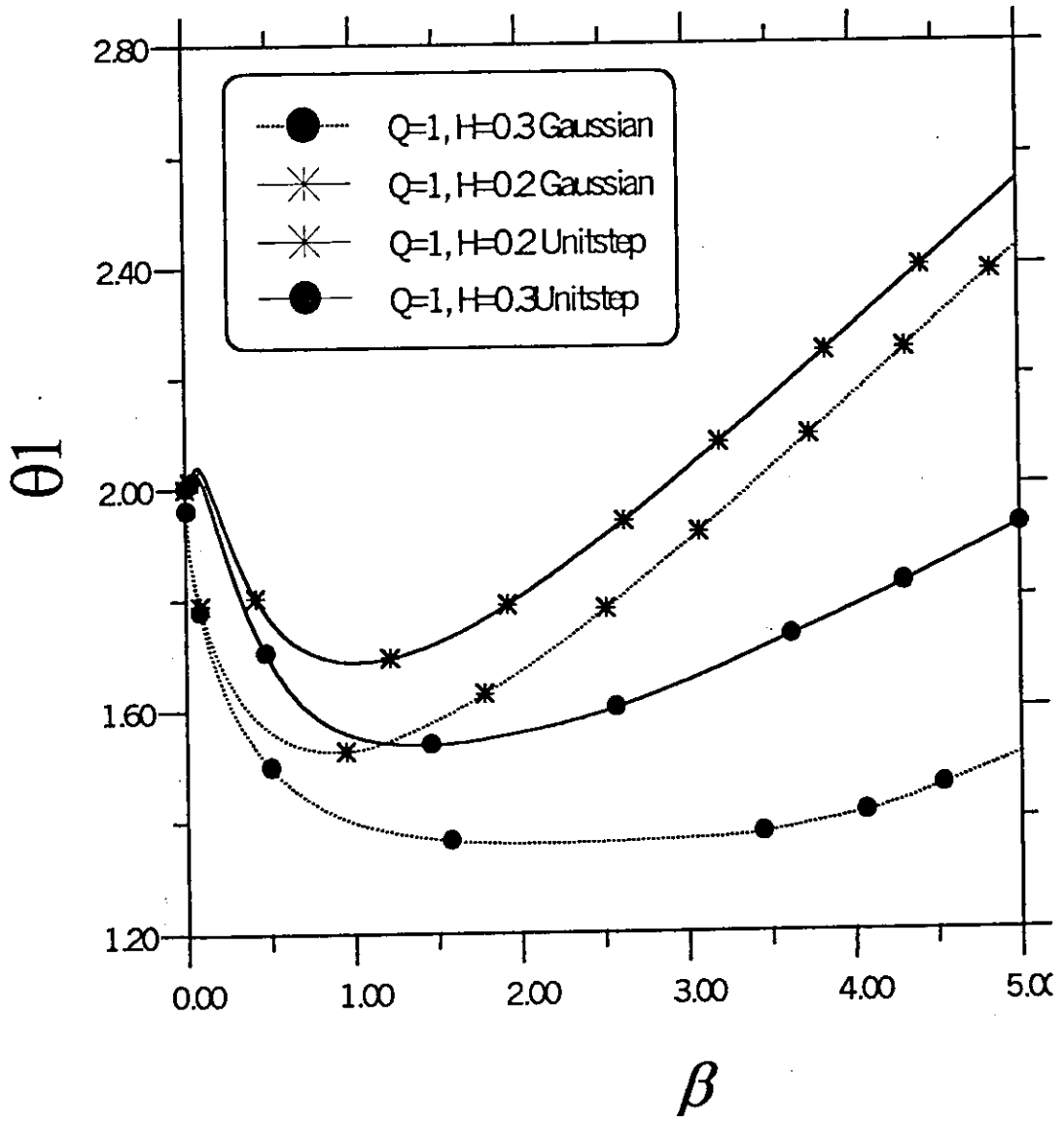

Figure (4.13): Comparison maximum temperature-time history (thermal stability) of typeII-superconductor based on diffusion model subjected to stepwise and Gaussian disturbance. (L=1.0, ε=0.0 and τ_i=0.0).

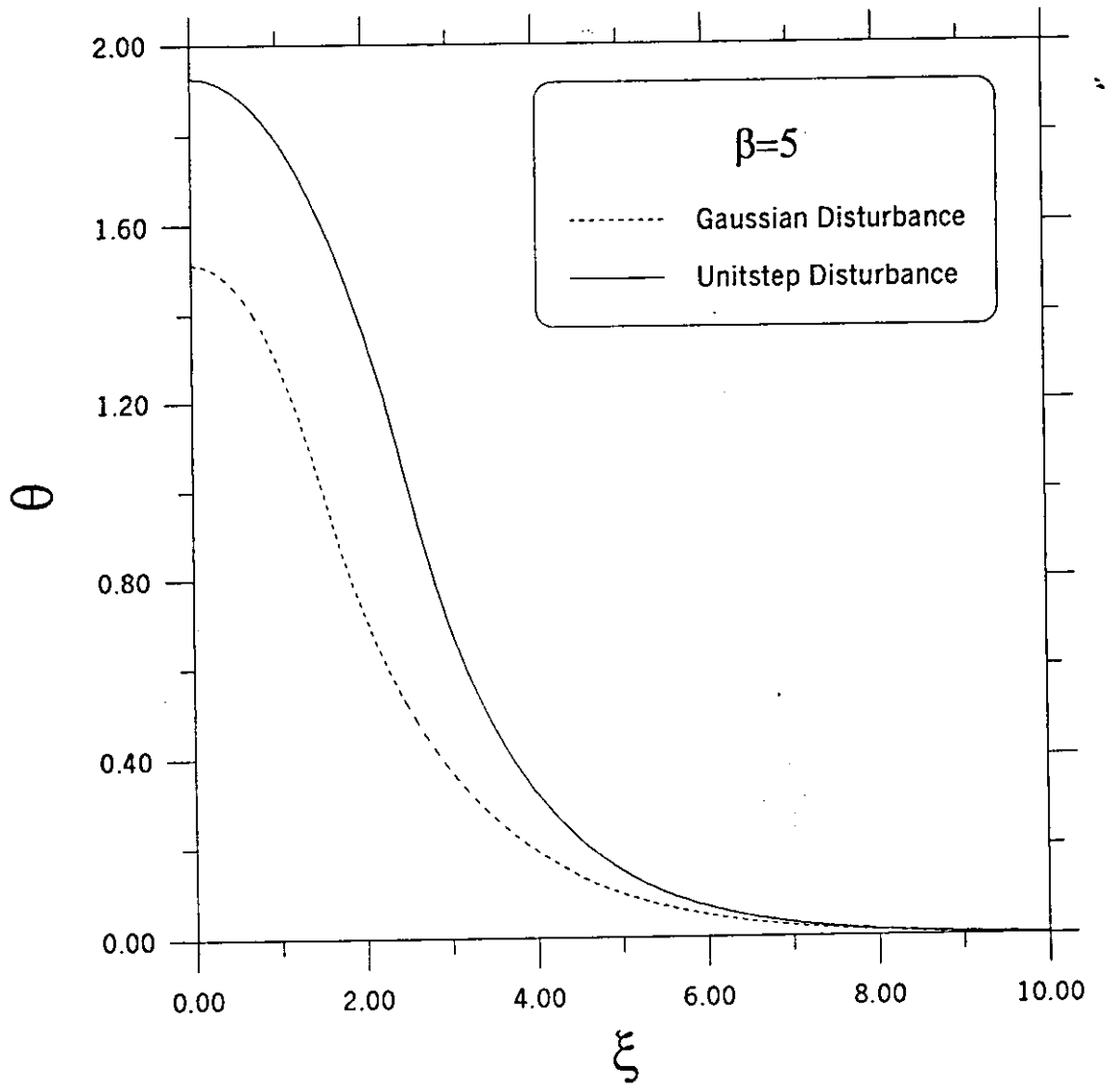

Figure (4.14): Comparison between temperature profiles for type II obtained based on diffusion model subjected to stepwise and Gaussian nature disturbances. (For Q=0.5, H=0.0, τ_i=0.0, ε=0.0 and β=5)

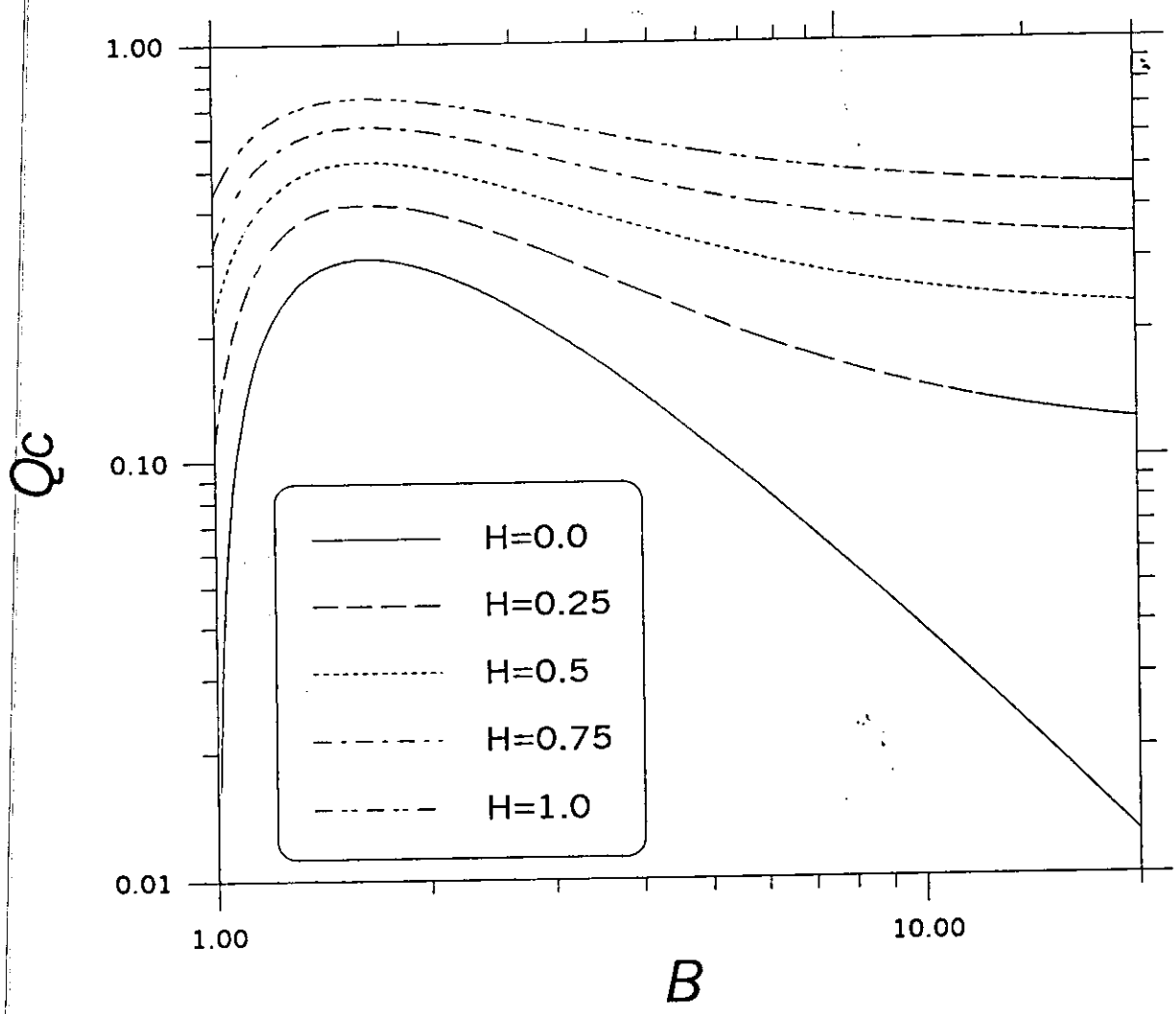

Figure (4.15): The stability criterion for type II-superconductor subjected to Gaussian type disturbance, based on diffusion heat conduction model. (For L=1.0, ε= 0.0, and τ_i=0.0).

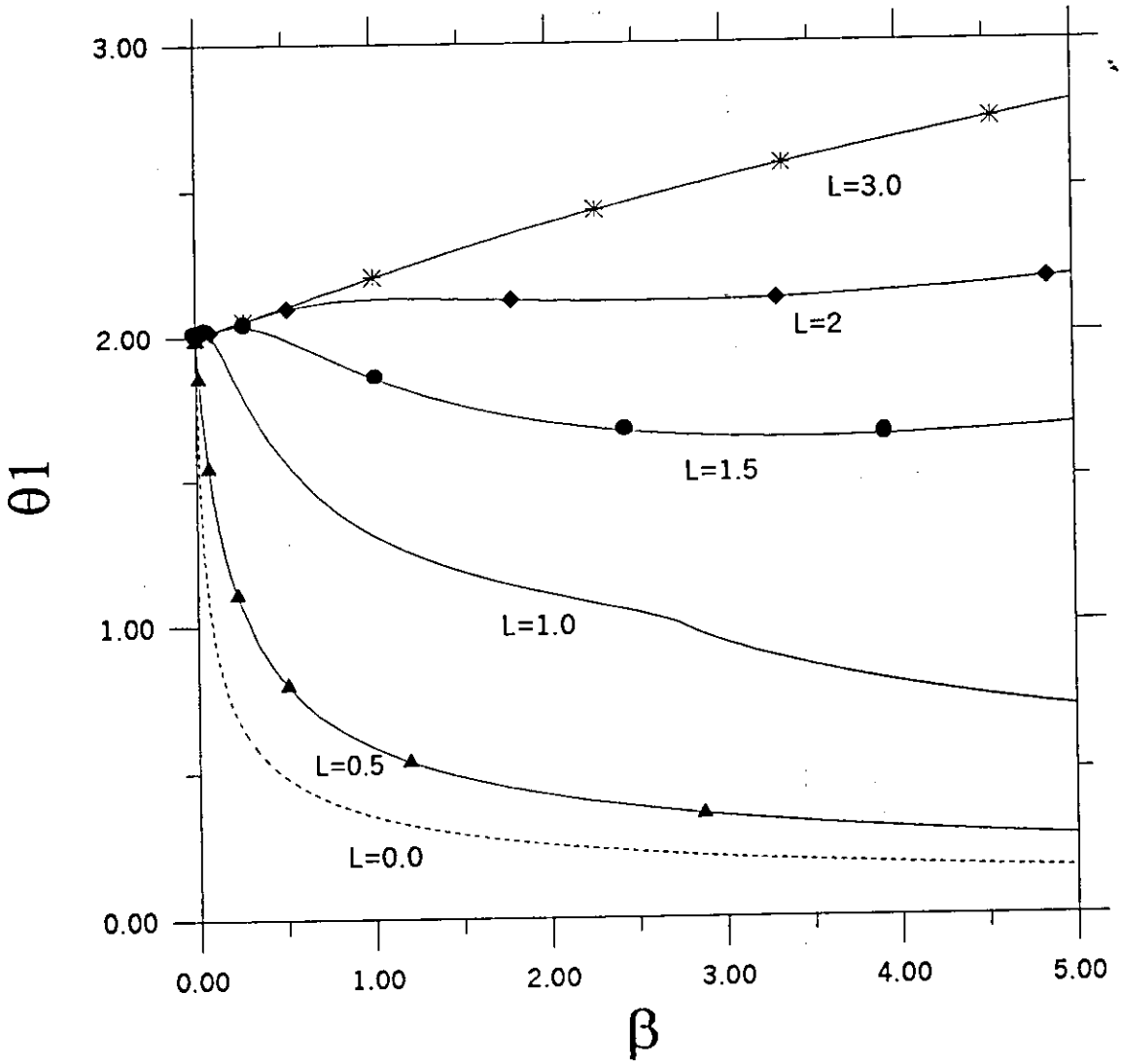

Figure (4.16): Effect of dimensionless disturbance length on typeII-superconductor thermal stability based on diffusion model. (For Q=0.2, τ_i=0.0, ε= 0.0, and H=0.0).

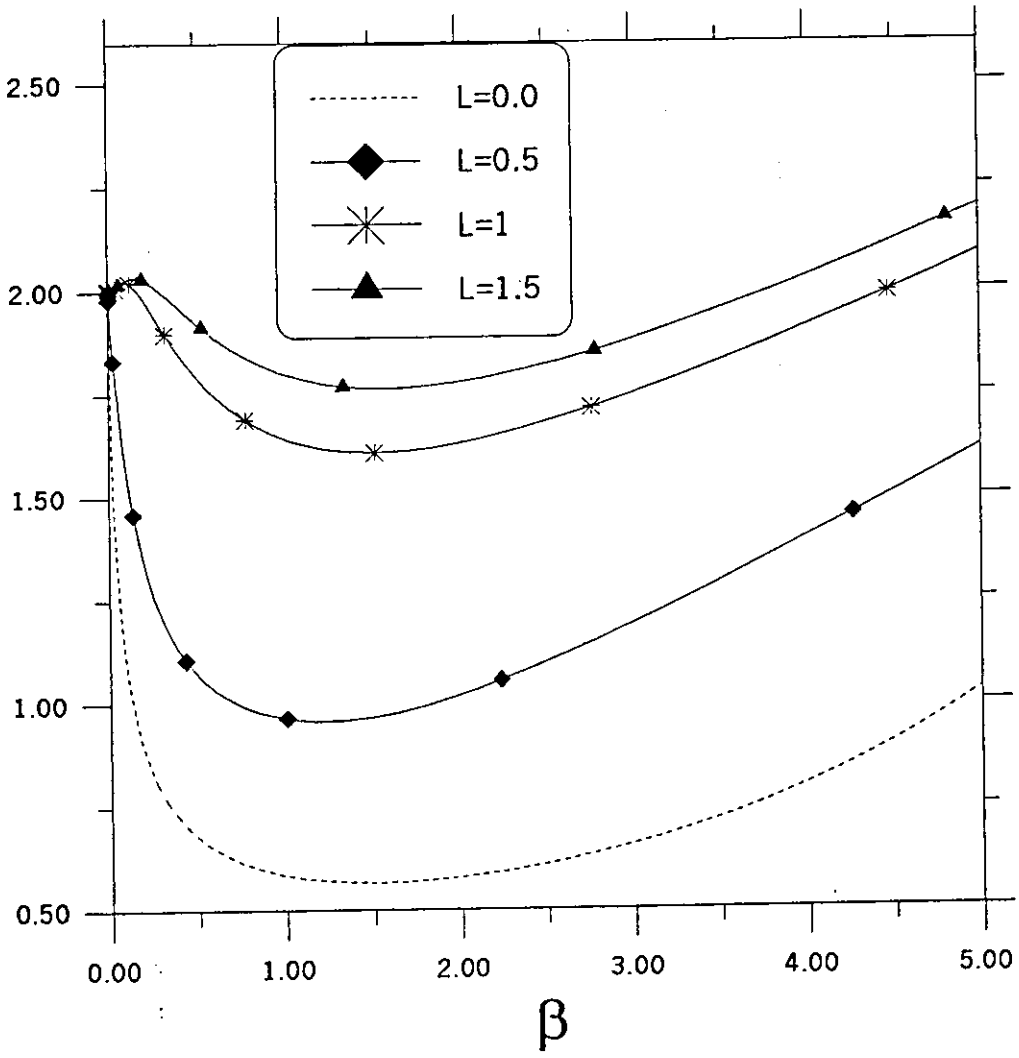

Figure (4.17): Effect of dimensionless disturbance length on type I superconductor thermal stability based on diffusion model. (For Q=0.2, θ_{c1}=0.1, τ_i=0.0, and H=0.0)

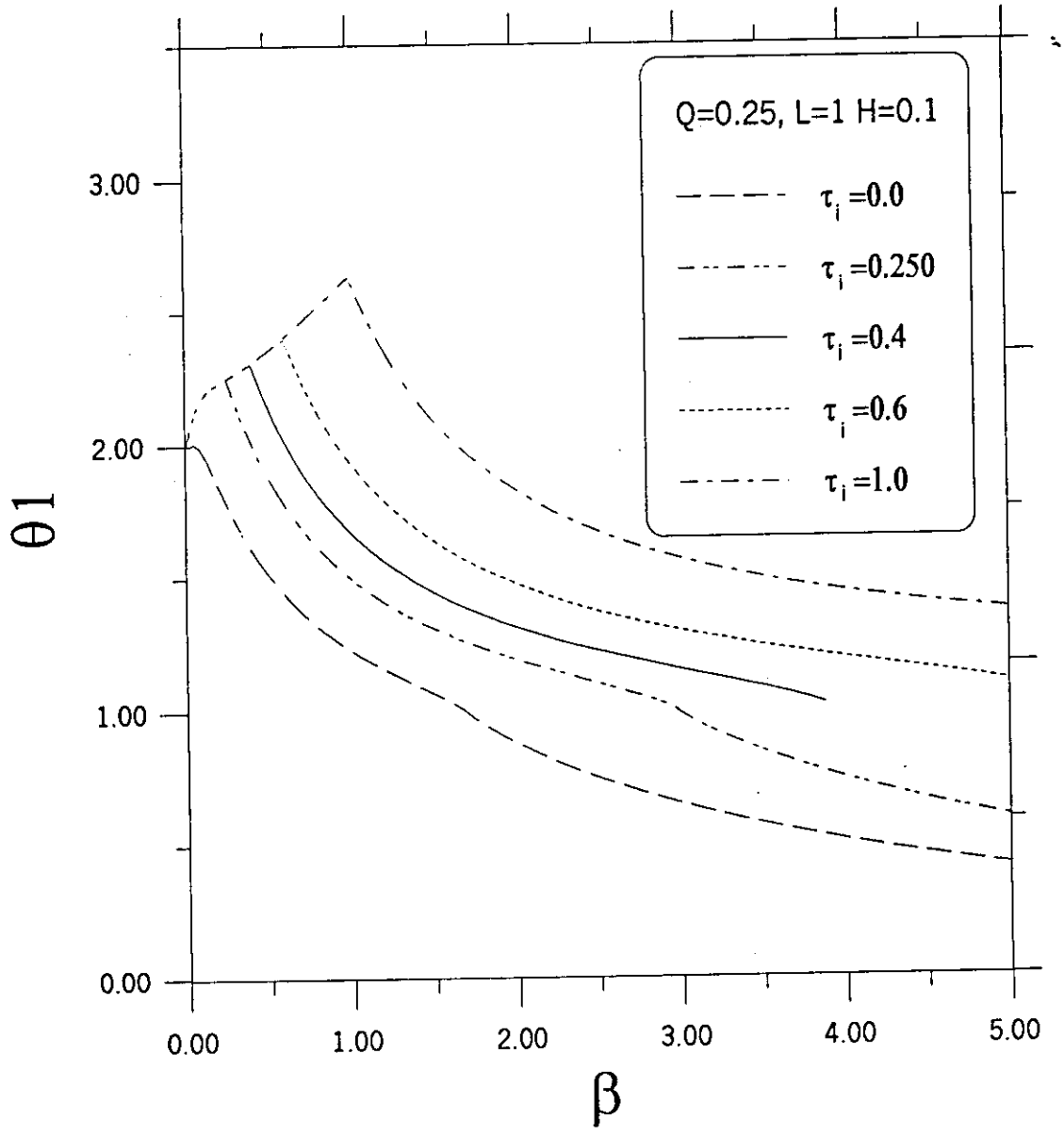

Figure (4.18a): Effect of dimensionless disturbance duration time on typeII-superconductor thermal stability based on diffusion model. (For Q=0.25, L=1, ε=2.0, B=2, and H=0.10).

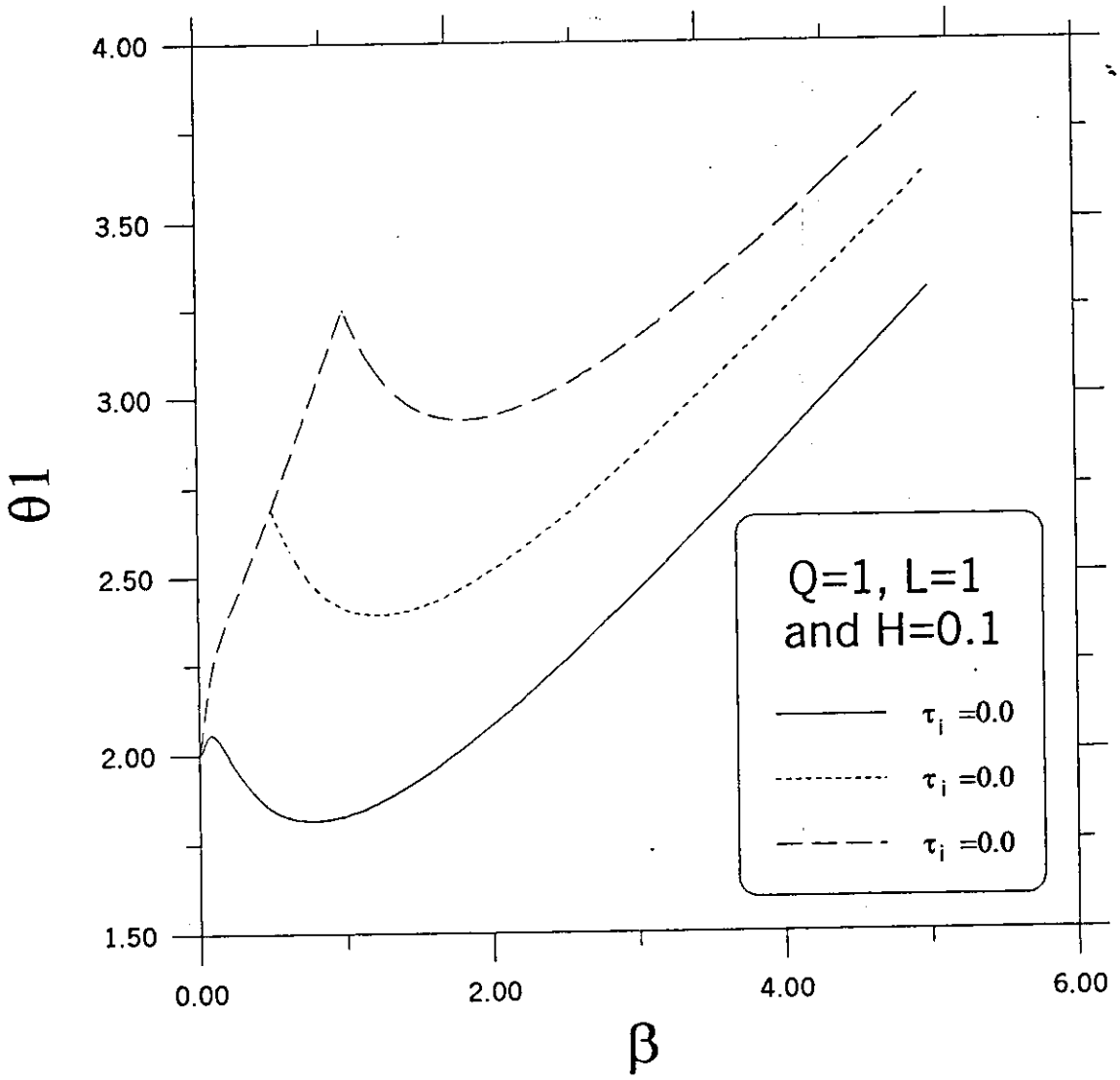

Figure (4.18b): Effect of dimensionless disturbance duration time on typeII-superconductor thermal stability based on diffusion model. (For Q=1, L=1, ε=2.0, B=2, and H=0.10).

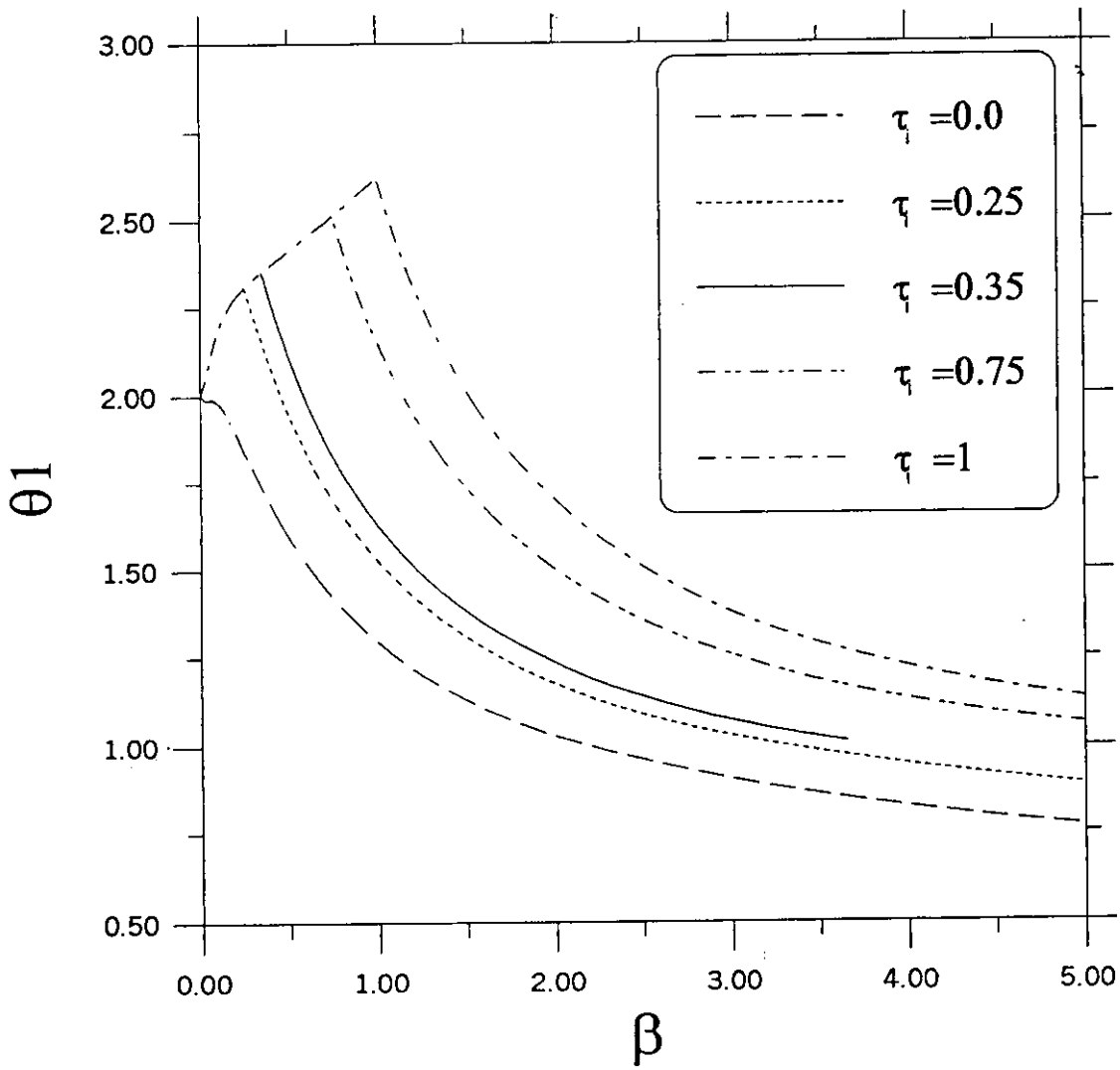

Figure (4.19): Effect of dimensionless disturbance duration time on type I-superconductor thermal stability based on diffusion model. (For Q=0.2, ε=2.0, B=2, θ_{cl}=0.1, L=1.0, and H=0.0)

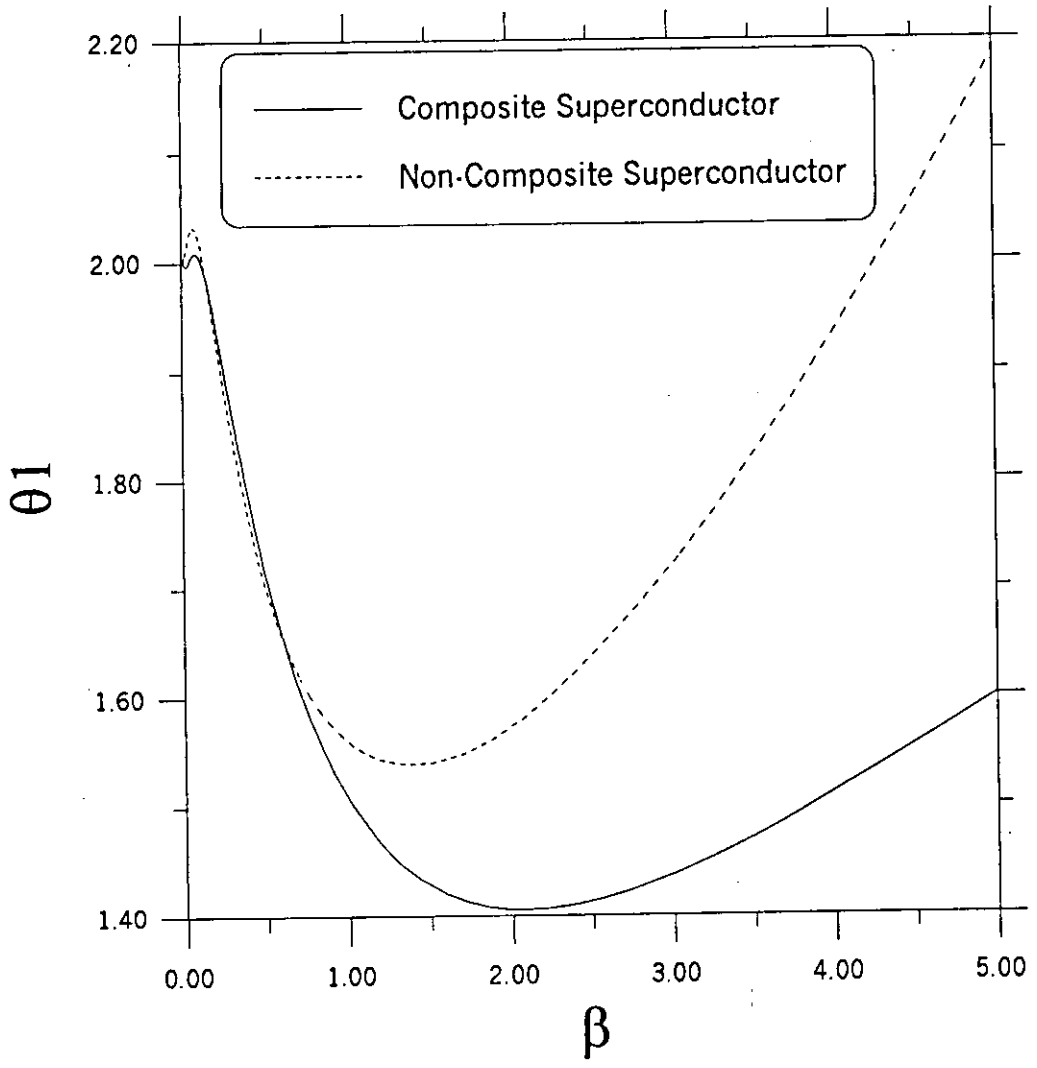

Figure (4.21): Comparison between thermal stability of typeI–superconductor and typeII -superconductor based on diffusion model. (For Q=0.5, H=0.0, ε=0.0, B=2, and τ_i=0.0).

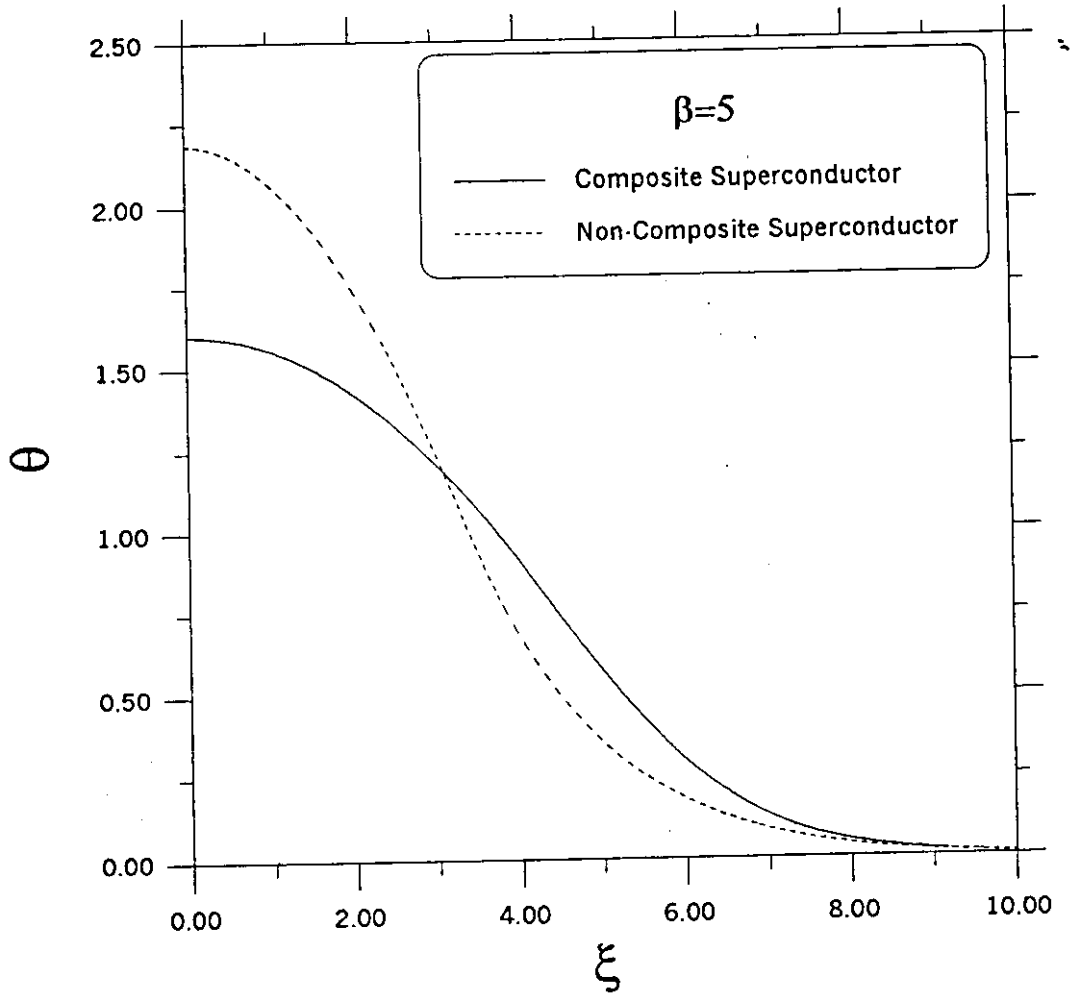

Figure (4.22): Comparison between temperature profile obtained for type1 –superconductor and typeII -superconductor based on diffusion model. (For Q=0.5, H=0.0, τ_i=0.0, ε=0.0, and B=2).

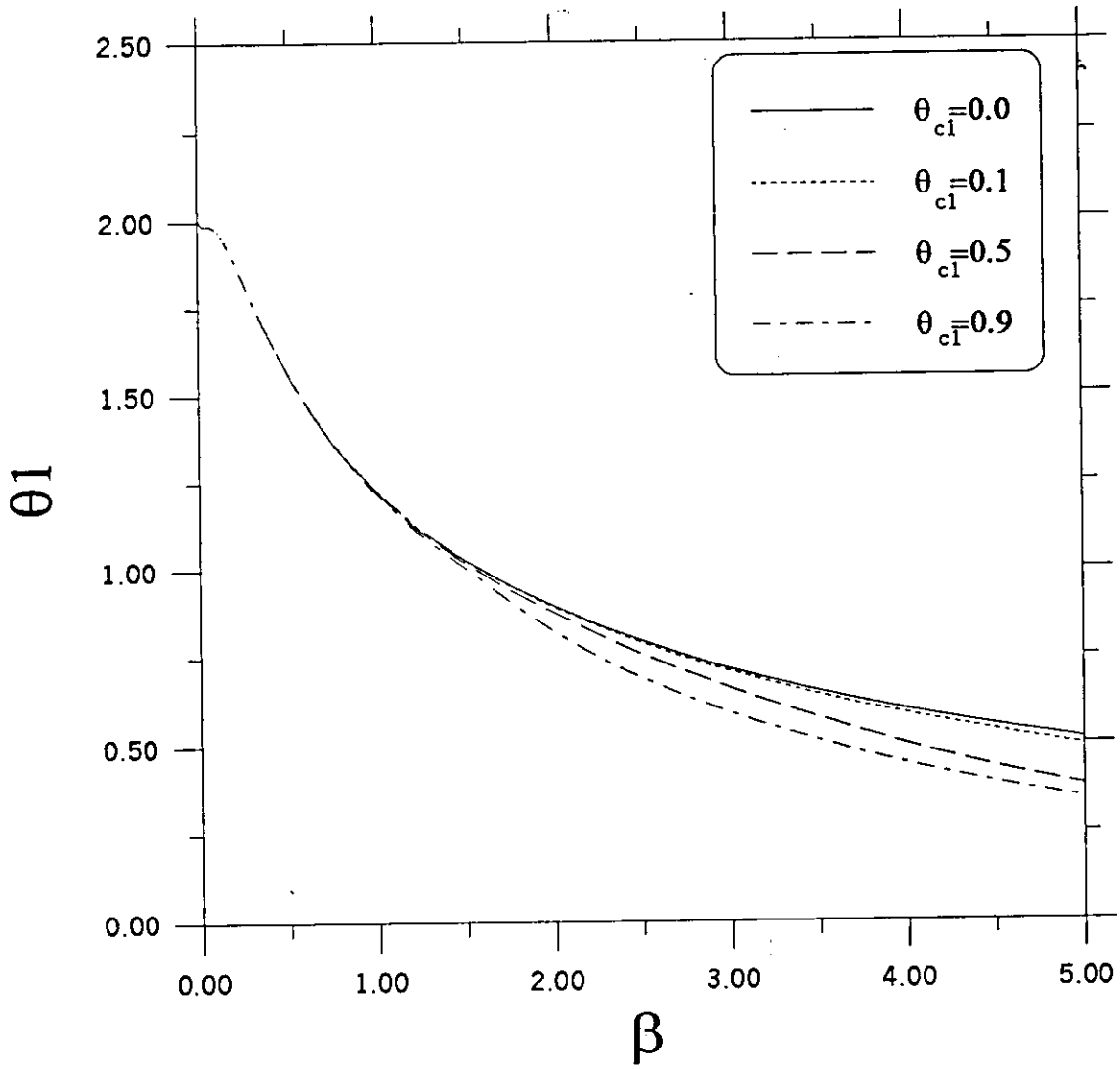

Figure (4.23a): Effect of dimensionless current sharing temperature on typeII -superconductor thermal stability based on diffusion model. (For Q=0.15, H=0.1, ε=0.0, B=2, τ_i=0.0, and L=1.0).

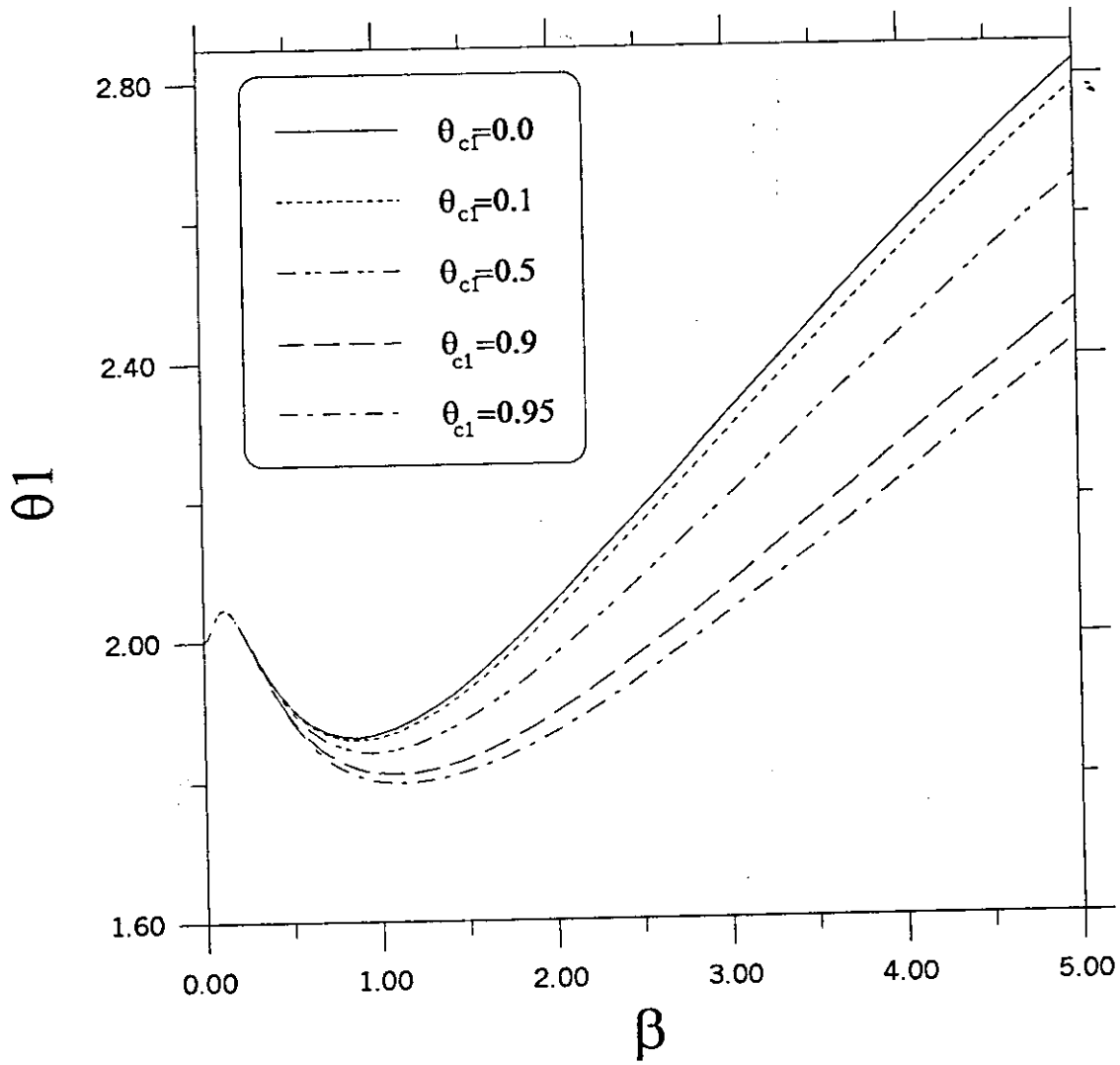

Figure (4.23b): Effect of dimensionless current sharing temperature on typeII -superconductor thermal stability based on diffusion model. (For Q=1, H=0.25, ε=0.0, B=2, τ_i=0.0, and L=1.0).

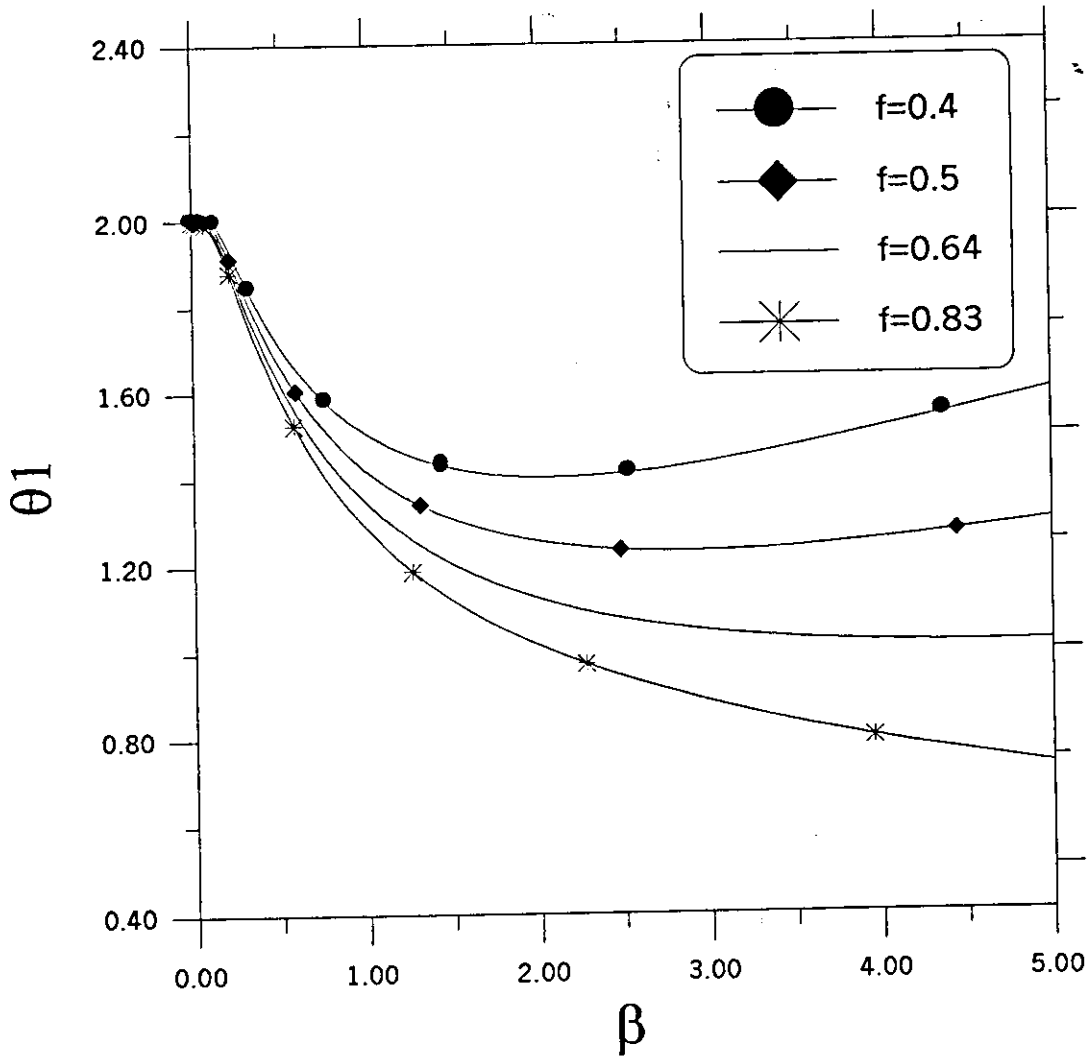

Figure (4.24a): The effect of stabilizer to superconductor ratio (f) on typeII-superconductor thermal stability based on diffusion model. (For L=1, θ_{cl}=0.1, H=0.2, τ_i=0.0, ε=0.0, B=2, and Q=0.25).

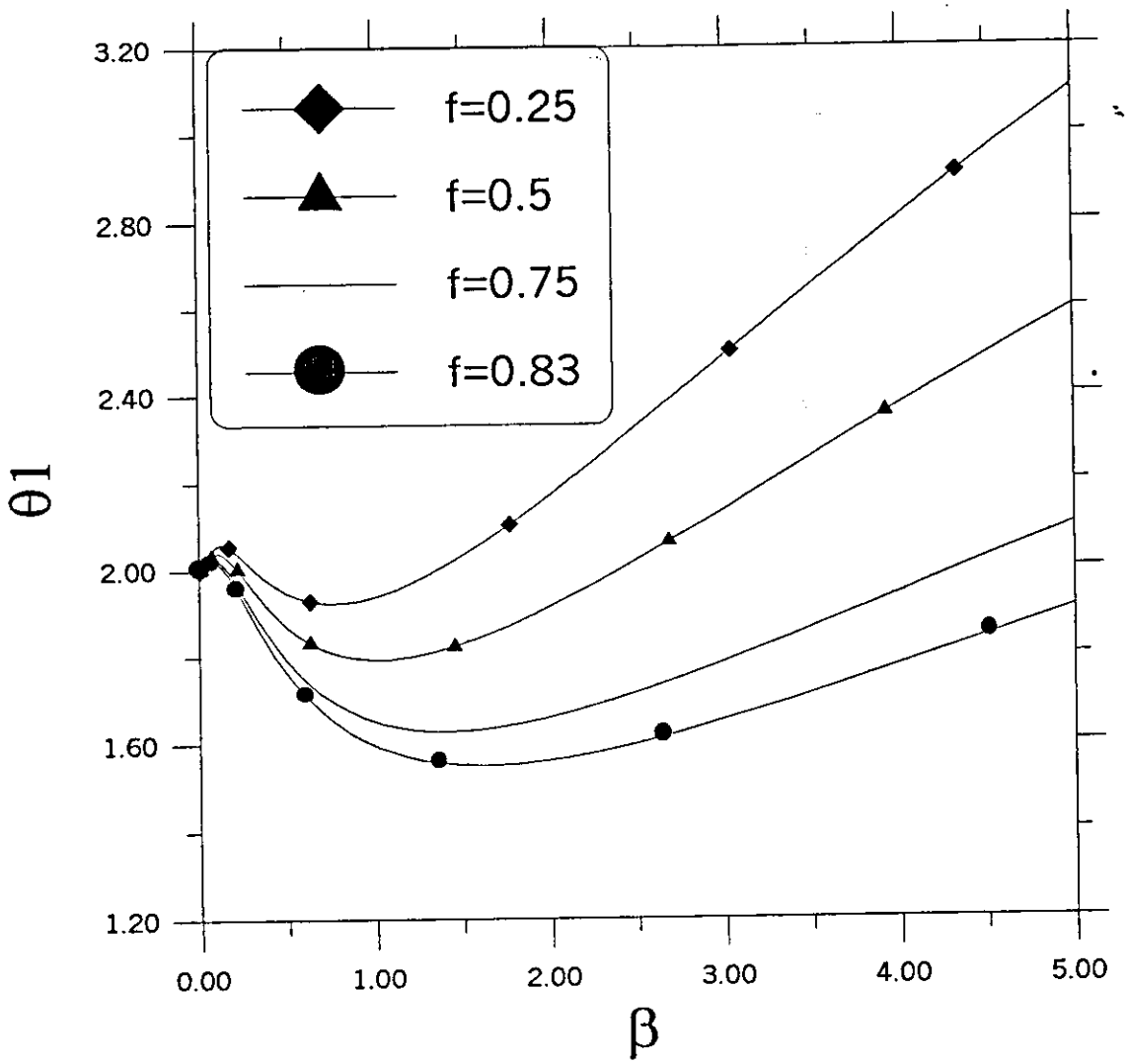

Figure (4.24b): The effect of stabilizer to superconductor ratio (f) on type II-superconductor thermal stability based on diffusion model. (For $L=1, \theta_{c1}=0.1, H=0.2, \tau_i=0.0, \varepsilon=0.0, B=2$, and $Q=0.5$).

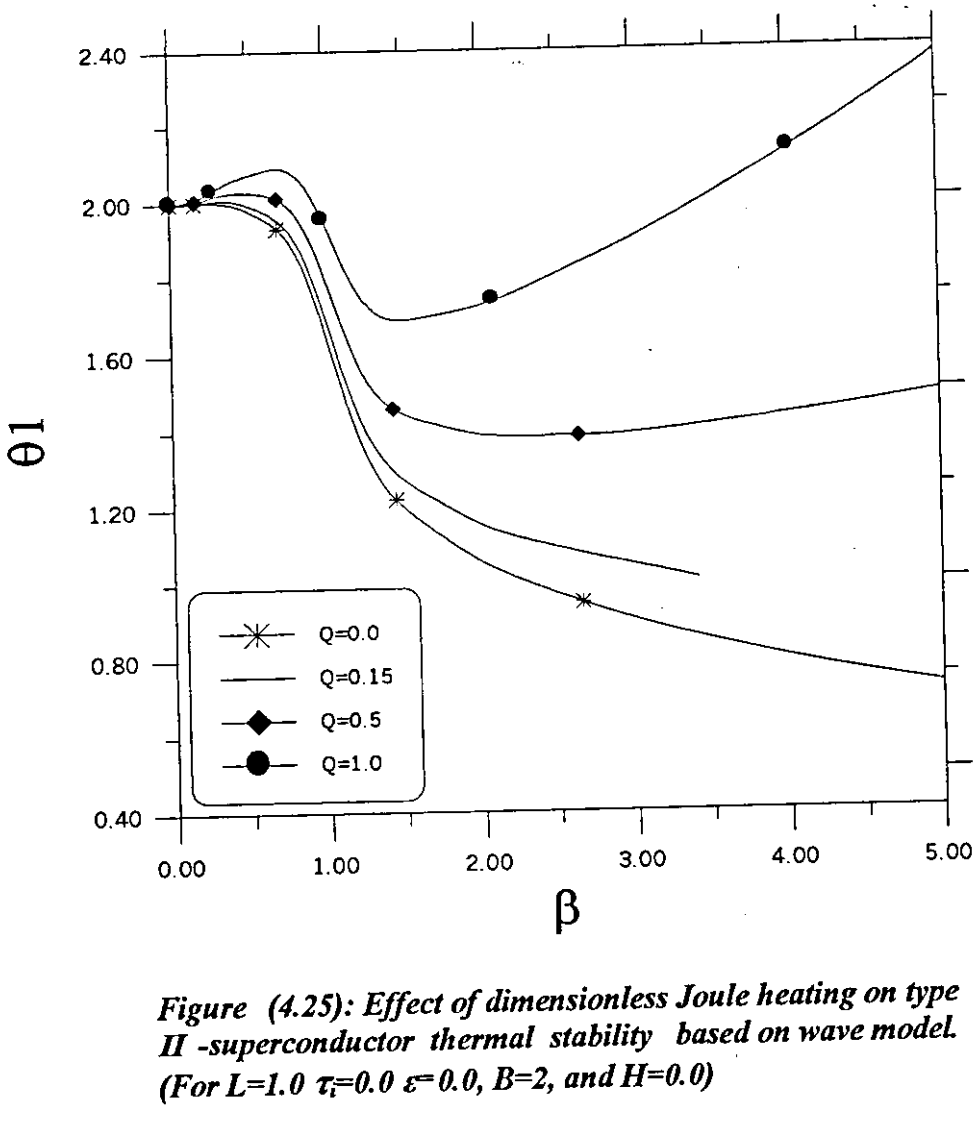

Figure (4.25): Effect of dimensionless Joule heating on type II -superconductor thermal stability based on wave model. (For L=1.0 τ_i=0.0 ε= 0.0, B=2, and H=0.0)

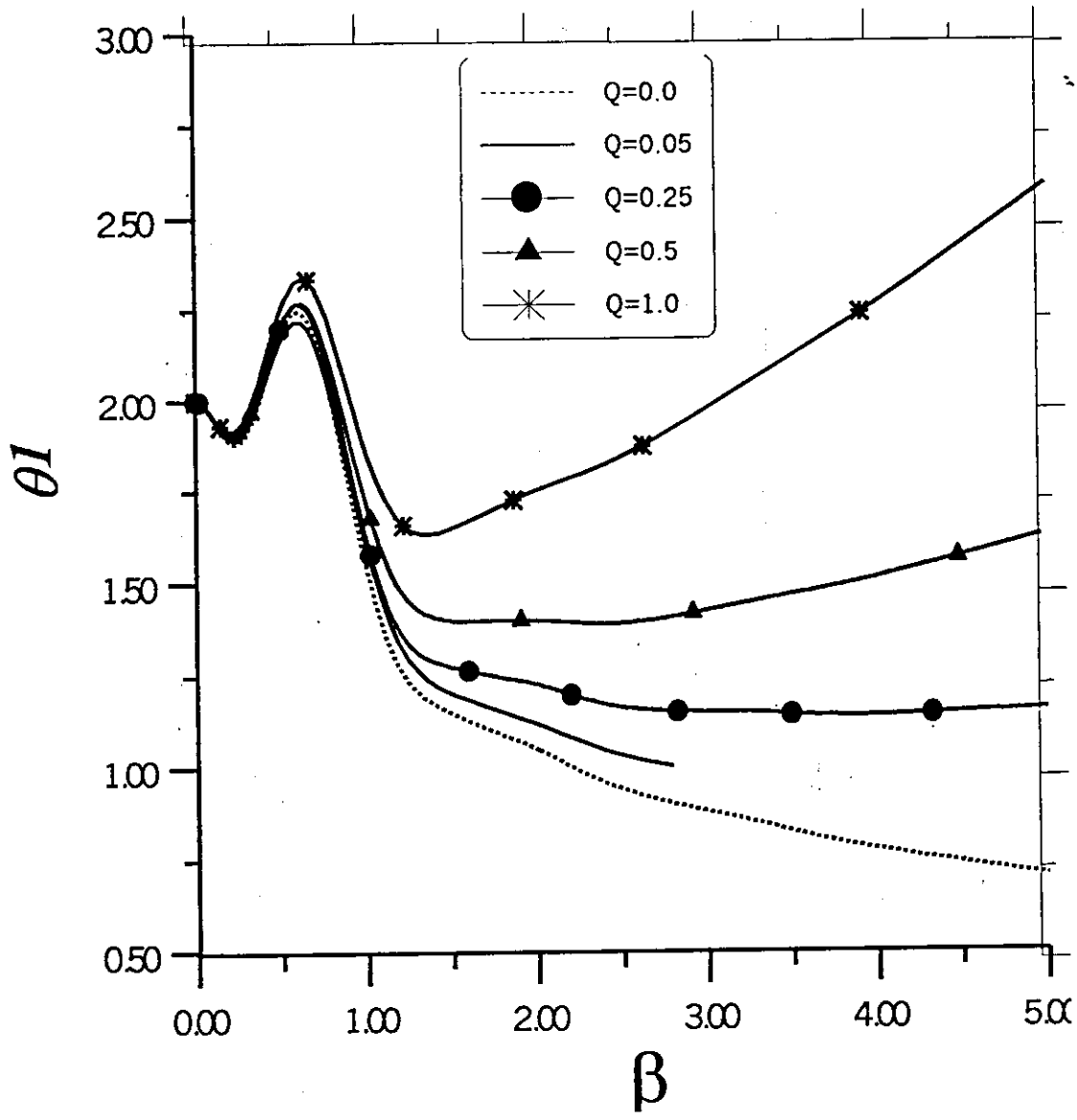

Figure (4.26): Effect of dimensionless Joule heating on typeI-superconductor thermal stability based on wave model. (For L=1.0, θ_{c1}=0.1, H=0.0 ε= 0.0, B=2, and τ_i=0.0)

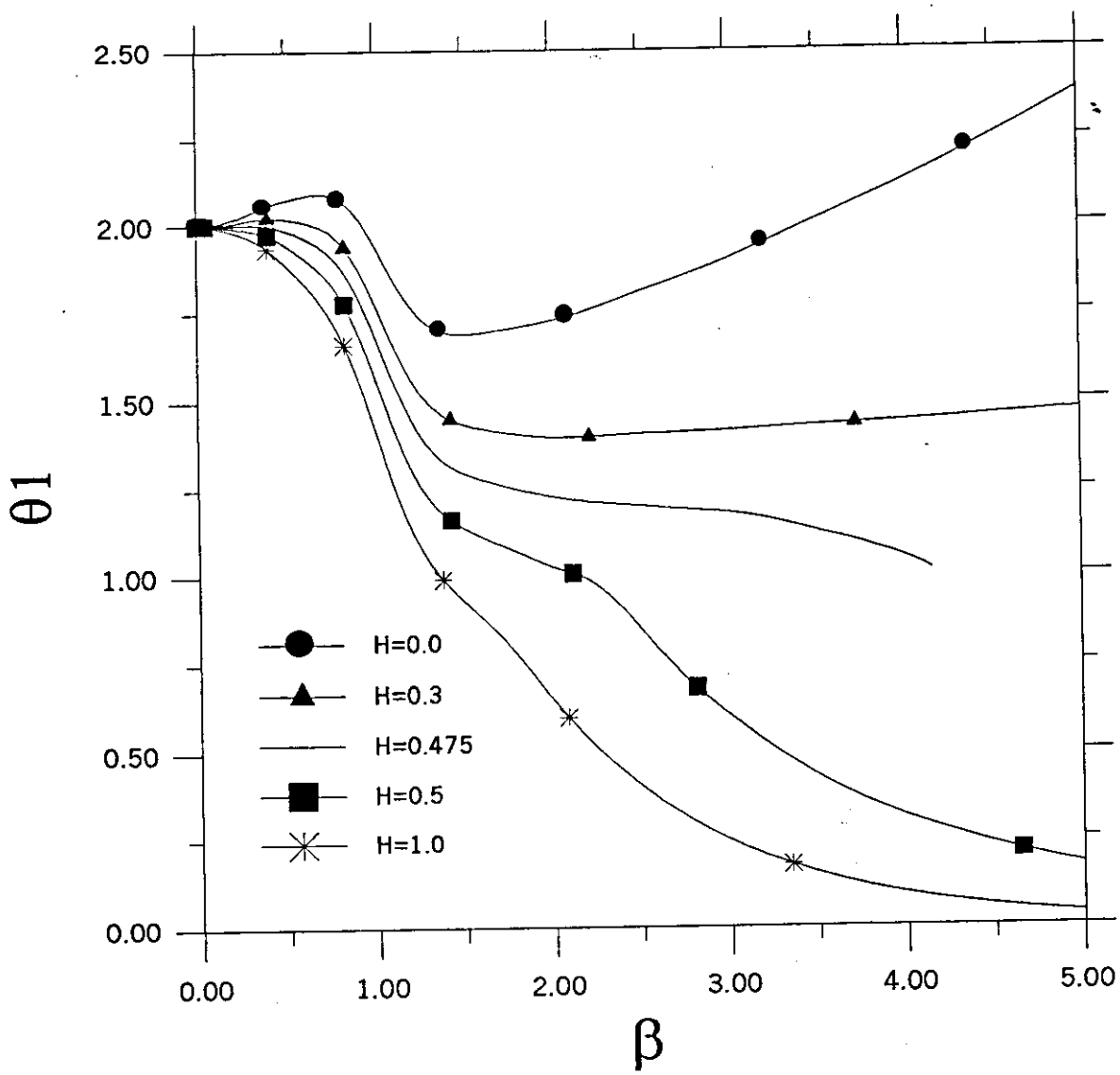

Figure (4.27): Effect of lateral cooling on type II superconductor thermal stability based on wave model. (For Q=1.0 τ_i=0.0, ε=0.0, B=2, and L=1.0).

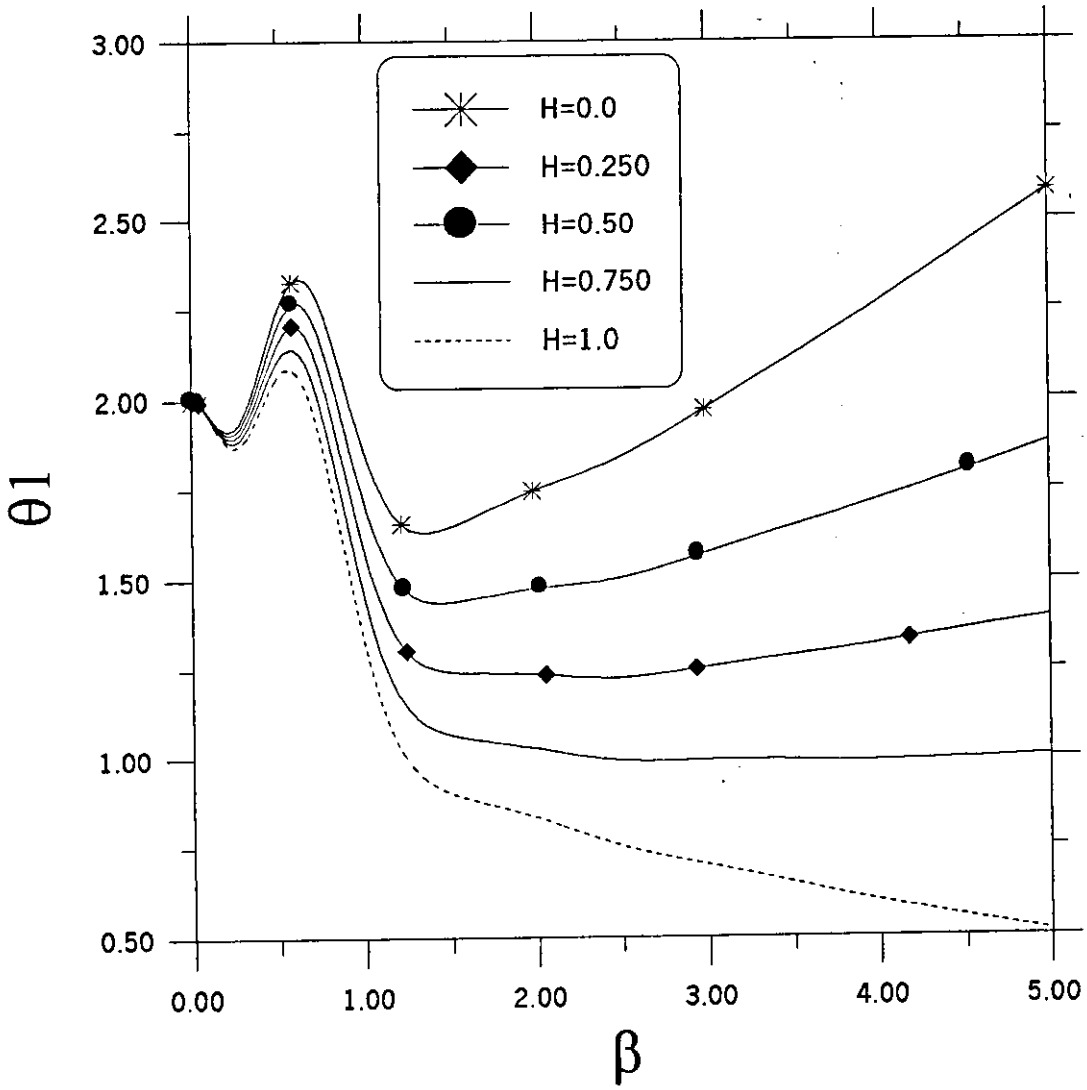

Figure (4.28): Effect of lateral cooling on type I-superconductor thermal stability based on wave model subjected to unit-step disturbance. (For Q=1.0, θ_{c1}=0.1, τ_i=0.0, ε= 0.0, B=2, and L=1.0).

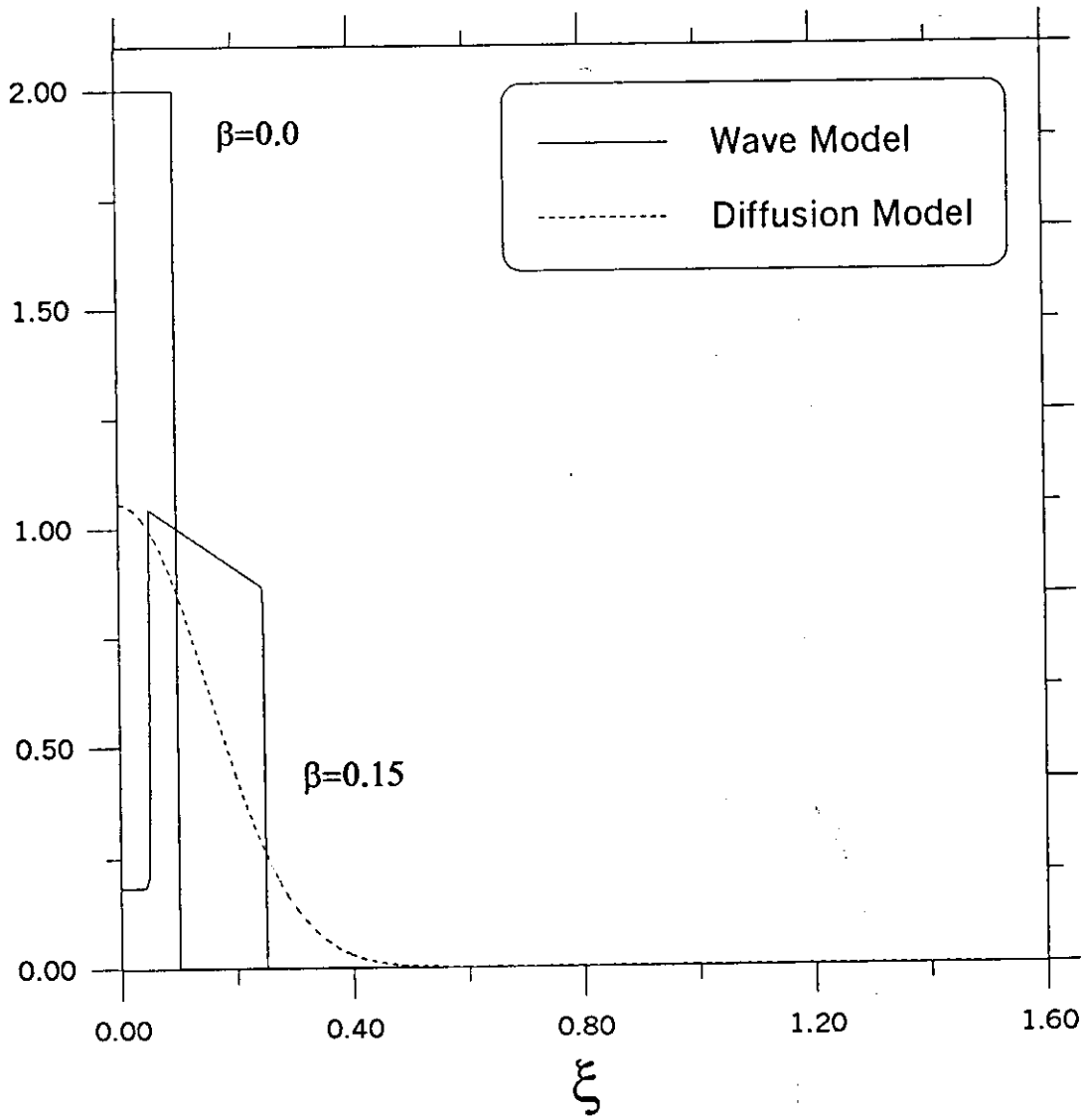

Figure (4.29a): Comparison between temperature profiles obtained based on diffusion model and wave model for typeII-superconductor. (For Q=0.0, no internal heat generation, θ_{c1}=0.1, τ_i=0.0, ε=0.0, B=2, and L=0.15).

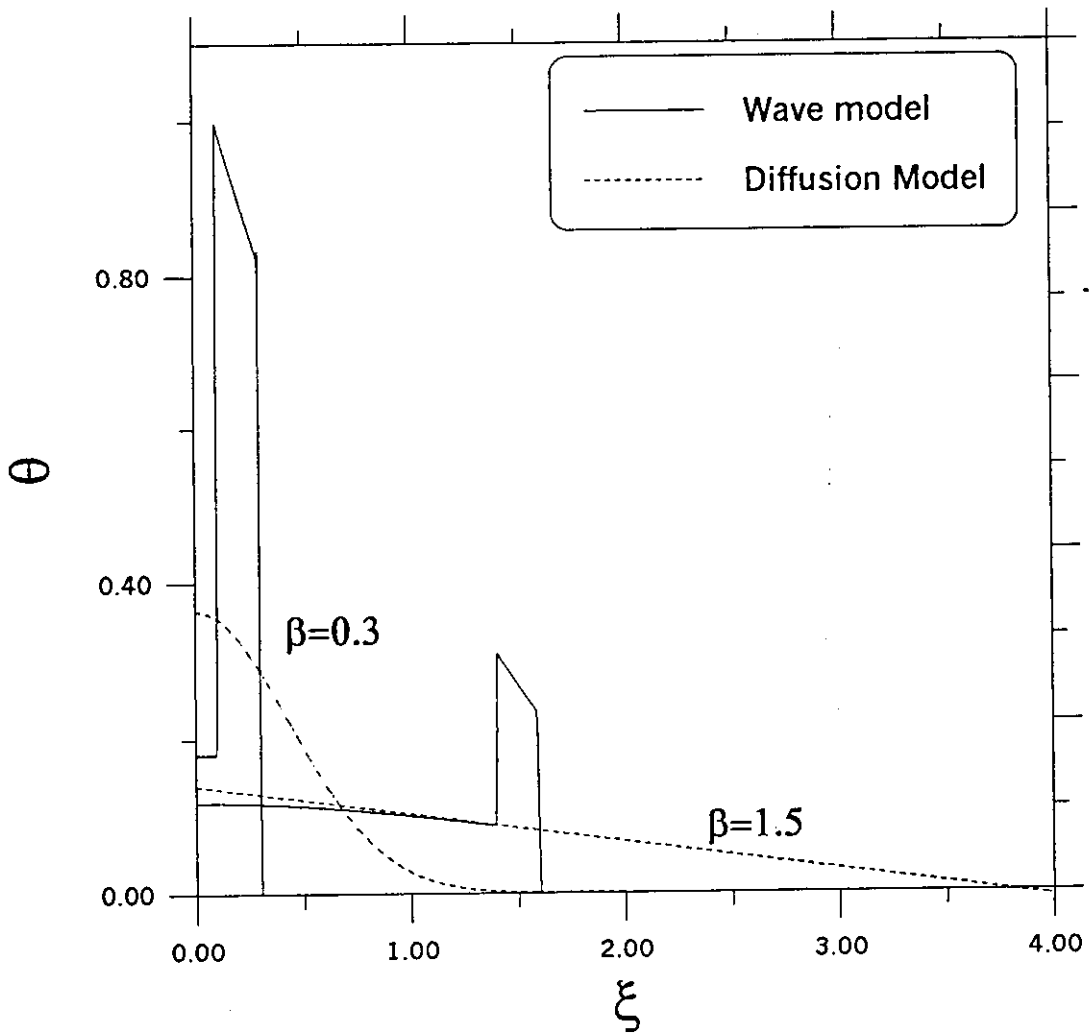

Figure (4.29b): Comparison between temperature profiles obtained based on diffusion model and wave model for typeII-superconductor. (For Q=0.0, no internal heat generation, θ_{cl}=0.1, τ_t=0.0, ε= 0.0, B=2, and L=0.15).

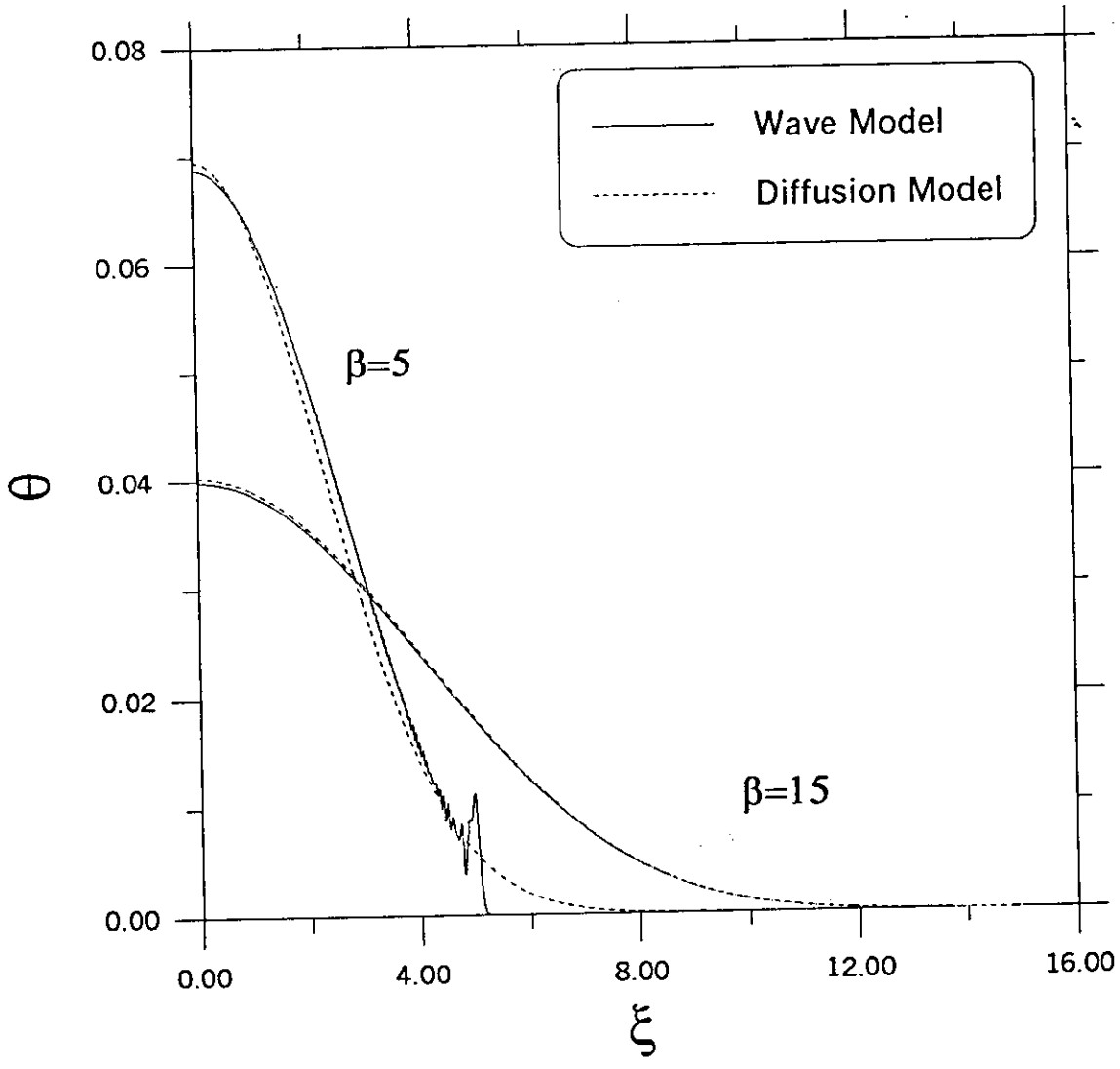

Figure (4.29c): Comparison between temperature profiles obtained based on diffusion model and wave model for typeII-superconductor. (For Q=0.0, no internal heat generation, τ_i=0.0, θ_{c1}=0.1, ε=0.0, B=2, ε=0.0, B=2, and L=0.15).

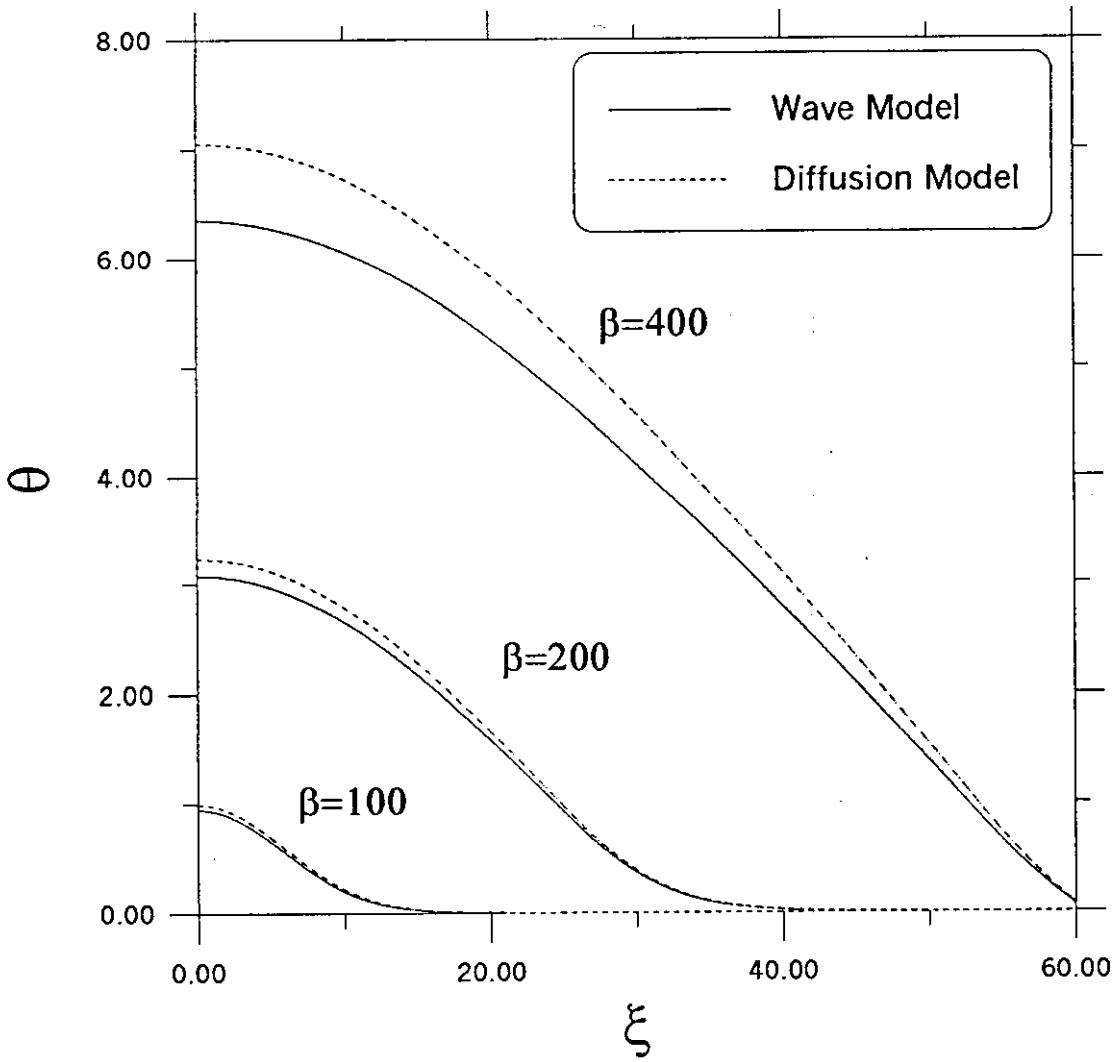

Figure (4.31): Effect of time on magnitude differences between wave and diffusion models. (For $Q=0.5, \theta_{c1}=0.1$, $L=1.5$, $\varepsilon=0.0$, $B=2$, and $\tau_i=0.0$)

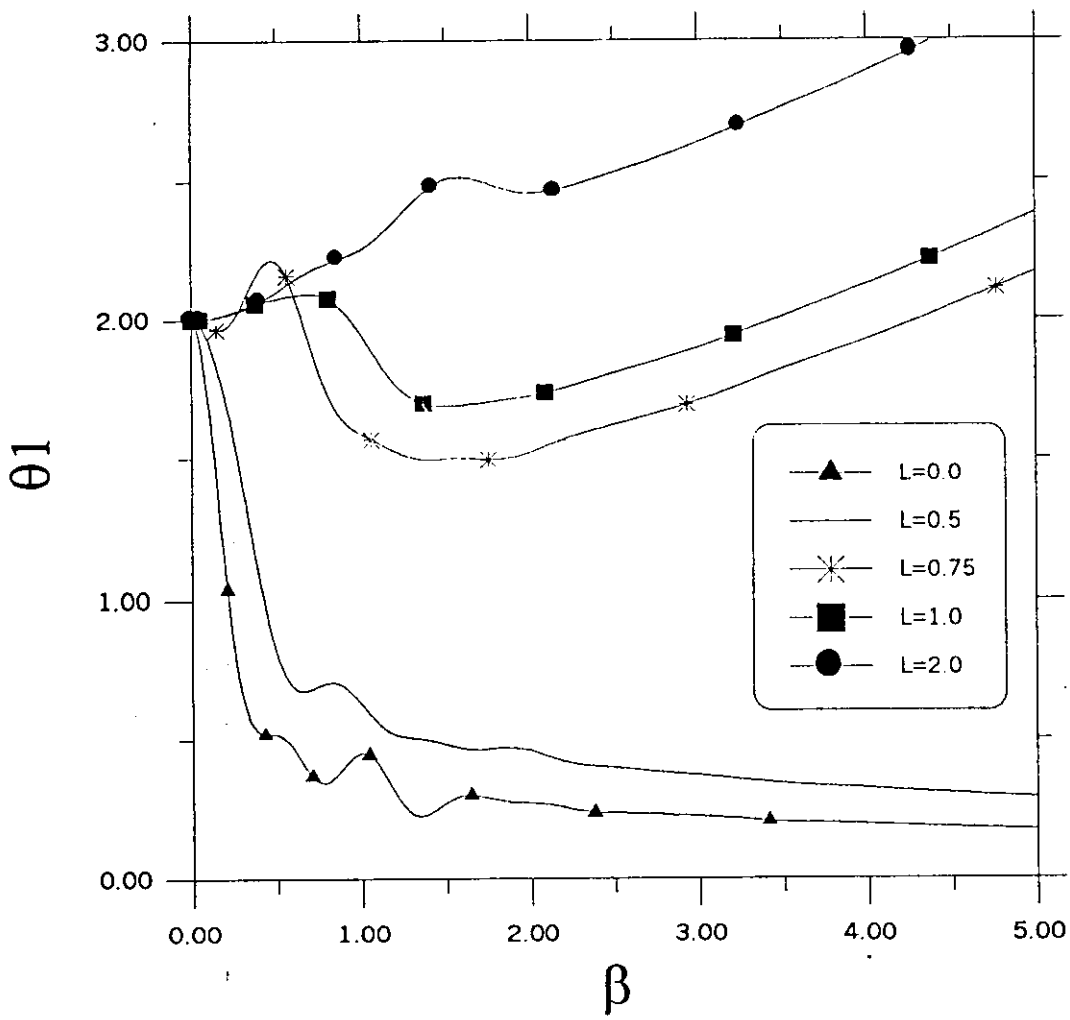

Figure (4.32a): Effect of dimensionless disturbance length on typeII-superconductor thermal stability based on wave model. (For Q=1, H=0.0, ε=0.0, B=2, and τ_i=0).

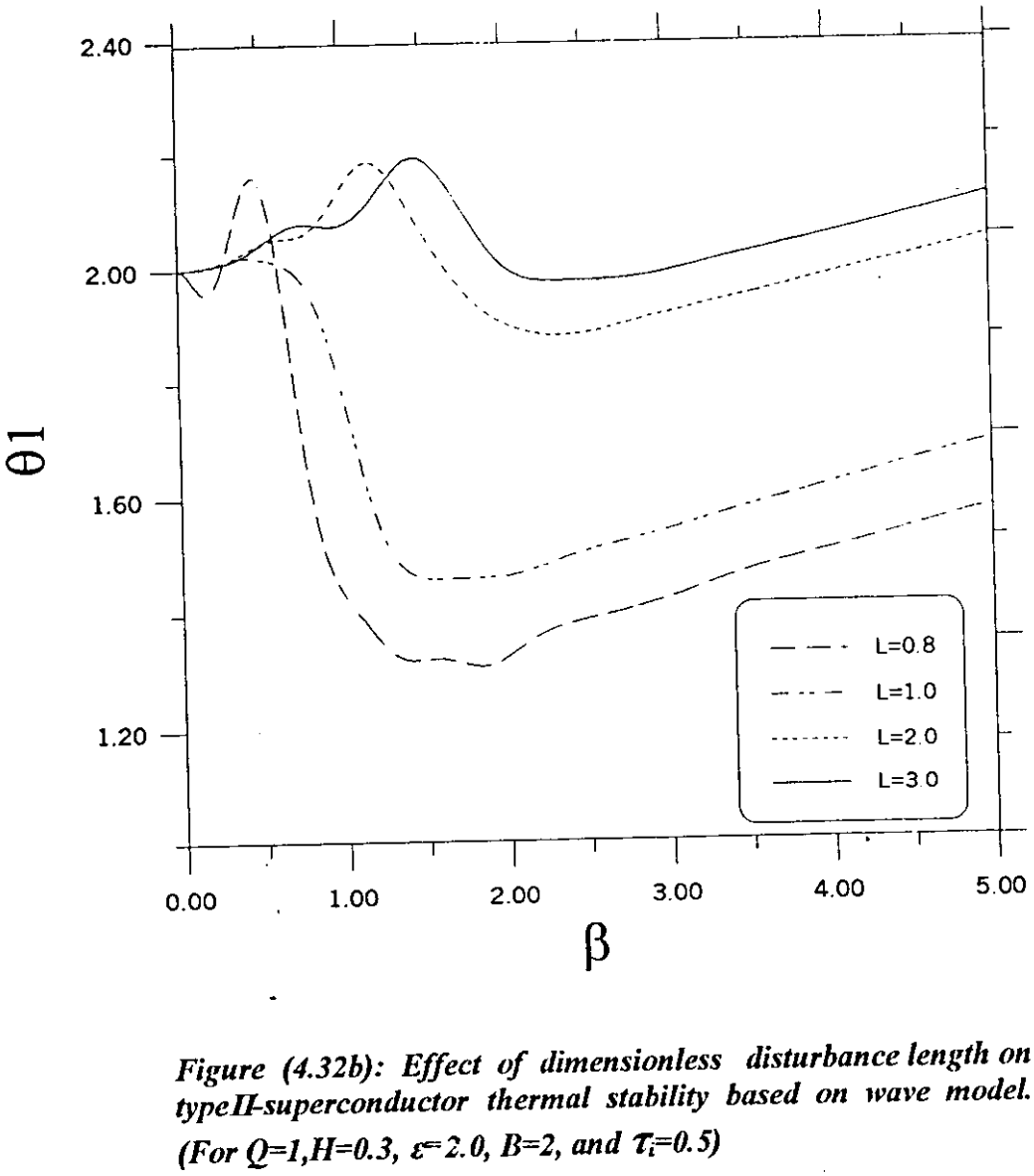

Figure (4.32b): Effect of dimensionless disturbance length on typeII-superconductor thermal stability based on wave model. (For Q=1,H=0.3, ε=2.0, B=2, and τ_i=0.5)

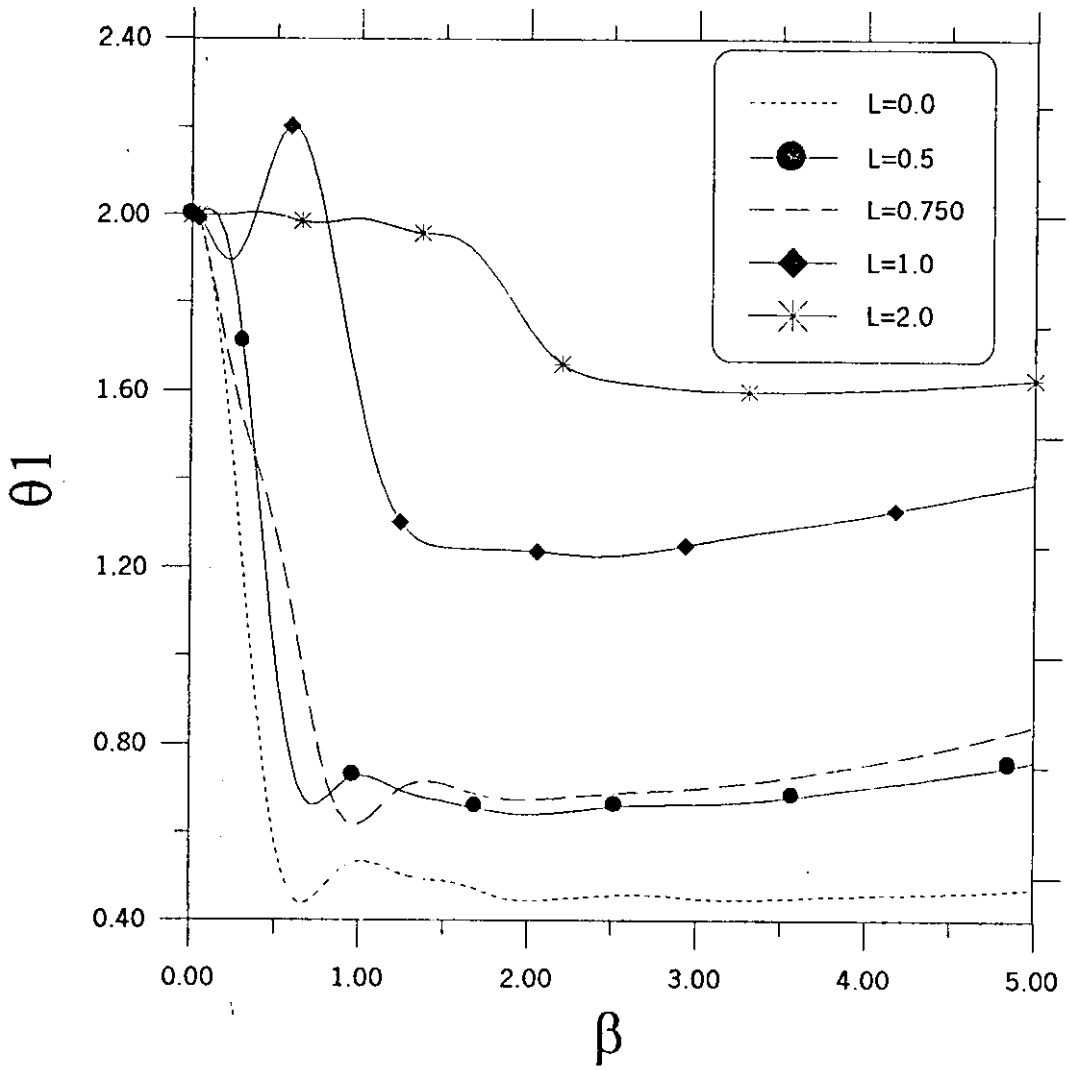

Figure (4.33): Effect of dimensionless disturbance length on type I-superconductor thermal stability based on wave model. (For Q=1,H=0.3, θ_{c1}=0.1, ε=0.0, B=2, and τ_i=0.0).

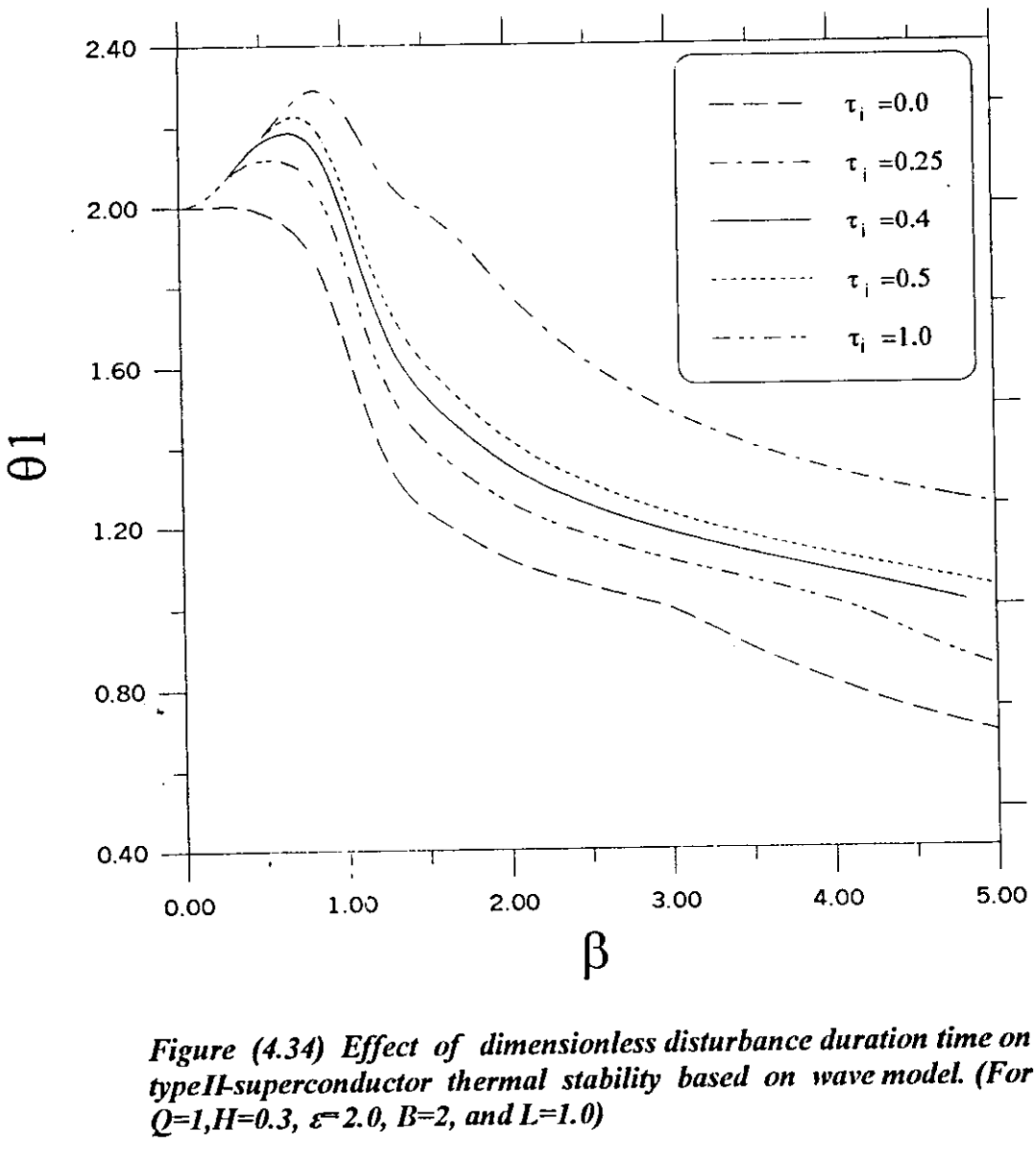

Figure (4.34) Effect of dimensionless disturbance duration time on typeII-superconductor thermal stability based on wave model. (For Q=1,H=0.3, ε=2.0, B=2, and L=1.0)

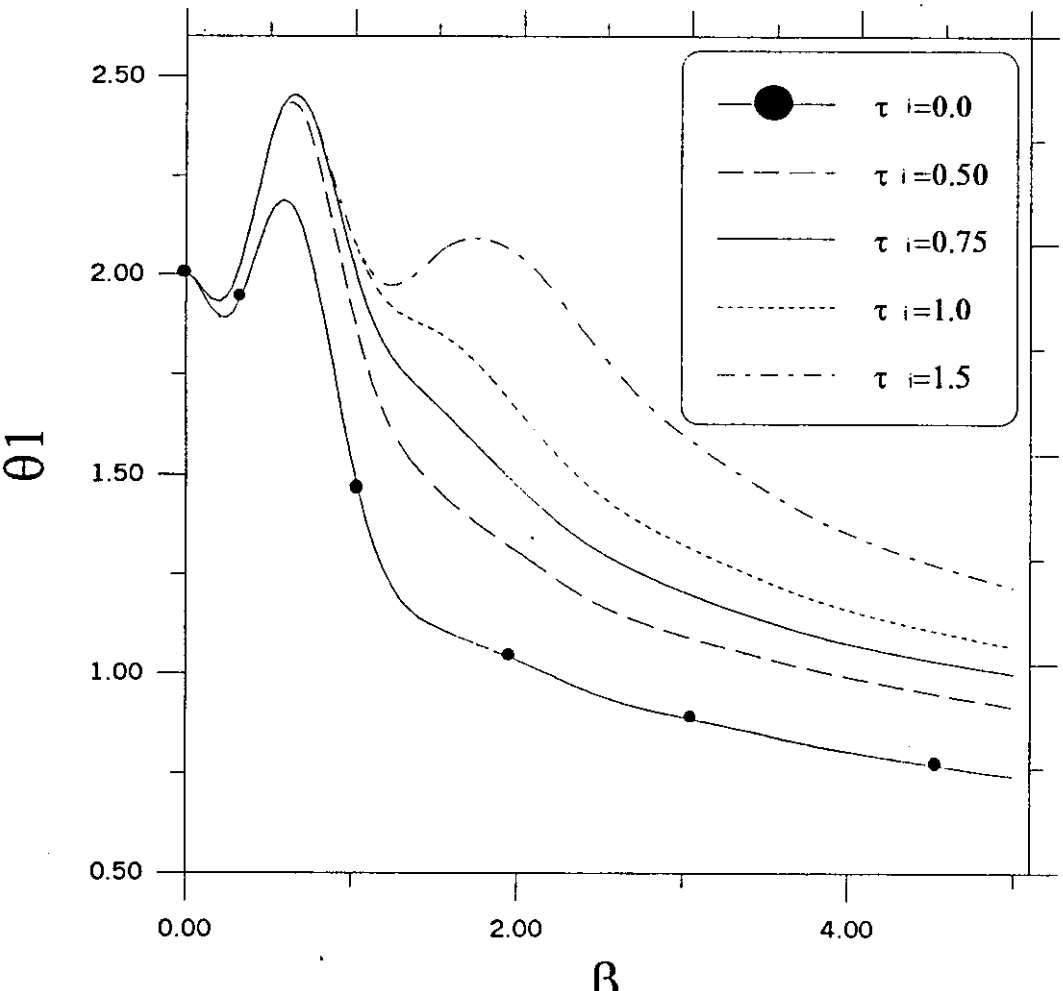

Figure (4.35): Effect of dimensionless disturbance duration time on typeI-superconductor thermal stability based on wave model. (For Q=1,H=0.3, θ_{c1}=0.1, ε=0.0, B=2, and L=1.0).

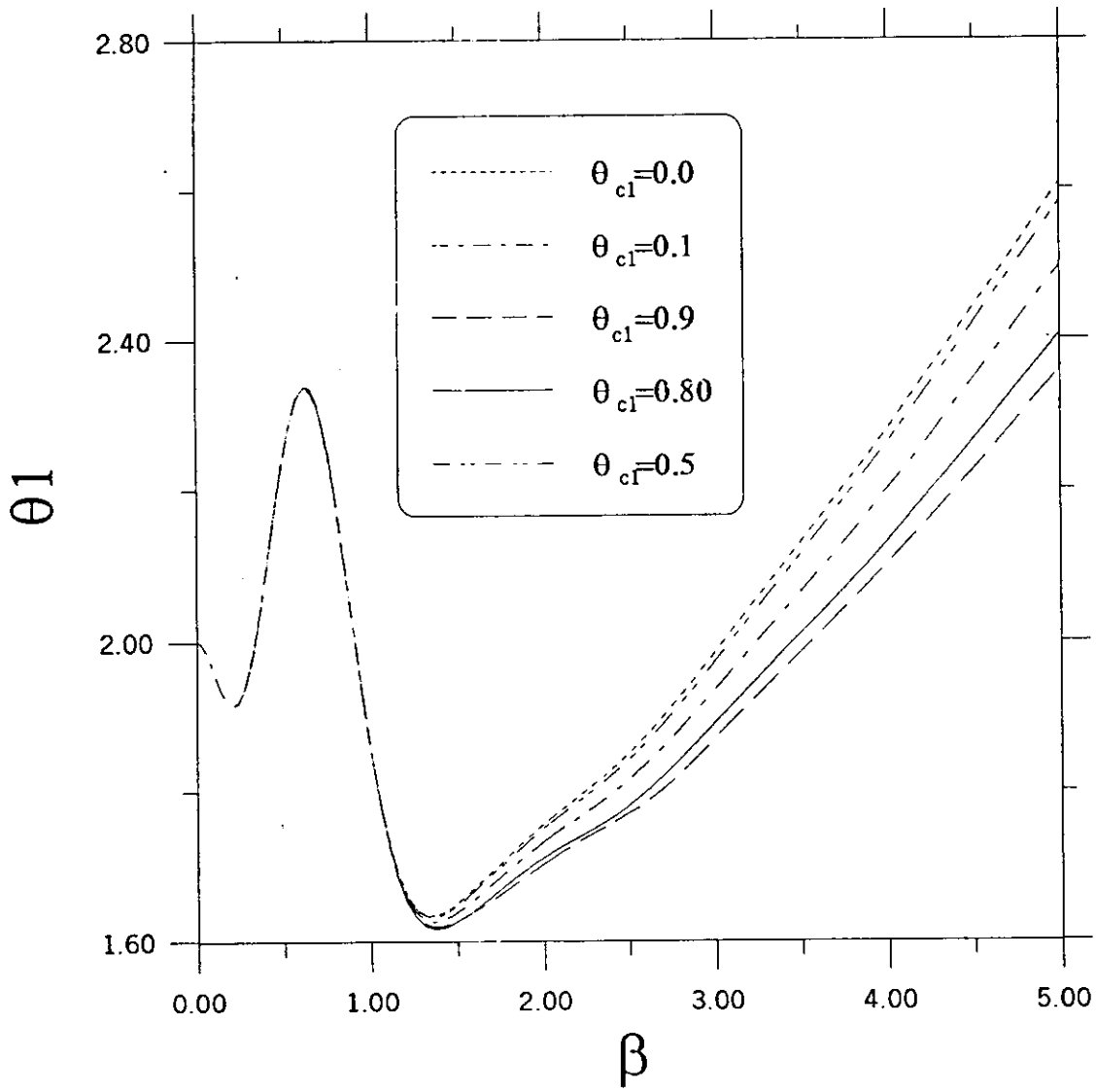

Figure (4.36): Effect of dimensionless current sharing temperature on typeII-superconductor thermal stability based on wave model subjected to stepwise disturbance. (For Q=0.5,H=0.0, τ_i=0.0 ε= 0.0, B=2, and L=1.0).

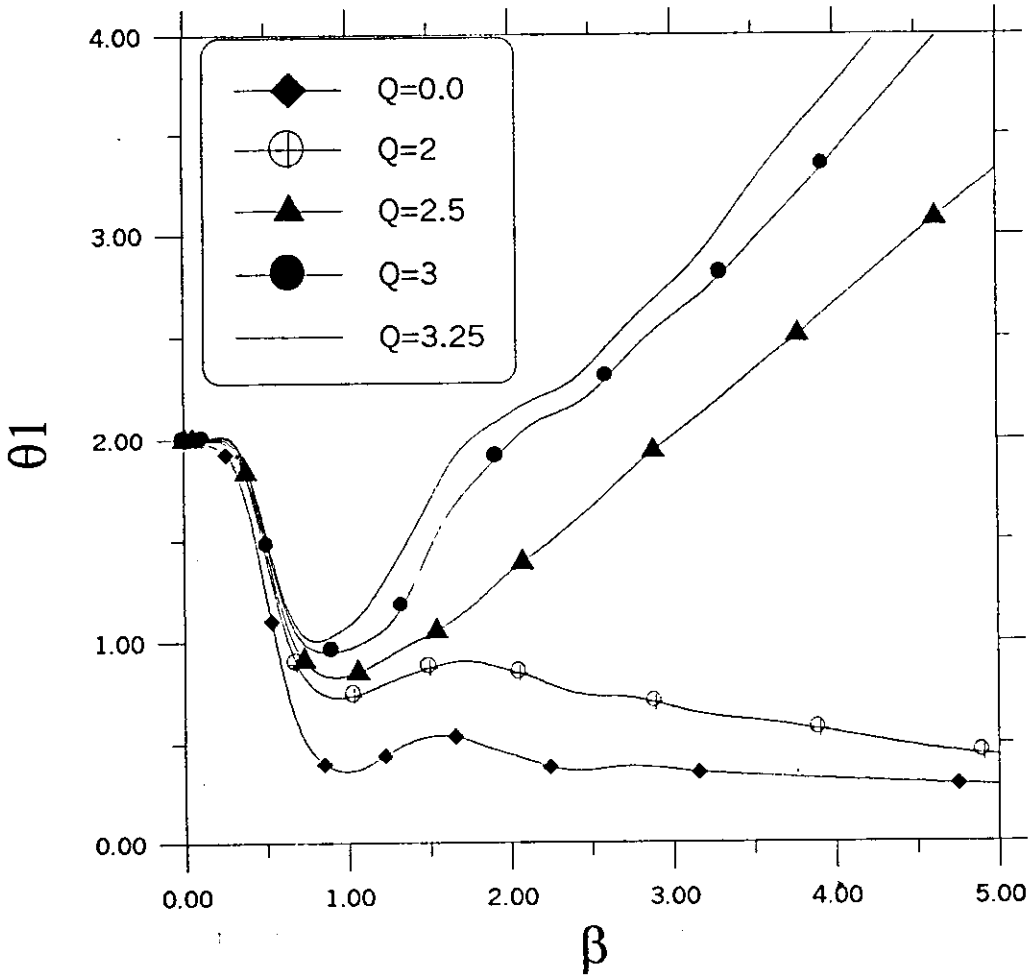

Figure (4.37): Effect of dimensionless Joule heating on typeII-superconductor based on dual-phase-lag model. (For L=1.0, R=5, H=0.0, ε=0.0, B=2, and τ_t=0.0).

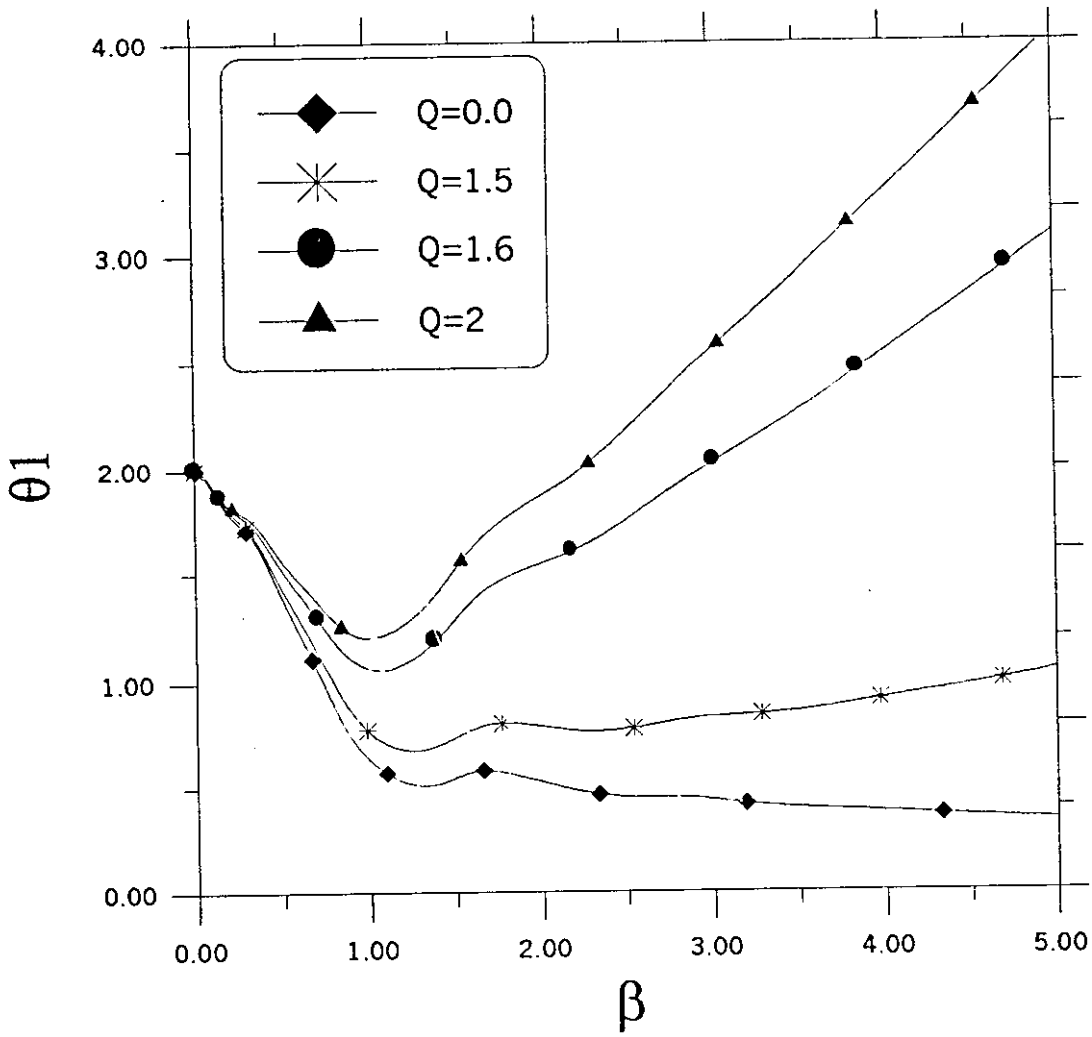

Figure (4.38): Effect of dimensionless Joule heating on type I-superconductor thermal stability based on dual-phase-lag model. (For $R=5.0$, $L=1.0$, $\theta_{c1}=0.1$, $\varepsilon=0.0$, $B=2$, $H=0.0$ and $\tau_t=0.0$).

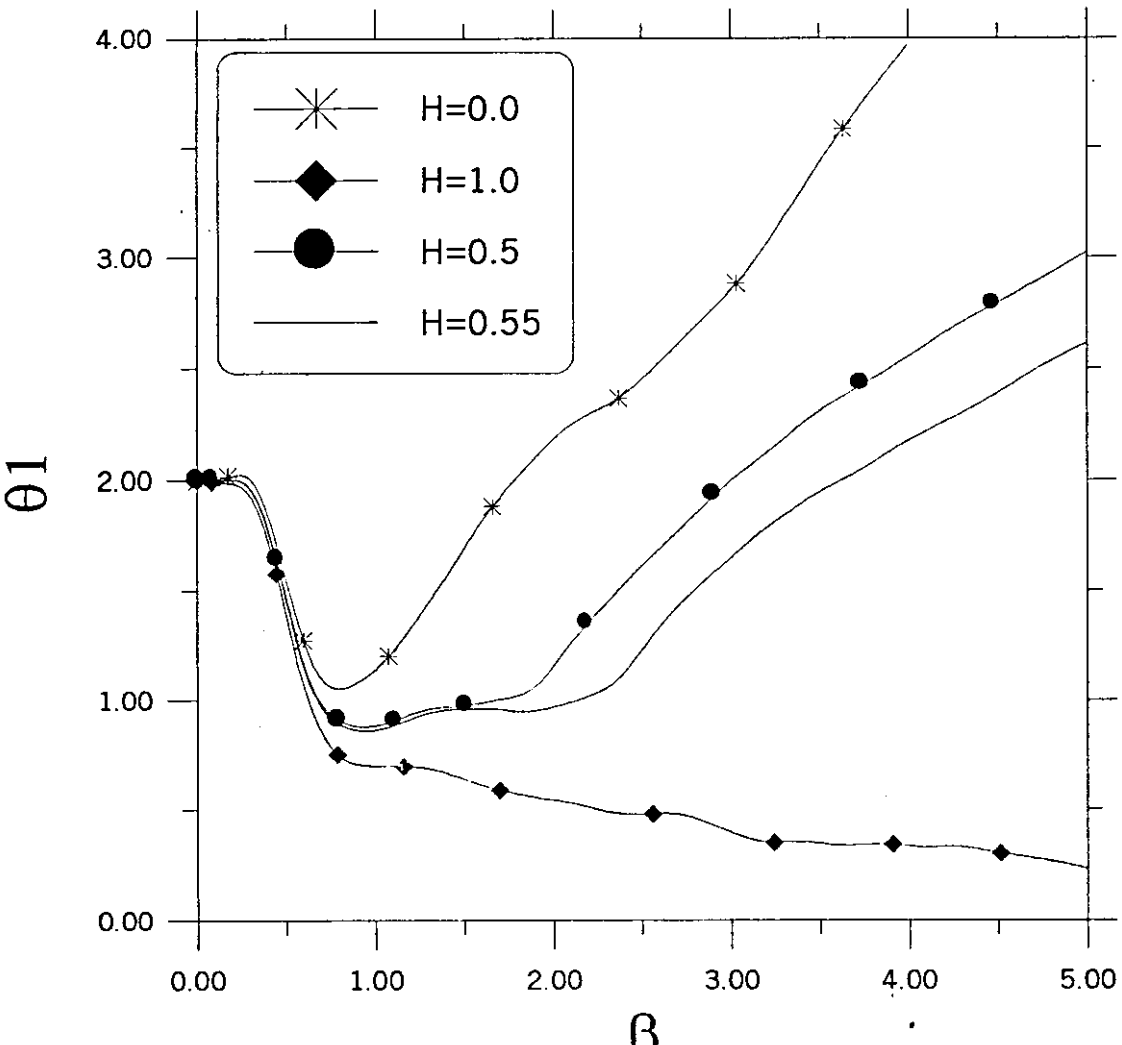

Figure (4.39): Effect of dimensionless lateral cooling on typeII-superconductor thermal stability based on dual-phase-lag model. (For Q=3.5, R=5.0, ε=0.0, B=2, H=0.0, L=1.0 and τ_i=0.0).

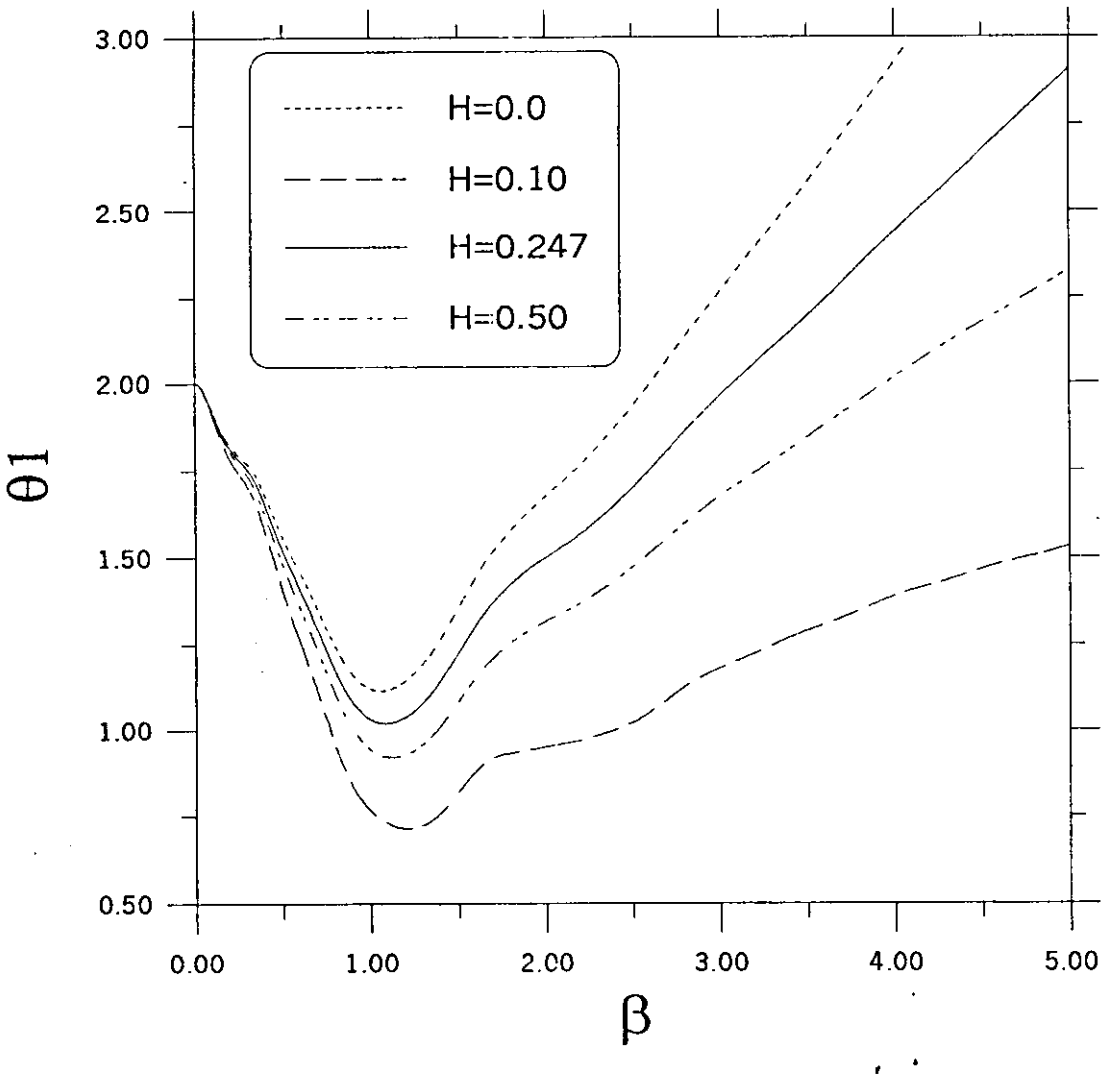

Figure (4.40): Effect of dimensionless lateral cooling on typeI-superconductor thermal stability based on dual-phase-lag model. (For Q=2.0, R=5.0, ε=0.6, B=2, L=1.0, θ_{c1}=0.10 and τ_t=0.0)

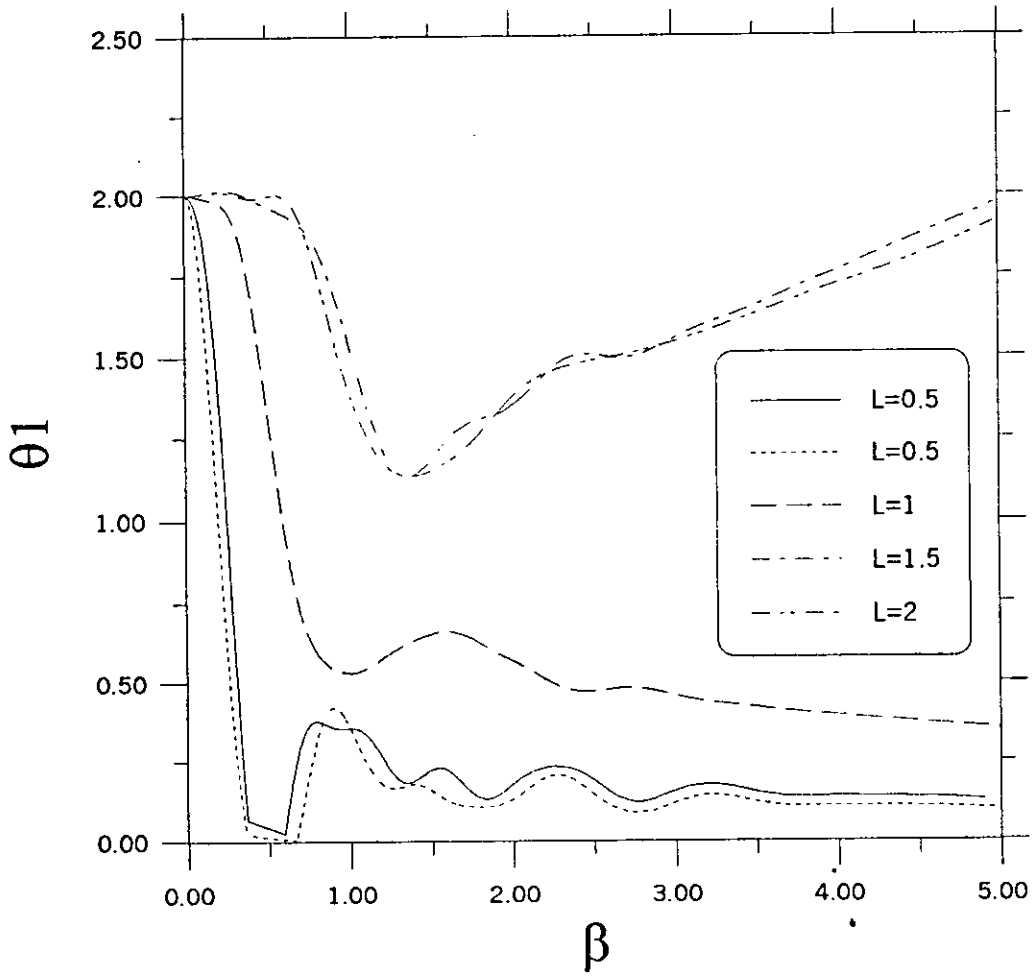

Figure (4.41): Effect of dimensionless disturbance length on typeII-superconductor thermal stability based on dual-phase-lag model. (For H=0, R=5.0, Q=4, ε=0.0, B=2, τ_t=0.0)

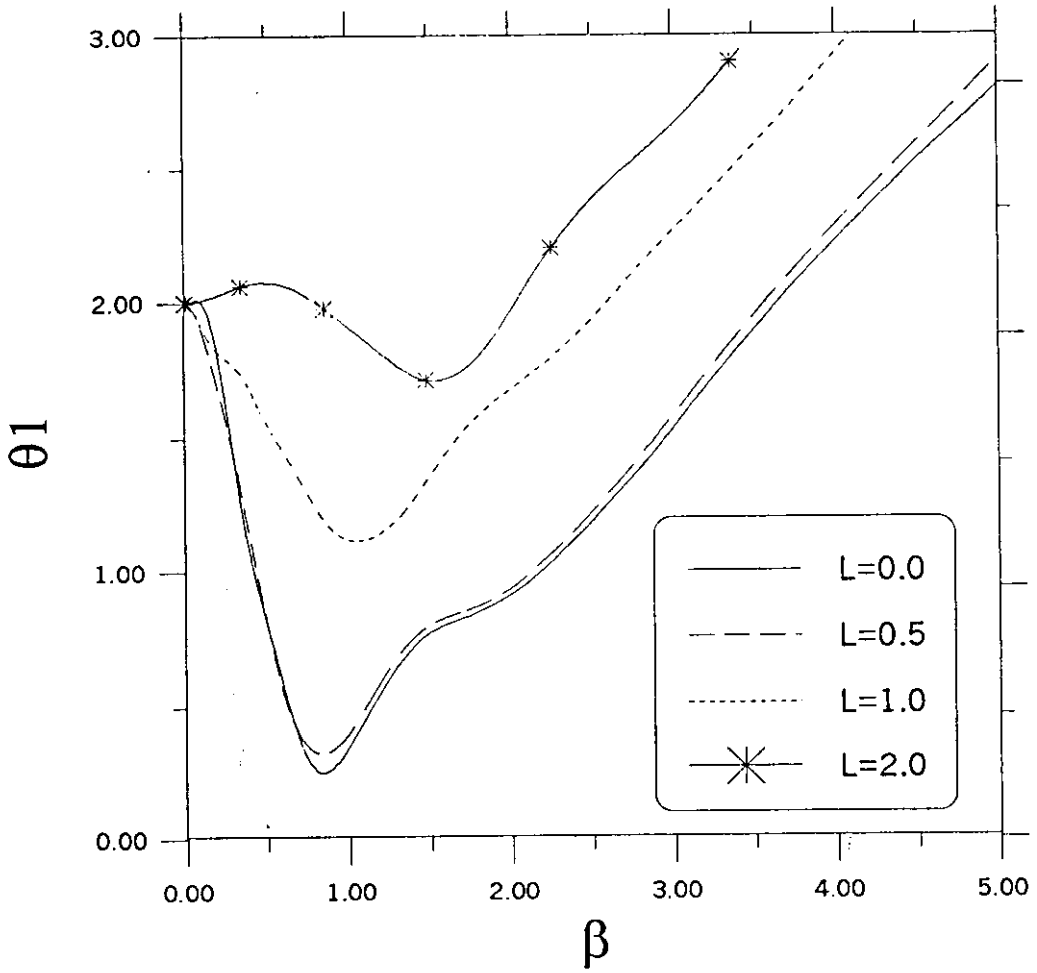

Figure (4.42): Effect of dimensionless disturbance length on type I-superconductor based on dual-phase-lag model. (For Q=2.0, R=5.0, ε=0.0, B=2, τ_i=0.0, θ_{c1}=0.1 and H=0.0)

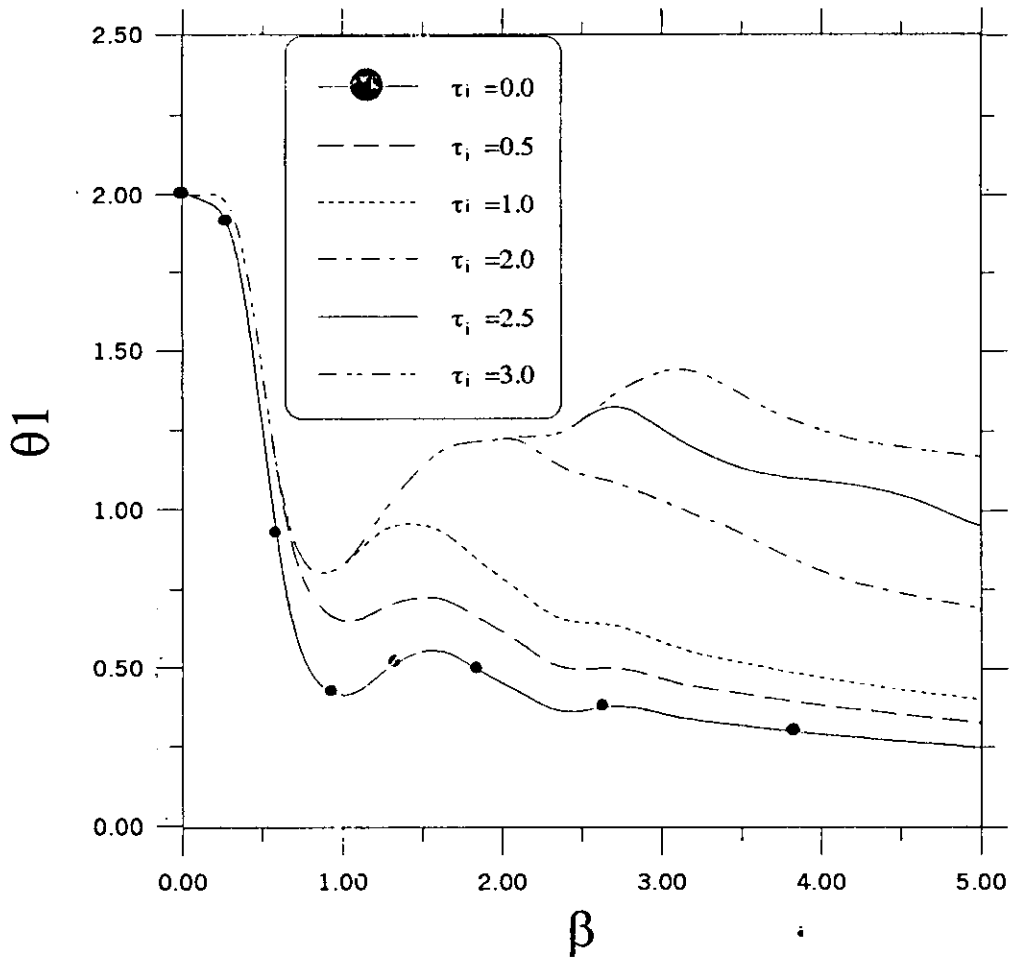

Figure (4.43): Effect of dimensionless disturbance duration time on typeII-superconductor thermal stability based on dual-phase-lag model. (For L=1.0, Q=0.5, R=5, ε=2.0, B=2, and H=0.1).

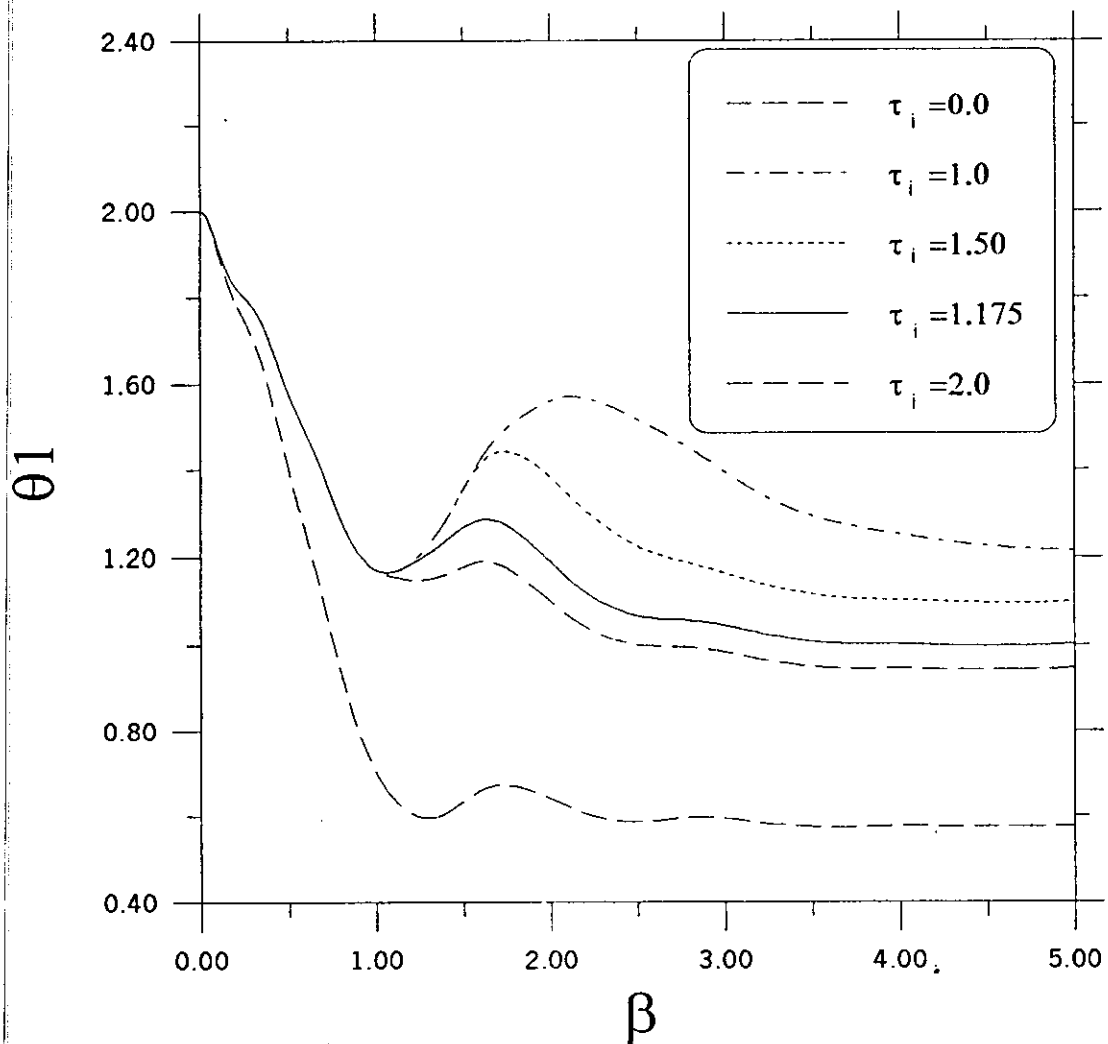

Figure (4.44): Effect of dimensionless disturbance duration time on type-I superconductor based on dual-phase-lag model. (For L=1.0, Q=1.0, θ_{c1}=0.1, R=5, ε=2.0, B=2, and H=0.10)

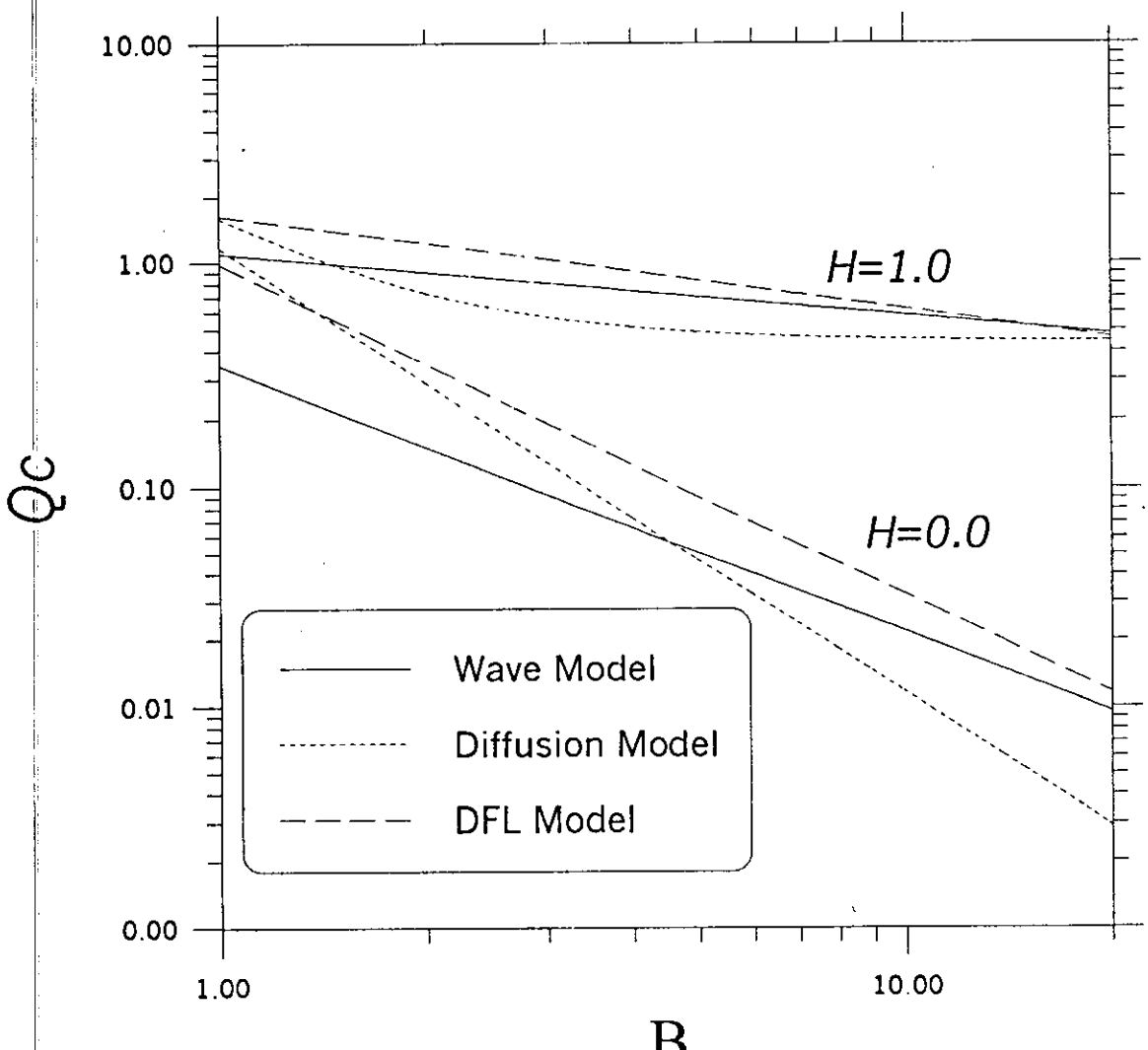

Figure (4.45): The stability criterion for type II-superconductor subjected to stepwise type disturbance, based on three different heat conduction model. (For τ_i=0.0, R=5, ε= 0.0, and L=1.0).

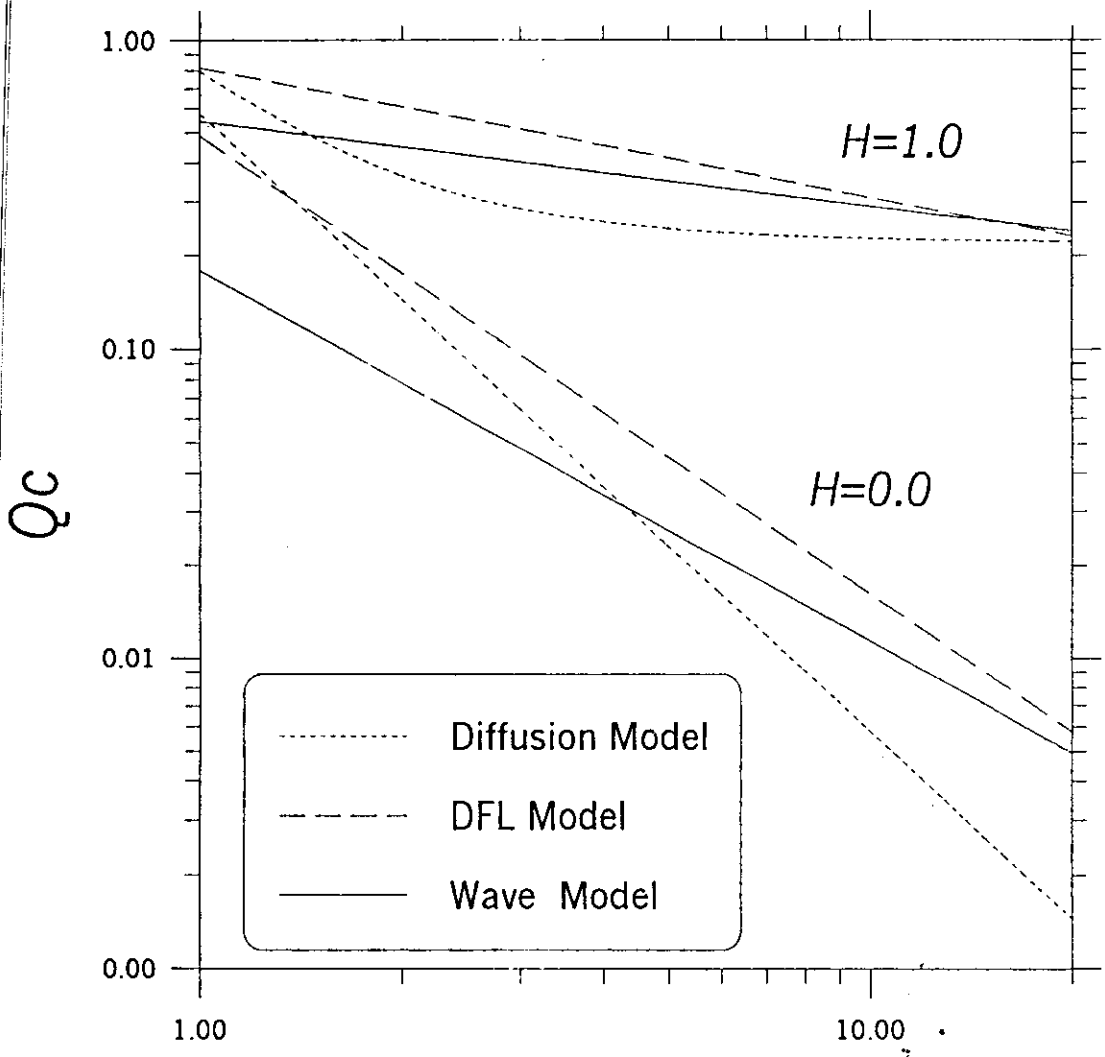

Figure (4.46): The stability criterion for typeI-superconductor subjected to stepwise type disturbance, based on three different heat conduction model. (For L=1.0, R=5, ε=0.0, θ_{cl}=0.10 and τ_i=0.0)

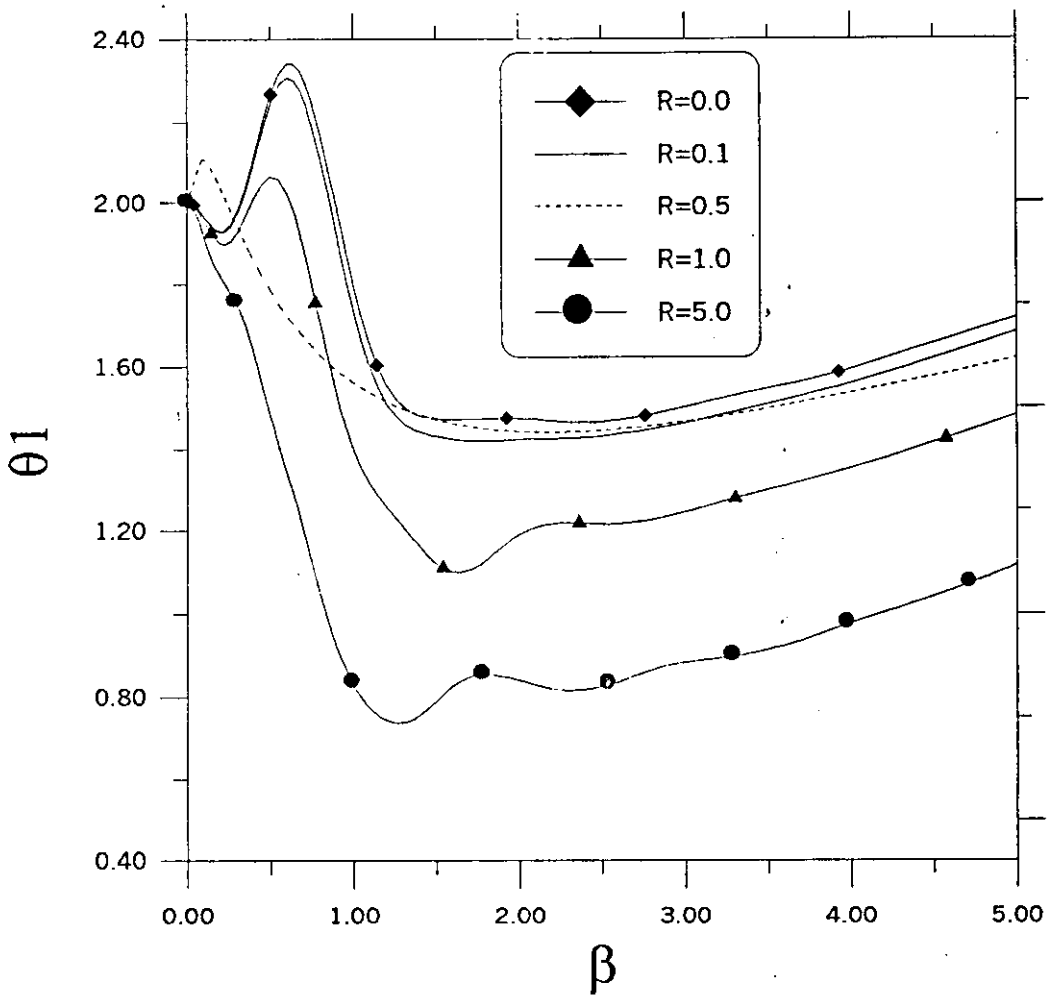

Figure (4.47b): comparison between dimensionless maximum temperature-time history of typeI-superconductor based on the three macroscopic heat conduction model. (For Q=1, L=1.0, ε=1.0, B=2, H=0.10 and τ_i=0.1)

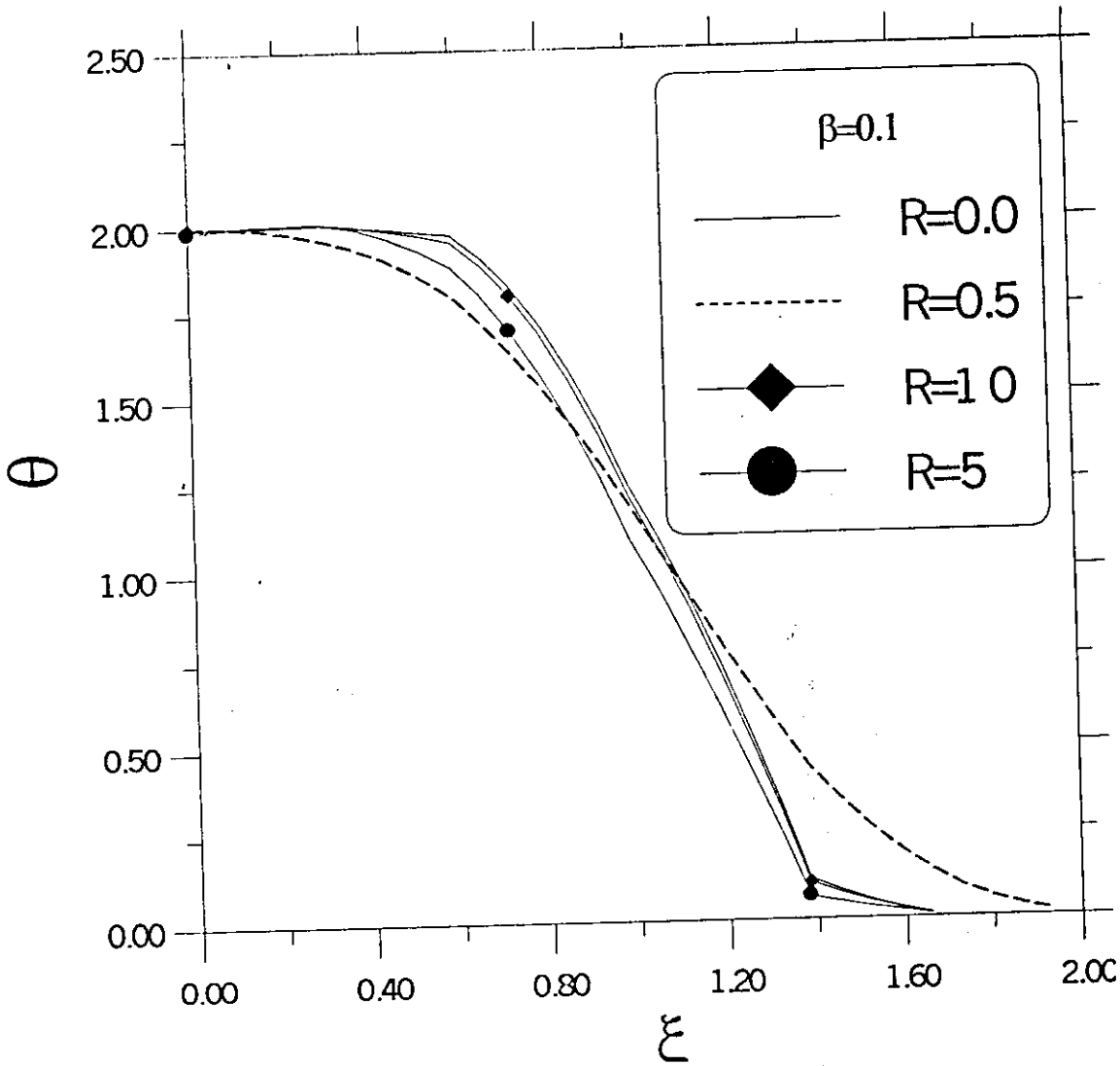

Figure (4.48a): Comparison between temperature profiles obtained based on different macroscopic heat conduction models for type I superconductor. (For Q=0.25, R=5, ε=0.0, B=2, L=1.0, H=0.0 and τ_i=0.0).

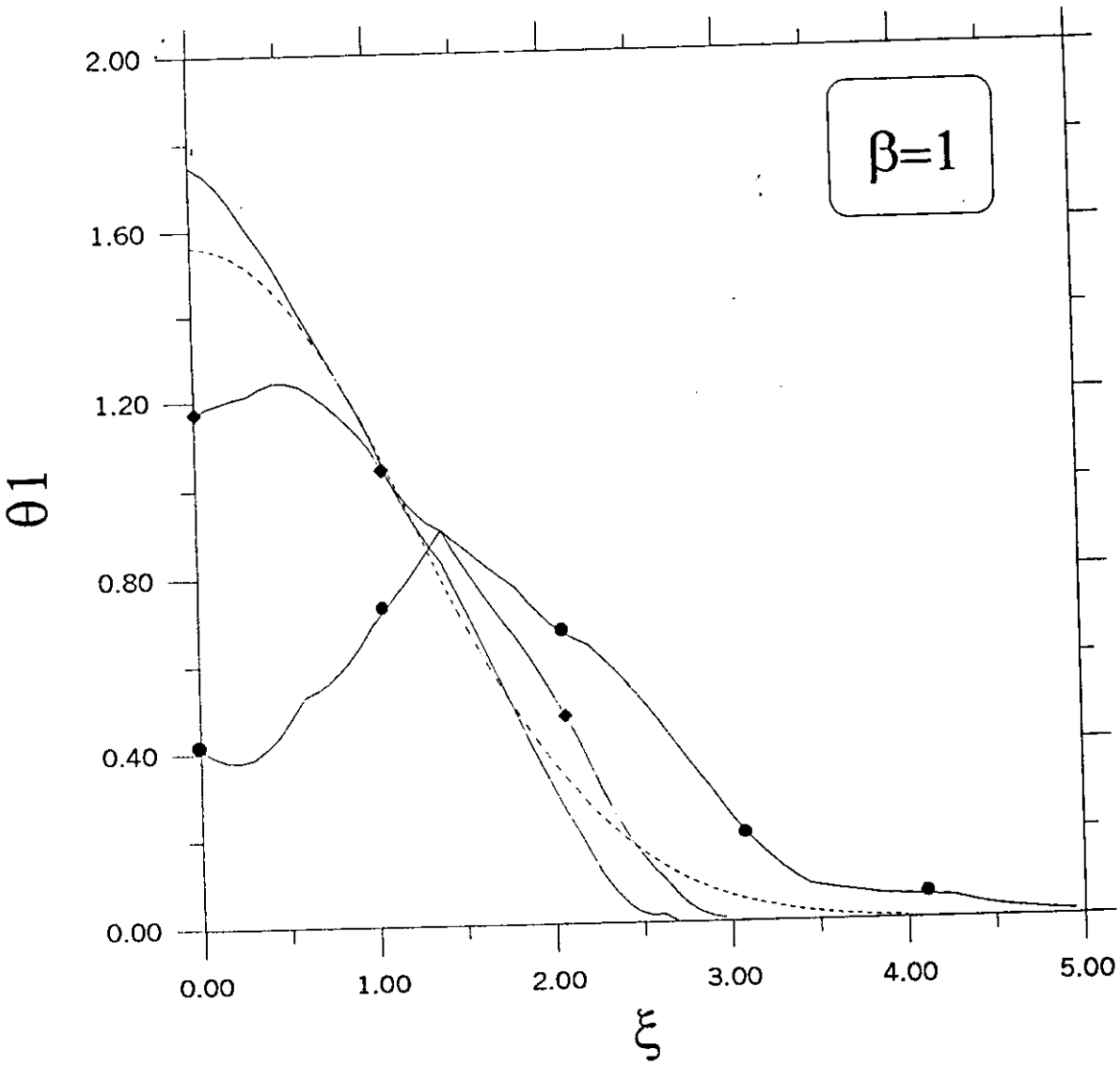

Figure (4.48b): Comparison between temperature profiles obtained based on different macroscopic heat conduction models for type-I superconductor. (For Q=0.25, ε=0.0, B=2, L=1.0, H=0.0 and τ_i=0.0).

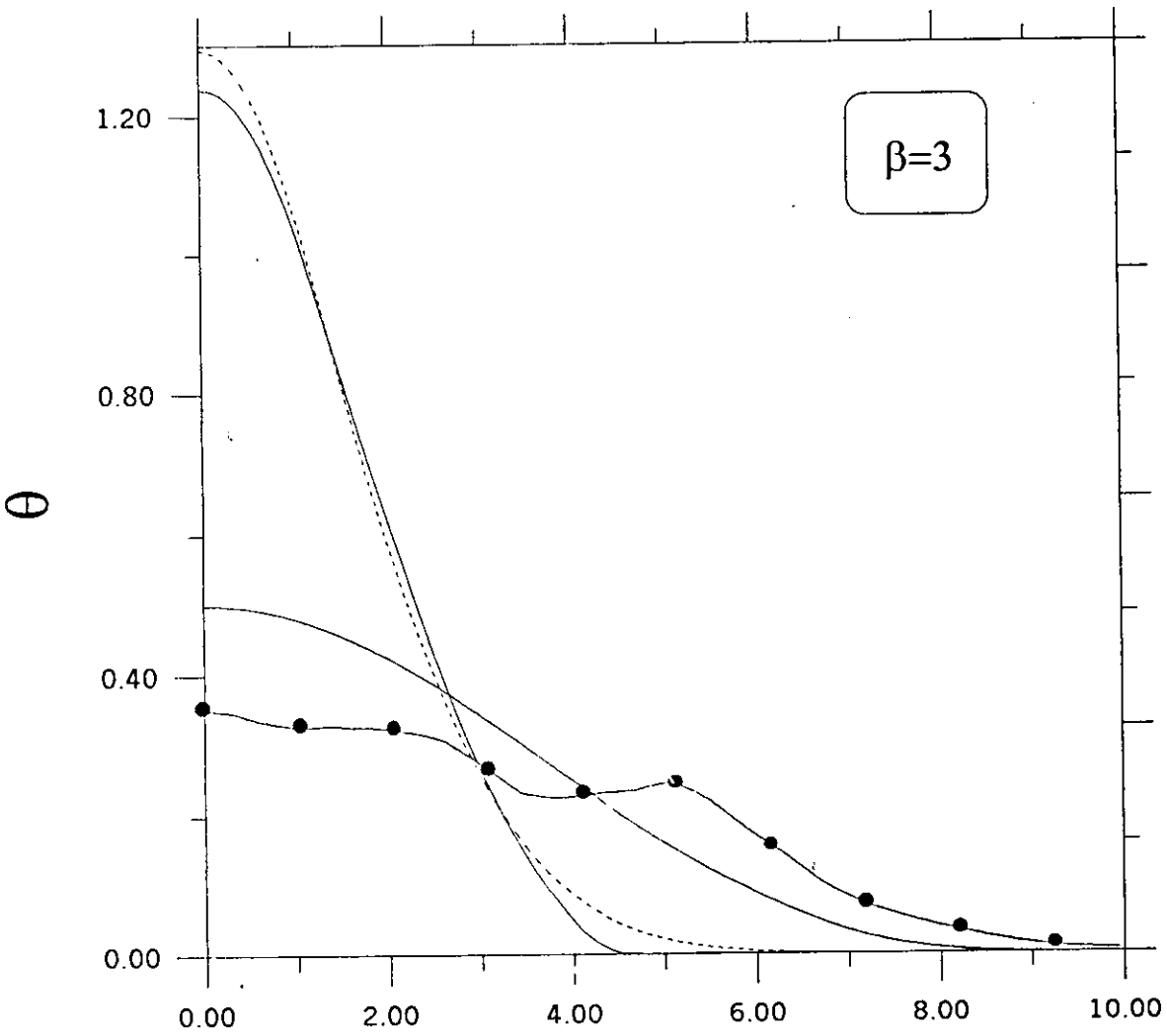

Figure (4.48c): Comparison between temperature profiles obtained based on different macroscopic heat conduction models for type I superconductor. (For Q=0.25, ε=0.0, B=2, L=1.0, H=0.0 and τ_i=0.0).

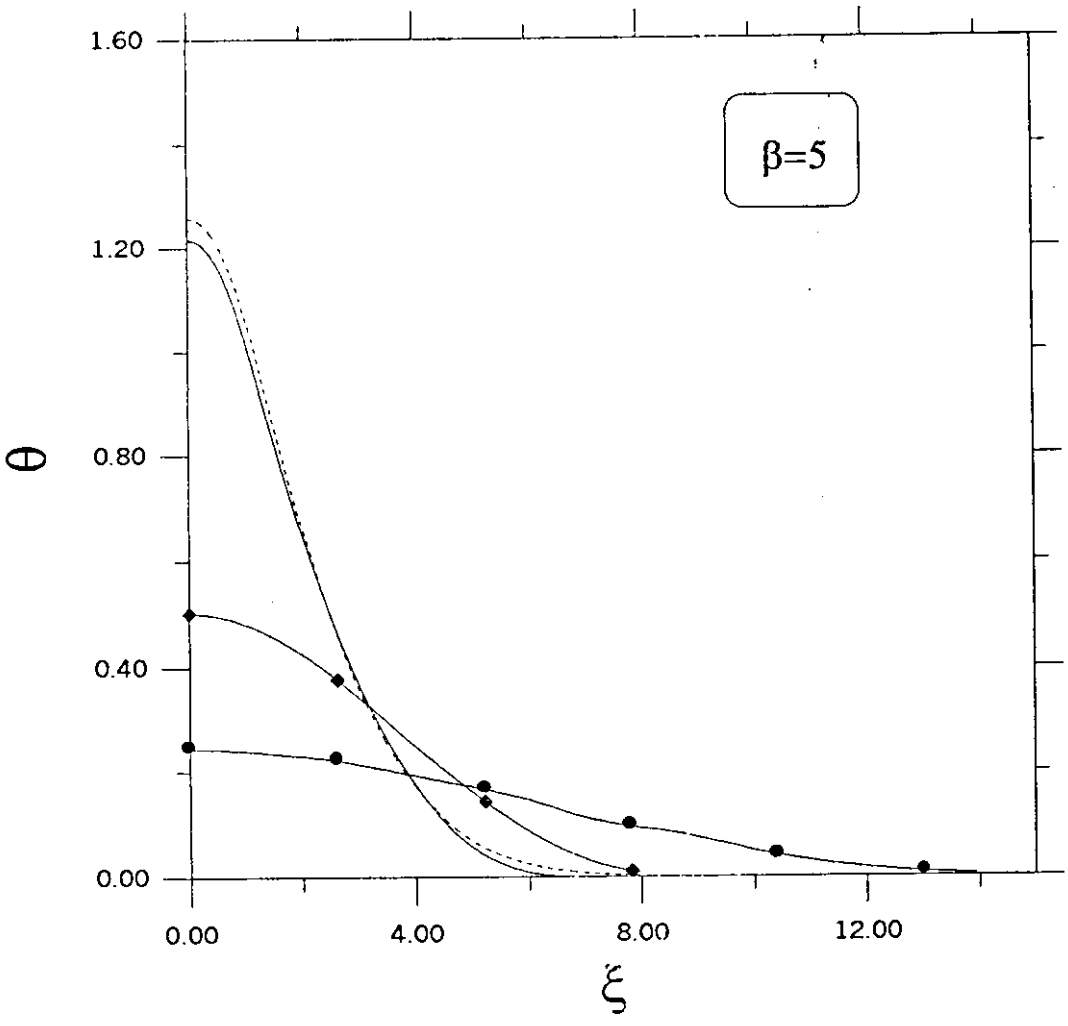

Figure (4.48d): Comparison between temperature profiles obtained based on different macroscopic heat conduction models for typeI-superconductor (For Q=0.25, ε=0.0, B=2, L=1.0, H=0.0 and τ_t=0.0).

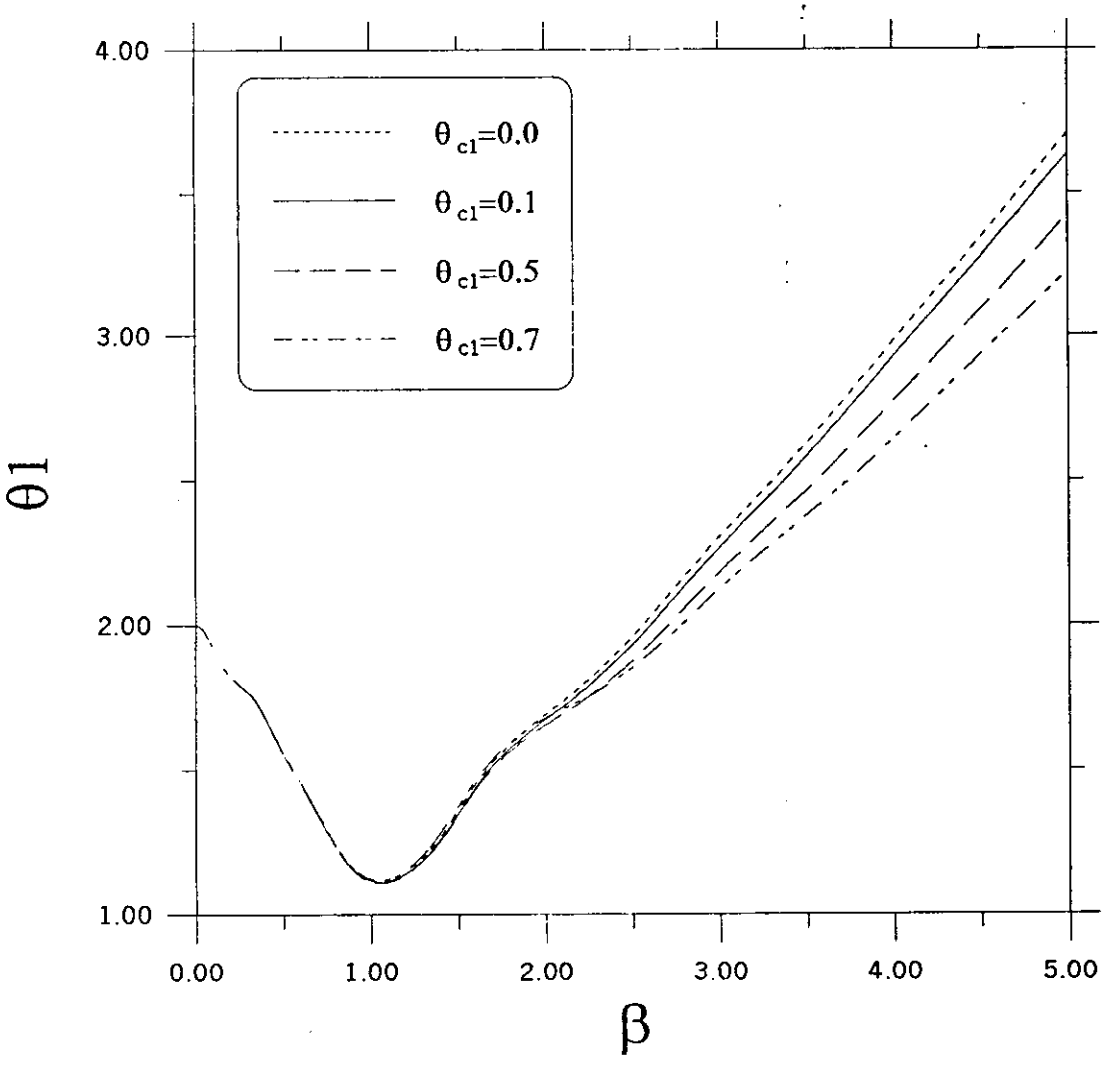

Figure (4.49): Effect of dimensionless current sharing temperature on typeII-superconductor thermal stability based on dual-phase-lag model. (For L=1.0, Q=1, τ_i=0.0, ε=0.0, B=2, and H=0.0)

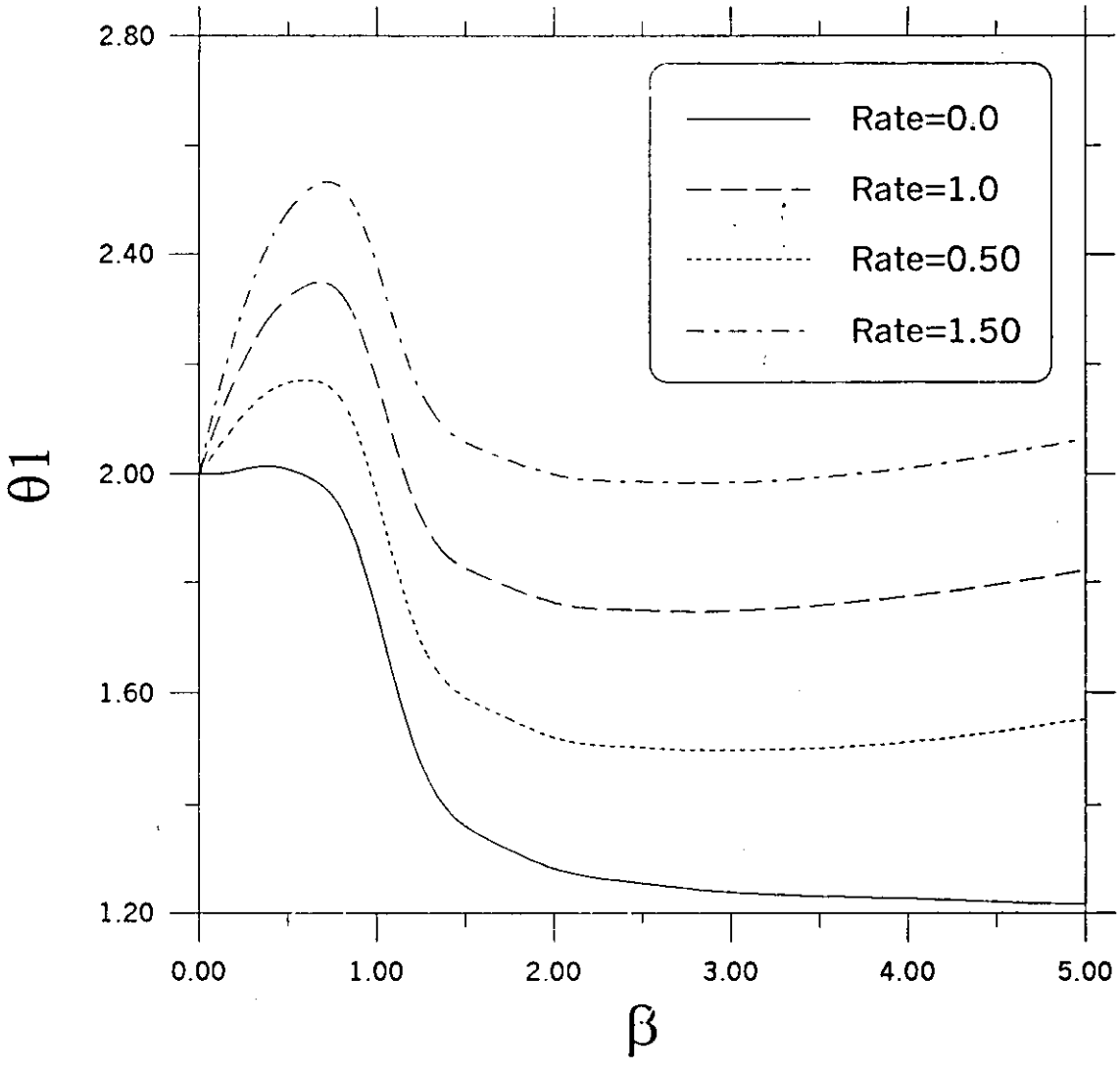

Figure (4.50): The effect of initial time-rate of temperature on type II-superconductor thermal stability based on wave model. (For L=1.0, Q=0.5, τ_i=0.0, R=0, ε=0.0, B=2, and H=0.1).

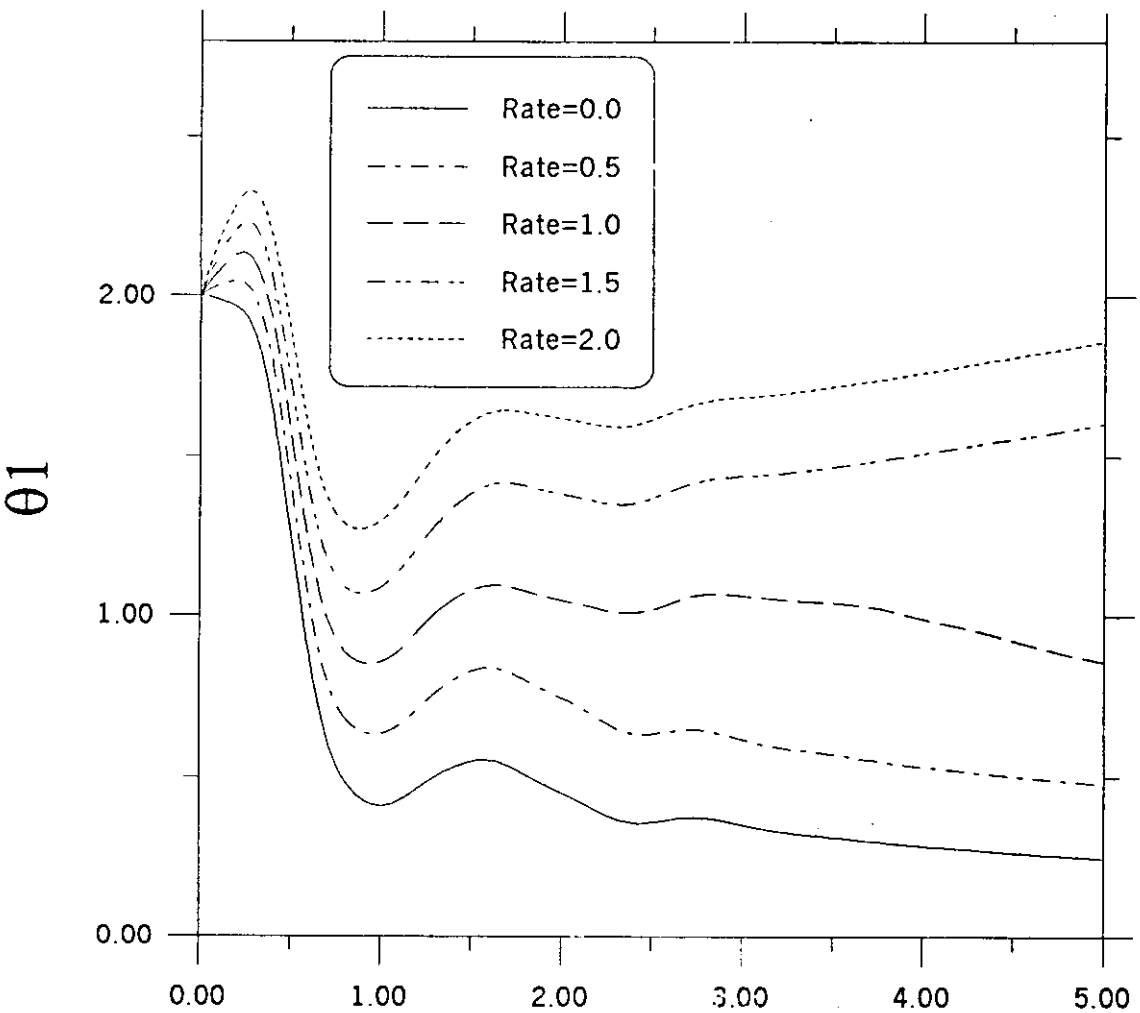

Figure (4.51): The effect of initial time-rate of temperature on type II-superconductor thermal stability based on dual-phase-lag model. (For L=1.0, H=0.0, R=5, ε=0.0, B=2, τ_i=0.0, and Q=1.5)

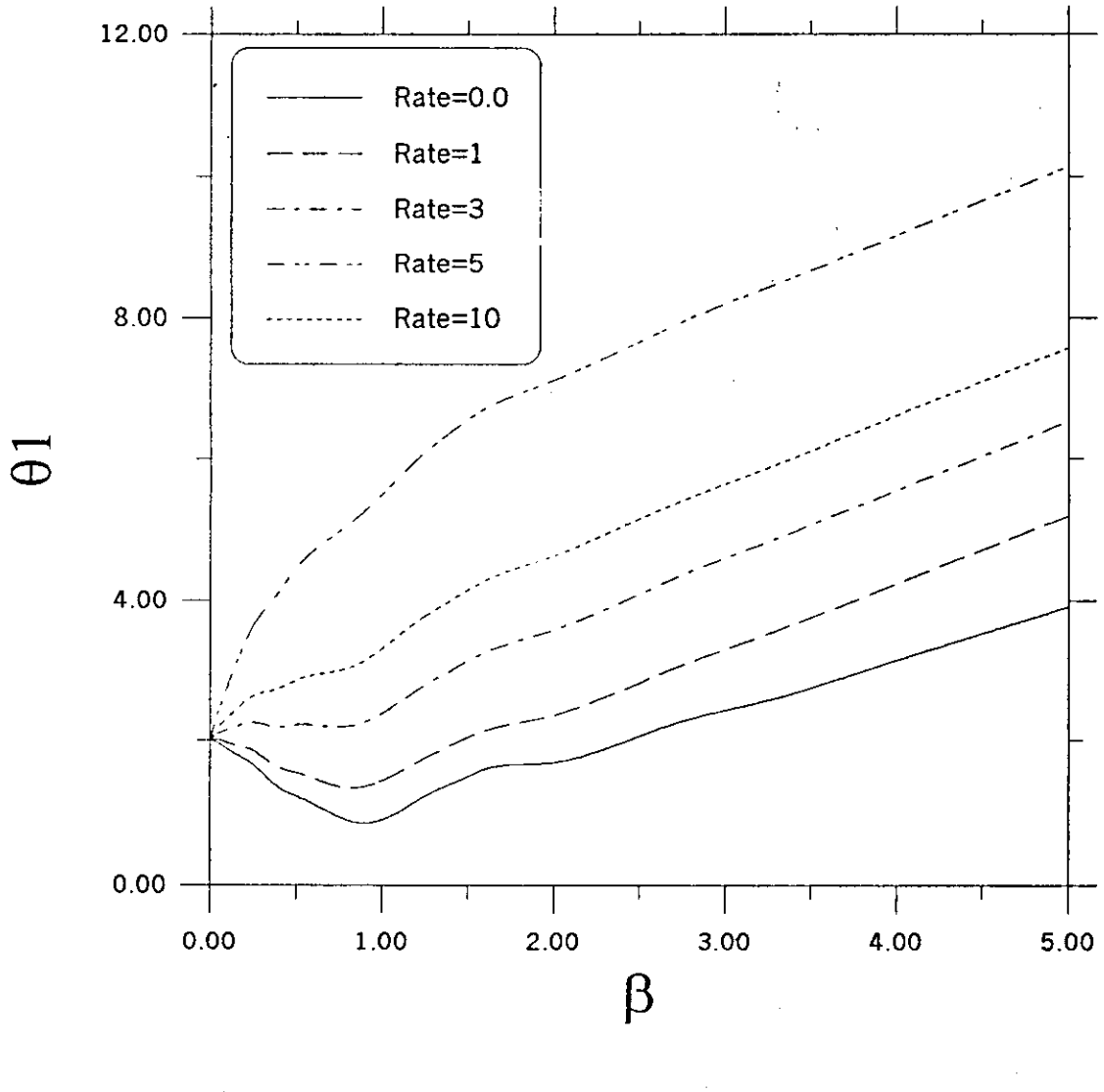

Figure (4.52): The effect of initial time-rate of temperature on typeI-superconductor thermal stability based on dual-phase-lag model. (For L=1.0, θ_{c1}=0.1, τ_i=0.0, R=5, ε=0.0, B=2, and Q=0.5)

5-Conclusions and Recommendations

The main conclusions of the study are presented in this chapter. The usefulness of the present analysis for the low and high-temperature superconducting wires is assessed. The superconducting wire thermal stability is studied numerically based on the different heat conduction models. The history of a given temperature disturbance is derived from the solution of the transient heat conduction model for an infinite laterally cooled conductor with temperature dependent heat source. The combined diffusion by axial heat conduction and the lateral heat transfer and its effect on superconductor thermal stability is presented numerically.

The following conclusions drawn from this study:

1. The superconductor thermal stability region decreases with the Joule heating, the disturbance intensity, length, energy, and duration time, while the stability region increases with the lateral cooling, the current sharing temperature.
2. The collapse of growth behavior of a local disturbance depends on a number of important dimensionless groups: the Joule heating, the lateral cooling, the disturbance intensity, length, duration time and energy.
3. For large values of lateral cooling (H) the effect of disturbance intensity (B) on stability is insignificant compared with that of Q, while for small H the effect of B on stability is comparable with the effect of Q.
4. The disturbance shape along the axial direction of the superconductor wire influences thermal stability. The stepwise disturbance has a stronger effect on the thermal stability compared to the normal distribution one. In spite of this, the stability criterion is not very sensitive to the particular shape of the initial temperature (disturbance) distribution.

5. Type II superconductors are likely to be much more stable in response to thermal disturbances than their type I counterparts. Also, type II superconductors require less lateral cooling to bring them into the thermal stability compared to type I.
6. As current sharing increases the thermal stability type II superconductor improves.
7. As the disturbance length (intial normal zone length), and duration time increase the thermal stability of both superconductor types becomes worst.
8. At small values of disturbance intensity the use of the wave model to investigate the thermal stability of superconductor underestimates the stability operation region, which will ensure thermal stability. While for large B the diffusion model should be used. The use of dual-phase-lag model with R=5 seems to overestimate the stability region.
9. The increase of initial time rate of change of temperature will contribute in the process of shifting superconductor of both types to operate outside the stability region.

The numerical solution of this study is conducting based on the assumption of constant physical properties, this assumptions valid only for very low temperature (below 25 K) where the matrix resistivity is in dependent of temperature. Since low Tc superconductors operate in this temperature range, this assumption is valid. However, it is not a good assumption for high Tc superconductors. So, Further works that takes into account the temperature dependent of the physical properties is required.

6-References

- Abeln, A., Klemt, E. and Riess, H. 1992.Stability consideration for design of a high temperature superconductor. *Cryogenics*, 32 (3): 269-278.
- Al-Huniti, N. S. and Al-Nimr, M. A. 2000. Behavior of thermal stresses in a rapidly heated thin plate. *J. Thermal Stresses*, 23(4): 293-308.
- Al-Nimer, M. A., and Naji, M. 2000. On the Phase-Lag Effect on the Non-equilibrium Entropy Production. *Microscale Thermophysical Engineering*, 4(4)..
- Al-Nimr, M. A. and Al-Huniti, N. S. 2000.Thermal stresses under the effect of dual-phase-lag heat conduction model. Accepted for publication in *J. Thermal Stresses.*
- Al-Nimr, M. A., and Arpaci, V. S. 1999. Picosecond thermal pulses in thin metal films. *Journal of Applied Physics*, 85(5): 2517-2521.
- Al-Nimr, M. A., and Arpaci, V. S. 2000. The thermal behavior of thin metal films in the hyperbolic two-step model. *Int. J. Heat Mass Transfer.* 43: 2021-2028.
- Al-Nimr, M. A., Haddad, O. M. and Arpaci, V. S 1999.Thermal Behavior of Metal Films- A Hyperbolic Two Step Model. *Heat and Mass Transfer*, 36: 459-464.
- Al-Nimr, M. A., Naji, M. and Arpaci, V. S. 2000. Non-equilibrium entropy production under the effect of dual-phase-lag heat conduction model. *ASME J. Heat Transfer.*
- Anderson, D.A., TannehillJ, A. C. and Pletch, R. H. .1984. *Computational Fluid Mechanics and Heat Transfer*. McGraw-Hill, New York, U.S.A.

- Bejan, A., and Tien, C.L. 1978. Effect of Axial Conduction and Metal Helium Heat Transfer on the Local Thermal Stability of Superconducting Composite Media. *Cryogenics*, 18: 433 – 441.
- Bellis, R. H. and Iwasa, Y. 1994. Quench propagation in high T_c superconductor. *Cryogenics,* 34: 129 – 144.
- Buznikov, N. A., Pukhov, A. A. and Rakhmanov, A. L. 1995. Local normal zone nucleation to 'global' transition: quench development in superconductor with changing current. *Cryogenics*, 35 (10) :623-630.
- Chen, Han-Taw, and Lin, Jae–Yuh.1994. Analysis of Two Dimensional Hyperbolic Heat Conduction Problems. *Int. J. Heat and Mass Transfer*, 37 (1): 153 – 164.
- Chidambrara, C., Raj, B. and Jean, B. H. 1991. Analysis of Joule Heating in Electro-phonetic Processes. *Int. Comm. Heat and Mass Transfer*, 18: 843-852.
- Flik, M. I. and Tien, L C. 1990. Intrinsic Thermal Stability of Anisotropic Thin-Film Superconductors. *J. Heat Transfer*, 112:10-15.
- Gladum, A., Eckert, B., Mobius, A., and Verges, P. 1981. A computer program simulating the quench of superconducting magnet system. *IEEE Trans. On Magnet,* Vol. 17.
- Ito, T., Takata, Y. and Kasao, D. 1992.Stability Analysis of Forced – Flow Cooled Superconductors. *Cryogenics*, 32:439-445.
- Kadambi, V. Dorri, B. 1986. Current decay and temperatures during superconducting magnet coil quench. *Cryogenics*, 26

- Kim, W.S., Hector, L.G. and, Ozisik M.N. 1990. Hyperbolic Heat Conduction Due To Axisymmetric Continuous or Pulsed Surface Heat Sources. *J. Applied Phys.*, 68: 5478 – 5485.
- Lopez, G. 1996. Constant heat conduction and stabilizing of bus bar conductor. *Cryogenics*, 36 (12): 1051-1052.
- Lue, J. W., Lubell, M. S., D., Campbell J. M. and Schwall R. E. 1996. Quenches in a high temperature superconducting tape and pancake coil. *Cryogenics*, 36 (5): 279-389.
- Maddock, B.J., Jaunes, G.B. and Narris, W.T.1969. Superconductive Composites: Heat transfer and Steady-State Stabilization. *Cryogenics*, 9:261-273
- Malineowski, L. 1991. Critical energy of thermally insulated composite superconductors. *Cryogenics*, 31: 444-449.
- Malineowski, L. 1993. Novel model for evolution of normal zones in composite superconductor. *Cryogenics*, 33 (7): 724-728.
- Mobius, A., Eckert, B., Gladum, A. and Verges, P. 1986. Numerical treatment of quenching process in superconducting magnet system. *Cryogenics*, 21: 413 – 422.
- Naji, M. N., Al-Nimr, M. A and Al-Huniti, Naser S. 2000. Thermal stresses under the parabolic two-step heat conduction model. Accepted for publication in *J Thermal Stresses*.
- Patanker, S. V. 1980. *Numerical Heat Transfer and Fluid Dynamics.* Hemisphere Publishing Corporation, U.S.A.
- Pradhan, S., Romanovkii, V. R. 1999. Thermal stability of superconducting multifilamentray wire with multiply connected stabilizing regions. *Cryogenics*, 39: 339-350.

- Qui, T.Q., and Tien, C.L. 1992. Short-Pulse Laser Heating on Metals. *Int. J. Heat and Mass Transfer*, 35 (3): 719 – 726.
- Qui, T.Q., and Tien, C.L. 1998. Heat Conduction Mechanism During Short-Pulse Laser Heating of Metals. *J. Heat Transfer,* 115: 835 – 841.
- Robert, G. N. and. Gunnar, B. 1999.*Fields of Physics by Finite Element Analysis – An Introduction.* Prentice-Hall, U.K.
- Seol, S.Y. and Chyu, M.C. 1994. Stability Criterion for Composite Super-Conductors of Large Aspect Ratio. *Cryogenics*, 37 (6):513-519
- Stekly, Z.J.J., and Zar, J.L. 1965. Stable Superconducting Coil. *IEEE Transactions on Nuclear Science* , 12(3): 367-372
- Takehiro, Ito and Hiromi, Kubota. 1996. Dynamic analysis of pool-cooled superconductor and MPZ. *Cryogenics*, 36 (3): 159-162.
- Tzou, D.Y. 1995a. A Unified Field Approach for Heat Conduction from Micro-to Macro-scale. *ASME JOURNAL of HEAT TRANSFER*, 117: 8-16.
- Tzou, D.Y. 1995b. The Generalized Lagging Response in small-Scale and High-Rate Heating. *International Journal of Heat and Mass Transfer*, 38: 3231-3240.
- Tzou, D.Y. 1995c. Experimental Support for the lag response in heat propagation. *AIAA Journal of Thermophysics and Heat Transfer*, 9:686-693.
- Tzou, D.Y., Ozisik, M.N., and Chiffele, R.J. 1994. The Lattice Temperature in Microscopic Two-Step Models. *J. Heat and Mass Transfer*, 116: 1034 – 1038.
- Ünal, A. and Chyu, M.C. 1995.Instability behavior of superconductor wires/cylinders under finite linear thermal disturbance. *Cryogenics*, 35 (2): 87-92.

- Ünal, A., Chyu, M.C. and Kuzay, T.M. 1993. Stability and Recovery Behavior of Tape / Film – Type Superconductors. *J. Heat Transfer*, 115: 467 – 469.
- Werner B. 1991. *Superconductivity Fundamentals and Applications. VCH Publishers*, New York, USA.
- Wetzko, M., Zahn, M. and Reiss, H. 1995. Current sharing and stability in a Bi2223/Ag high temperature superconductor. *Cryogenics*, 35 (6): 375-386.
- Wilson, M.N. 1983. *Superconducting Magnets*, Clarendon Press. Oxford, U.K.
- Wipf, S.L. 1978. Stability and degradation of superconducting current carrying devices. *LASL Report, La-7275*.
- Xiao, L. Y., Kiyoshi, T., Ozaka, O. and Wada H. 1999. Case study on quenches evolution and passive protection of high Tc superconducting pancake coil. *Cryogenics*, 39: 293-298.

7-Appendix

Computer Program to Calculate T(ξ,β)

```
**************************************
C       PROGRAM PARABOLIC
C
INTEGER JMAX,NSTEP
(PARAMETER(JMAX=33,NSTEP=4
INTEGER i,j,midl
(DOUBLE PRECISION f(33,33),u(33,33
do 12 i=1,JMAX
do 11 j=1,JMAX
u(i,j)=0.d0
continue          11
continue         12
midl=JMAX/2+1
u(midl,midl)=2.d0
(call mglin(u,JMAX,2
':write(*,'(1x,a)') 'MGLIN Solution
do 13 i=1,JMAX,NSTEP
write(*,'(1x,9f8.4)')
((u(i,j),j=1,JMAX,NSTEP
continue         13
write(*,*) "Test that solution satisfies
":Difference Eqns
do 15 i=NSTEP+1,JMAX-1,NSTEP
do 14 j=NSTEP+1,JMAX-1,NSTEP
f(i,j)=u(i+1,j)+u(i-1,j)+u(i,j+1)+u(i,j-1)-
(4.d0*u(i,j
continue         14
('(write(*,'(7x,7f8.4
f(i,j)*(JMAX-1)*(JMAX-1),j=NSTEP+1,JMAX-)   &
(1,NSTEP
continue         15
END
(SUBROUTINE mglin(u,n,ncycle
INTEGER n,ncycle,NPRE,NPOST,NG,MEMLEN
(DOUBLE PRECISION u(100,100
PARAMETER
(NG=5,MEMLEN=13*2**(2*NG)/3+14*2**NG+8*NG-
(100/3
(PARAMETER (NPRE=1,NPOST=1
C       USES
addint,copy,fill0,interp,maloc,relax,resid,rstrct,slvsml
INTEGER
(j,jcycle,jj,jpost,jpre,mem,nf,ngrid,nn,ires(100
```

```
(INTEGER   irhs(100),iu(100),maloc,irho(100
DOUBLE PRECISION z
COMMON /memory/ z(MEMLEN),mem
mem=0
nn=n/2+1
ngrid=NG-1
(irho(ngrid)=maloc(nn**2
(call rstrct(z(irho(ngrid)),u,nn
if (nn.gt.3) then          1
nn=nn/2+1
ngrid=ngrid-1
(irho(ngrid)=maloc(nn**2
call
(rstrct(z(irho(ngrid)),z(irho(ngrid+1)),nn

go to 1
endif
nn=3
(iu(1)=maloc(nn**2
(irhs(1)=maloc(nn**2
(((call slvsml(z(iu(1)),z(irho(1
ngrid=NG
do 16 j=2,ngrid
nn=2*nn-1
(iu(j)=maloc(nn**2
(irhs(j)=maloc(nn**2
(ires(j)=maloc(nn**2
(call interp(z(iu(j)),z(iu(j-1)),nn
if (j.ne.ngrid) then
(call copy(z(irhs(j)),z(irho(j)),nn
else
(call copy(z(irhs(j)),u,nn
endif
do 15 jcycle=1,ncycle
nf=nn
do 12 jj=j,2,-1

do 11 jpre=1,NPRE
(call relax(z(iu(jj)),z(irhs(jj)),nf
continue            11
call
(resid(z(ires(jj)),z(iu(jj)),z(irhs(jj)),nf
nf=nf/2+1
(call rstrct(z(irhs(jj-1)),z(ires(jj)),nf
(call fill0(z(iu(jj-1)),nf
continue              12
(((call slvsml(z(iu(1)),z(irhs(1
nf=3
```

```
do 14 jj=2,j
nf=2*nf-1
call addint(z(iu(jj)),z(iu(jj-
(1)),z(ires(jj)),nf
do 13 jpost=1,NPOST
(call relax(z(iu(jj)),z(irhs(jj)),nf

continue          13
continue            14
continue       15
continue       16
(call copy(u,z(iu(ngrid)),n
return
END
(SUBROUTINE relax(u,rhs,n
INTEGER n
(DOUBLE PRECISION rhs(100,100),u(100,100
INTEGER i,ipass,isw,j,jsw
DOUBLE PRECISION h,h2
(h=1.d0/(n-1
h2=h*h
jsw=1
do 13 ipass=1,2
isw=jsw
do 12 j=2,n-1
do 11 i=isw+1,n-1,2
U(i,j)=0.25d0*(u(i+1,j)+u(i-
(1,j)+u(i,j+1)+u(ı,j-1
((h2* rhs(i,j-    &

continue          11
isw=3-isw
continue       12
jsw=3-jsw
continue      13
return
END
(SUBROUTINE addint(uf,uc,res,nf
INTEGER nf
DOUBLE PRECISION
(res(100,100),uc(51,51),uf(100,100
CU     USES interp
INTEGER i,j
(call interp(res,uc,nf
do 12 j=1,nf
do 11 i=1,nf
(uf(i,j)=uf(i,j)+res(i,j
continue          11
continue       12
```

```
return
END
(SUBROUTINE copy(aout,ain,n
INTEGER n
DOUBLE PRECISION
(ain(100,100),aout(100,100
INTEGER i,j
do 12 i=1,n
do 11 j=1,n
(aout(j,i)=ain(j,i
continue          11
continue         12
return
END
(SUBROUTINE fill0(u,n
INTEGER n
(DOUBLE PRECISION u(100,100
INTEGER i,j
do 12 j=1,n
do 11 i=1,n
u(i,j)=0.d0
continue          11
continue         12
return
END
(SUBROUTINE interp(uf,uc,nf
INTEGER nf
(DOUBLE PRECISION uc(51,51),uf(100,100
INTEGER ic,if,jc,jf,nc
nc=nf/2+1
do 12 jc=1,nc
jf=2*jc-1
do 11 ic=1,nc
(uf(2*ic-1,jf)=uc(ic,jc
continue          11
continue         12
do 14 jf=1,nf,2
do 13 if=2,nf-1,2
((uf(if,jf)=.5d0*(uf(if+1,jf)+uf(if-1,jf
continue           13
continue         14
do 16 jf=2,nf-1,2
do 15 if=1,nf
((uf(if,jf)=.5d0*(uf(if,jf+1)+uf(if,jf-1
continue         15
continue         16
return
END
(FUNCTION maloc(len
```

```
continue          11
continue        12
do 13 ic=1,nc
(uc(ic,1)=uf(2*ic-1,1
(uc(ic,nc)=uf(2*ic-1,2*nc-1
continue        13
do 14 jc=1,nc
(uc(1,jc)=uf(1,2*jc-1
(uc(nc,jc)=uf(2*nc-1,2*jc-1

continue        14
return
END
(SUBROUTINE slvsml(u,rhs
(DOUBLE PRECISION rhs(3,3),u(3,3
C  U    USES fill0
DOUBLE PRECISION h
(call fill0(u,3
h=.5d0
u(2,2)=-h*h*rhs(2,2)/4.d0
return
END
```

الخلاصة

دراسة الاستقرار الحراري للمواد مفرطة الموصلية الكهربائية باستخدام نماذج ماكرو سكوبية مختلفة لانتقال الحرارة بالتوصيل

إعداد محمد العودات
المشرف الرئيسي: ا.د. محمد حمدان
المشرف المشارك: د. محمد النمر

تتعرض المواد مفرطة الموصلية الكهربائية إلى حالات من عدم الاستقرار الحراري تؤدي إلى فقدانها لخاصية التوصيل المفرط للكهرباء -في ظاهره تعرف ب الكبت (Quench) حيث تتجاوز قيم المجال المغناطيسي و درجة الحرارة وكثافة التيار القيم الحرجة، ويفشل النظام باستعادة حالة الاستقرار. وعموما تبدأ هذه الظاهرة باضطرابات خارجية موضعية تحدث منطقة عادية (ذات مقاومة كهربائية). ويمكن أن تنمو المنطقة العادية أو تختفي وذلك اعتمادا على الموازنة بين التسخين الحراري في السلك والفقد الحراري منة. فإذا لم تسحب الجرارة بعيدا عن المنطقة العادية بشكل أسرع من تولدها فان المنطقة العادية ستنمو وعندها نقول أن الموصل غير مستقر. يعتبر الاستقرار الحراري من أهم القضايا في تصميم الأجهزة التي تستخدم لمواد ذات الموصلية الفائقة للكهرباء. ويحدد الاستقرار الحراري للمواد مفرطة الموصلية الكهربائية كميا بواسطة بعض العوامل المحددة، والتي تسمى بمؤشرات الاستقرار، حيث تحدد منطقة التشغيل المستقر للمواد مفرطة الموصلية الكهربائية. وتستخدم عوامل الاستقرار في تصميم الأجهزة التي تستخدم المواد ذات الموصلية الفائقة للكهرباء. تقدم هذه الرسالة تحقيق عددي لحساب عوامل الاستقرار الحراري والتي تشمل درجة الحرارة القصوى للموصل والطاقة الحرجة. وقد تم حساب هذه العوامل بناءا على عدة نماذج ماكروسكوبية لانتقال الحرارة بالحمل، وهذه النماذج هي النموذج الانتشاري التقليدي، والنموذج الموجي،والنموذج ثنائي الطور. إن الجزء الجوهري في هذا العمل هو استخدام والنموذج الموجي،والنموذج ثنائي الطور والتي تستخدم لوصف العمليات ذات التغير السريع أو

ذات معدلات التسخين العاليـة فـي الوصـلات الفائقـة. وهـذه النمـاذج تـأخذ بعيـن الاعتبـار السـرعة المحدودة لانتشار التدفق الحراري وأسبقية كل من الانحدار والتدفق الحراري.

ولقد تم نمذجة لاستقرار الحراري بواسطة كود عددي باستخدام طريقـة الفـروق المتناهيـة لحالة النموذج الانتشاري وباستخدام برنامج FlexPDE في حالتي النموذج الموجي وثنائي الطور. ويأخذ النموذج العددي بالاعتبار كلا من الانتقال الغير مستقر فـي الموصـل وفـي وسـيط التبريد، والطول المحدود وفترة البقاء المحدودة للاضطراب الحراري.

لقد دلت الدراسة على أن استخدام كلا من النموذج الموجي وثنائي الطور له اثـر حاسـم علـى توقـع الاستقرار الحراري للموصلات. وكذلك أوضحت الدراسة أنة هنالك تسخين جـول حـرج لكـل شـدة اضطراب وان منطقة الاستقرار الحراري المحسوبة بناءا على النموذج ثنائي الطور تبدو مضخمة. ولقيم اضطراب صغيرة فان النموذج الموجي يتوقـع منطقـة اسـتقرار حـراري أضيـق مـن المنطقـة المتوقعة من النموذج الانتشاري، والوضـع معكـوس عنـد قيـم الاضطـراب الكبيـرة. وكذلـك بينـت الدراسة الأثر الإيجابي للتبريد العرضي للموصل على الاستقرار الحراري والأثـر السـلبي لطـول الاضطراب وطول فترة مكوثه على الاستقرار الحراري.

وباستخدام النتائج العددية تم تحديد العوامل الأساسية للاستقرار الحراري. وبناء عل ذلك تم استخلاص عدد مـن الاسـتنتاجات العامـة. ولقد تـم مقارنـة لنتـائج هـذه الدراسـة مـع بعـض النتـائج المتوفرة في المراجع المختصة وكان التوافق مقبولا.